CONFIGURATIONAL STUDIES OF

SCALING PHENOMENA

by

RODERICK CHARLES DEWAR

A thesis submitted for the degree of

DOCTOR OF PHILOSOPHY

Department of Physics

University of Edinburgh

September 1986

To my mother and father

ACKNOWLEDGEMENTS

I am indebted to many people for the help and support I have been offered during my studies at Edinburgh.

It is a pleasure to thank Alastair Bruce and David Wallace who have actively encouraged my interest in physics, and from both of whom I have learned a great deal. In particular, I would like to thank Alastair for his excellent supervision throughout the duration of this work, and David for his valuable support and encouragement at several critical moments.

I have enjoyed the friendship and co-operation of many members of the Physics Group at Edinburgh; in particular Andrew Brass, David Chalmers, David Nicolaides, David Scott and Charlie Wall; I especially thank Chris Harris, with whom I collaborated in the work of chapter 3, for many helpful comments during the time he spent on my behalf. In my first year I benefitted greatly from discussions with Alan McKane.

Finally, I would like to thank the Science and Engineering Research Council for full financial support during my studies, and for part-support enabling participation in the 6th Trieste International Symposium, July 1985.

The work in chapter 3 was done in collaboration with CK Harris. Elsewhere, the contents of this thesis are entirely my own work apart from where otherwise stated.

Roderick Dawes

2/9/86

ABSTRACT

The renormalisation group approach to problems involving scale-invariance is briefly reviewed. Then, using renormalisation group ideas and techniques, various scaling phenomena are studied directly in terms of the scaling properties of the configurations or patterns that underlie them.

(i) we study the universal scaling properties of configurations of block-spins near the critical point of an O(n)-symmetric ferromagnet, as characterised by the block-spin probability density function (p.d.f.). Critical scaling properties of this p.d.f. are obtained for $n > 2$ and $d=2+\epsilon$ within a perturbative calculation for small ϵ. A non-perturbative approximation to the renormalisation group transformation is used to calculate the p.d.f. at the transition of the d=3 XY model (n=2). Then we carry out a Monte-Carlo simulation of this model on the ICL Distributed Array Processor (DAP), which supports the result of the calculation. Our results suggest that universal scaling features of the underlying spin patterns should be revealed in some characteristic distribution of spin angles; we discuss the possible role played by topological excitations (vortices) at the d=3 XY transition.

(ii) we study the problem of percolation in terms of scaling properties of the underlying clusters. Following a recent controversy regarding the scaling behaviour of the mean number of clusters, we present numerical evidence for the validity of the

currently-accepted scaling picture. For our finite-size scaling analysis we use a purpose-written fast parallel cluster-counting algorithm, implemented on the ICL DAP. A noise reduction scheme is adopted to suppress the considerable fluctuation in the numerical data. A clear discrepancy with the controversial scaling picture is thus established.

(iii) we study scaling in a model of random epidemic growth. From numerical simulations, we find that the interface between healthy and infected sites exhibits both static and dynamic scaling properties. Results are in close agreement with the predictions of a recently-proposed Langevin equation for interface growth, from which universality classes have been extracted using the dynamical renormalisation group. We thus identify the essential large-distance, long-time physics of the epidemic model.

CONTENTS

CONTENTS (continued)

CHAPTER 1

RENORMALISATION GROUP APPROACH TO SCALE-INVARIANCE

1.1 Introduction to scale-invariance

This thesis is about problems which involve scale-invariance through the formation of patterns which look the same on different length scales. Examples include (i) phase transitions and other critical phenomena in many-body systems and (ii) processes of growth and aggregation.

At the critical point of water ($T=647^{o}K, p=217$ atmospheres) for example, where the distinction between liquid and gas disappears, density fluctuations develop in the form of co-existing droplets of liquid and bubbles of gas on scales ranging from the size of one molecule to the size of the container. Statistically, the picture of such a system looks the same on all length scales. Contrast this with, say, the problem of the large-scale motion of ocean waves which is essentially uncorrelated with the small-scale molecular structure of the water.

Problems in physics with many length scales are more difficult to solve than those like the ocean waves, which are confined to only a narrow range of length scales. The renormalisation group (RG) is a general method for dealing with such problems. It was first introduced as a technical device in quantum electrodynamics to get

rid of (renormalise) certain unphysical infinities in the theory. It happened to lead to many physically-equivalent definitions of the physical electric charge (coupling constant) differing only by a choice of length scale.

KG Wilson (1971a,1971b) realised its potential for problems with many length scales. In his iterative version, at each step the degrees of freedom associated with the smallest length scales in the picture (Hamiltonian) are "eliminated" and their effect is incorporated into a new, but physically-equivalent, picture of the remaining degrees of freedom. The change in the smallest length scale is a scale transformation $x \to x' = \lambda x$ and the change induced in the Hamiltonian is a renormalisation group transformation (RGT) $H \to H'(\lambda)$.

Scale-invariance may then be described fruitfully in terms of fixed points of the RGT. It means roughly that after the scale transformation $x \to x'$ the transformed Hamiltonian is the same as the original Hamiltonian. The scale-invariant system is therefore described by a fixed-point Hamiltonian H^* with the property that under the scale transformation $H^* \to H^*$.

The aim of this introductory chapter is to review briefly the ideas of scaling and the RG that form a background to the work presented in chapters 2-4. The set up of this chapter is the following: in section 1.2 we describe scaling and universality as they appear at phase transitions. I have chosen the context of phase transitions in ferromagnets to do this because their intrinsic symmetry makes them easier to think about. The liquid-gas transition

would serve the same purpose; moreover it is a remarkable fact that even quantitatively, many such superficially distinct systems share the same (universal) critical behaviour.

In section 1.3 we shall outline the emergence of the scaling hypothesis by which scaling may be understood as the consequence of a single characteristic length scale - the correlation length ξ - diverging at the critical point. On the way we discuss the ideas of Widom scaling and Kadanoff blocking. In section 1.4 we introduce the ideas of Wilson's RGT as the physical and mathematical refinement of Kadanoff blocking. It is seen as a natural formalism in which both scaling and universality arise explicitly, as well as a powerful tool for calculating critical properties.

Section 1.5 outlines some techniques of field theory, mostly for chapter 2. After a brief description of the field formalism that allows us to perform systematic calculations perturbatively, we indicate the way in which renormalised field theory techniques can be used to control calculations near the critical point. The connection of these techniques with Wilson's RGT is then exposed. Finally, in section 1.6 we set out the plan of the remaining chapters in the context of these introductory ideas.

1.2 Phase transitions in magnets, critical exponents, scaling and universality

Ferromagnetism

In zero magnetic field h and above temperature T_c=1044^{o}K, iron has no magnetisation M. When it is cooled below T_c it becomes

spontaneously magnetised. Nickel behaves similarly at $T_C=632^oK$. Iron and nickel are examples of ferromagnets. We understand ferromagnetism as follows.

The source of magnetism is the magnetic moments of the electron spins; M is the average magnetic moment of the sample. Electron spins tend to align themselves due to their quantum-mechanical exchange interaction. This tendency to order competes with the tendency to disorder due to thermal fluctuations. At high temperatures the spins are randomly aligned and so M=0. At zero temperature all the spins lie parallel to each other and so $M=M_{max}$. The temperature T_C marks the onset of co-operative alignment of the spins throughout the material.

Scaling near T_C

Now M goes to zero smoothly as T approaches T_C from below. Experimentally this behaviour seems power-like:

$$M \sim (T_c - T)^{\beta} \quad , \quad T \leq T_c \qquad (1.2.1)$$

where $\sim$ means "behaves like". β, a critical exponent, is 0.34(2) for Fe, 0.33(3) for Ni, i.e. the same to within experimental error (experimental values are taken from Ma (1976) p.12). (1.2.1) exhibits scaling behaviour in the sense that the equation stays the same under the scale changes $(T-T_C)\rightarrow\lambda(T-T_C)$, $M\rightarrow\lambda^{\beta}M$.

When iron is at $T=T_C$ then M=0 but if we switch on a small magnetic field h, the spins align to the field direction and M scales with h like

$$M \sim h^{1/\delta} \quad , \quad T = T_c \tag{1.2.2}$$

where the critical exponent δ is 4.2(1) for Ni. (1.2.2) is invariant under the scale changes $h \to \lambda h$, $M \to \lambda^{1/\delta} M$.

As $T \to T_c$ the isothermal susceptibility $\chi = (\partial M/\partial h)|_T$ for $h=0$ diverges as a power-law

$$\chi \sim (T - T_c)^{-\gamma} \quad , \quad T > T_c \tag{1.2.3a}$$

$$\sim (T_c - T)^{-\gamma'} \quad , \quad T < T_c \tag{1.2.3b}$$

γ=1.333(15) for Fe, 1.32(2) for Ni. Similarly the specific heat C at h=0 diverges like

$$C \sim (T - T_c)^{-\alpha} \quad , \quad T > T_c \tag{1.2.4a}$$

$$\sim (T_c - T)^{-\alpha'} \quad , \quad T < T_c \tag{1.2.4b}$$

α is -0.12(1) for Fe, -0.10(3) for Ni.

In addition to the thermodynamic exponents above, we can define two other exponents describing the space correlations of the critical spin fluctuations. The correlation function G(x) is defined by

$$G(x) = \langle \delta s(x)\, \delta s(0) \rangle \tag{1.2.5}$$

where s(x) is the local magnetic moment at x and δs is its value

relative to the average. G(x) can be measured for example by inelastic scattering of slow neutrons. One then finds that for large distances x, G(x) varies like

$$G(x) \sim e^{-x/\xi} \quad , \quad x \longrightarrow \infty \qquad (1.2.6)$$

where ξ, the correlation length, measures the range within which spins tend on average to be parallel to each other. The onset of long range order at T_c is marked by the divergence of ξ with a power-law singularity

$$\left.\begin{matrix} \\ \xi \end{matrix}\right\} \sim (T-T_c)^{-\nu} \quad , \quad T > T_c \qquad (1.2.7a)$$

$$\sim (T_c-T)^{-\nu'} \quad , \quad T < T_c \qquad (1.2.7b)$$

with $\nu \simeq 0.7$ for both Fe and Ni. For O(n)-symmetric systems below T_c, ξ so-defined is infinite; instead it can be defined as a crossover length for the behaviour between T=0 and $T=T_c$ (see e.g. Amit 1984).

At $T=T_c$, G(x) falls off much more slowly than exponentially, like

$$G(x) \sim \frac{1}{|x|^{d-2+\eta}} \quad , \quad x \longrightarrow \infty \qquad (1.2.8)$$

where η is very small, about 0.1 for Fe.

Scaling laws

The critical behaviour at T_c therefore is characterised by the nine exponents $\alpha, \alpha', \beta, \gamma, \gamma', \delta, \nu, \nu', \eta$. Apart from the relations

$$\alpha = \alpha' \tag{1.2.9}$$

$$\gamma = \gamma' \tag{1.2.10}$$

and

$$\nu = \nu' \tag{1.2.11}$$

experiments support other relations:

$$\alpha + 2\beta + \gamma = 2 \tag{1.2.12}$$

$$\gamma = \beta(\delta - 1) \tag{1.2.13}$$

$$\gamma = \nu(2 - \eta) \tag{1.2.14}$$

$$d\nu = 2 - \alpha \tag{1.2.15}$$

(1.2.9)-(1.2.15) are called scaling laws. Evidently, only two exponents are independent.

Universality

Also striking is the observed universality of exponent values amongst diverse systems like magnets, alloys and fluids which have different bulk properties and even critical temperatures. Fe and Ni are isotropic ferromagnets with different critical temperatures that share the same critical exponents. However, $YFeO_3$ is a uni-axial magnet which has different exponents from Fe and Ni (it shares the same exponents as those describing the liquid-gas transition), as

have magnets whose moment interactions are restricted to 2-dimensional planes. Thus the internal spin symmetry and the space dimensionality of interactions are relevant to critical behaviour. In addition, a change from short to long-range (dipolar) interactions will alter the exponent values. The implication then is that, modulo these rather general features, critical behaviour is insensitive to the detailed nature of the inter-particle interactions.

The observed scaling laws inspired the powerful scaling hypothesis (section 1.3) whose proper understanding, together with that of universality, became possible by the RG formulation (section 1.4).

1.3 Widom scaling, Kadanoff blocking and the scaling hypothesis

Widom scaling

Widom (1965) found a way to reproduce the scaling laws involving the thermodynamic exponents α', α, β, γ', γ, δ. He hypothesised that near the critical point the singular part of the free energy $F(T,h)$, the part responsible for critical behaviour, is a generalised homogeneous function, i.e.

$$F(\lambda^a t, \lambda^b h) = \lambda F(t,h) \qquad (1.3.1)$$

where $t=(T-T_C)/T_C$ is the reduced temperature. Using standard thermodynamic relations it follows that all the above exponents can be written in terms of the two unknown parameters a and b. This induces relations between the exponents which are just the scaling laws.

Kadanoff blocking

Kadanoff (1966) extended the understanding of scaling laws by giving a physical explanation of (1.3.1) for the Ising model in terms of how a system could behave under a blocking transformation. He was then also able to derive the remaining scaling laws involving the correlation exponents ν, ν', η.

Starting with an Ising model in d-dimensions with nearest-neighbour coupling J and magnetic field h, he imagines dividing the lattice into blocks of side L sites. Near T_c the correlation length is very large, and so if $L<<\xi$ it is assumed that all the spins in a block would be mostly up or down. He then argues that one could treat a block as a single effective spin, again either up or down, and that there exists effective parameters J_L (or t_L) and h_L with which one could write an effective Hamiltonian for the block spins in Ising form.

This means that the free energy per block $f(t_L,h_L)$ has the same functional form as the original free energy per site f(t,h) so that

$$f(t_L, h_L) = L^d f(t, h) \qquad (1.3.2)$$

To get Widom's scaling form from this physical picture, Kadanoff proposed

$$t_L = L^u t \qquad (1.3.3)$$

$$h_L = L^v h \qquad (1.3.4)$$

Then

$$f(L^u t, L^v h) = L^d f(t,h) \tag{1.3.5}$$

which is Widom's hypothesis with $\lambda=L^d$, u=ad, v=bd.

To re-express the magnetic energy $(h \sum_{\text{sites}} s)$ as $(h_L \sum_{\text{blocks}} s_L)$ using (1.3.4), the block-spin s_L must be defined as

$$S_L = L^{-v} \sum_{i \in \text{block}} S_i \tag{1.3.6}$$

Within Kadanoff's block-spin picture it is then easy to derive the following result for the correlation function (1.2.5)

$$G(L^{-1}x, L^u t) = L^{2(d-v)} G(x,t) \tag{1.3.7}$$

valid if x is large. Choosing L=x gives the scaling form

$$G(x,t) = x^{2(v-d)} f(t x^u) \tag{1.3.8}$$

and a comparison with the scaling forms (1.2.6)-(1.2.8) leads to the identifications

$$u = 1/2 \tag{1.3.9}$$

$$v = \frac{1}{2}(2+d-\eta) \tag{1.3.10}$$

Therefore, via u and v, ν and η are related to the thermodynamic exponents and the remaining scaling laws (1.2.14), (1.2.15) follow.

(Kadanoff argued the result $\nu'=\nu$ on slightly weaker grounds in terms of the regularity of $t_L(t)$ at $t=0$). So if we could work out u and v by explicitly constructing the transformations (1.3.3),(1.3.4) then we could calculate all the critical exponents.

Kadanoff blocking exposes the connection between coarse-graining spins and scaling properties at the critical point. However, it involves assumptions that are hard to justify physically. For instance, interactions less direct than between nearest neighbour block-spins would be generated by blocking. Furthermore, a block-spin would behave like an Ising spin only near T=0. Near T_c, spin fluctuations on all length scales up to the correlation length ξ would wash out the discreteness of the block-spin even when $L<<\xi$. Finally, Kadanoff had to assume the special transformations (1.3.3), (1.3.4) in order to recover Widom scaling. On account of these fairly uncontrollable approximations, Kadanoff blocking is not a very useful tool for calculating exponents; as with most real-space techniques, it is difficult to compute systematic corrections. However it does form the basis for Wilson's momentum shell renormalisation group (section 1.4) and provides this with a physically intuitive interpretation in terms of real-space blocking.

Scaling hypothesis

This hypothesis (Fisher 1967) is a more appealing statement of the ideas behind Kadanoff blocking. It states that all singular behaviour comes from the long-range correlation of spin fluctuations near T_c. Mathematically it can be expressed by saying that the divergence of the correlation length ξ is responsible for the singular dependence on $|T-T_c|$ of physical quantities and that ξ is

the only relevant length near T_c; physical quantities depend on $|T-T_c|$ only through their dependence on ξ. The temperature dependence of a physical quantity can then be understood from the way it behaves under a change of length scale, an idea already explicit in Kadanoff blocking.

Scaling laws then follow directly from dimensional analysis. Dimension here is defined in terms of scale transformations. For example, the free energy per site f(t,h) has dimensions of $(\text{length})^{-d}$; in other words, under the scale transformation $x \to x' = \lambda x$, $f \to f' = \lambda^{-d} f$. Dimension so-defined is often called anomalous dimension d_a. In general however, it is not the same as the d_n of naive dimensional analysis; d_a is defined only "locally" i.e. with respect to a particular region of parameter space such as the locale of $T=T_c, h=0$. The exponents u and v defined by the transformations (1.3.3),(1.3.4) are examples of anomalous dimensions near the critical point.

Now if we take h=0, the scaling hypothesis implies f(t)= function of ξ, $F(\xi)$, so that

$$F(\xi/\lambda) = \lambda^{d} F(\xi) \qquad (1.3.11)$$

Putting arbitrary $\lambda = \xi$ gives

$$f(t) = F(\xi) \sim \xi^{-d} \sim t^{d\nu} \qquad (1.3.12)$$

and hence $d\nu = 2-\alpha$, reproducing (1.2.15).

Another example is the magnetisation M below T_c. From the definition of the correlation function (1.2.5) and its behaviour at T_c (1.2.8), we see that at $T=T_c$ and $h=0$ M has anomalous dimension $d_a={}^1/_2(2-d-\eta)$. Thus, according to the scaling hypothesis and analogous to (1.3.12), at criticality the singular behaviour of M arises from the divergence of ξ like

$$M \sim \xi^{\frac{1}{2}(2-d-\eta)} \sim t^{\frac{1}{2}\nu(d-2+\eta)} \qquad (1.3.13)$$

and hence $\beta={}^1/_2\nu(d-2+\eta)$, consistent with (1.2.12),(1.2.14),(1.2.15). Other scaling laws follow similarly, and thus are simply conditions for the consistency of (anomalous) dimensions near the critical point.

The scaling hypothesis already contains the recipe for understanding universality as well. Short-range, system-specific correlations are irrelevant to critical behaviour. In addition, we see that scale-invariance arises at T_c because ξ is infinite and there is no relevant length parameter.

The most successful framework in which to discuss the scaling hypothesis is the RG (section 1.4), which focuses on the behaviour of the correlation length.

1.4 Wilson's "renormalisation group"

Wilson (1971a,1971b) extracted the good physics from Kadanoff blocking. First, the discrete block-spins are replaced by continuous coarse-grained variables $s_L(\underline{x})$ restricted to have fluctuations only

on length scales > L (here, we take s to be a scalar). This may be done by defining

$$S_L(\underline{x}) = \frac{1}{\sqrt{V}} \sum_{|\underline{k}|<\frac{1}{L}} e^{i\underline{k}.\underline{x}} s(\underline{k}) \qquad (1.4.1)$$

in which V is the lattice volume and the $s(\underline{k})$ are Fourier components of the local spin variables $s(\underline{x})$. Then $s_L(\underline{k})$, the Fourier transform of $s_L(\underline{x})$, given by

$$S_L(\underline{k}) = \frac{1}{\sqrt{V}} L^d \sum_{x} e^{-i\underline{k}.\underline{x}} S_L(\underline{x}) \qquad (1.4.2)$$

is zero for $k > 1/L$ (where $k=|\underline{k}|$). Qualitatively, $s_L(\underline{x})$ is the same as a block-spin of size L centred at the point $\underline{x}$. Next, instead of two parameters t_L and h_L, an infinite number of L-dependent parameters is included in the effective Hamiltonian $H_L\{s_L(\underline{x})\}$. Finally, a recursion formula (the RGT) is derived which determines $H_{bL}\{s\}$ from $H_L\{s\}$. The RGT is briefly outlined here.

The renormalisation group transformation R_b

Here we give a short description of what a renormalisation group transformation does. We refer to the large literature on this topic (e.g. Wilson 1971a,1971b, Wilson and Kogut 1974, Ma 1976, Wallace and Zia 1978, Amit 1984) for fuller discussion of the ideas and their implementation in practice.

Consider a large number of probability distributions $\{P\}$ for the $s_L(\underline{x})$. Any distribution is specified by a set of parameters and we can associate each P with a point μ in a parameter space. This parameter space can be defined by the set of all points

$\mu=(u_1,u_2,u_3,....)$ where the u_i are coupling constants specifying the effective Hamiltonian H_L, and then

$$P \propto \exp(-H_L) \tag{1.4.3}$$

A RGT is a transformation R_b from P to P' (represented by μ and μ' respectively) so we write

$$\mu' = R_b \mu \tag{1.4.4}$$

R_b is constructed as a (refined) Kadanoff blocking followed by a scale change by a factor b. The Kadanoff blocking is implemented as an integration of the distribution P over Fourier components $s_L(\underline{k})$ with momenta in the shell $1/bL < k < 1/L$. This downgrades the spatial resolution of spin variations to bL. Then in the scale change, the surviving Fourier components $s_L(\underline{k})$ with $k < 1/bL$ are relabelled $s_L'(\underline{k}')$ by shrinking the system size V by a factor b^d ($\underline{k}'=b\underline{k}$, $V'=V/b^d$) and rescaling the spins by a factor λ_b. Thus the block size remains the same, a fact which is essential to the recovery of scale-invariance. We may then define P' by

$$P' \propto \exp(-H_L') = \left[\prod_{\frac{1}{bL}<k<\frac{1}{L}} \int ds_L(\underline{k}) \exp(-H_L) \right]_{s_L(\underline{k})=\lambda_b s_L'(b\underline{k})} \tag{1.4.5}$$

and then μ' is defined by writing H' in the same form as H. Before rescaling, H' is just a refined version of Kadanoff's effective Hamiltonian for blocks of size bL. The set of R_b ($1<b<\infty$) is called (perversely) the renormalisation group and the group property $R_bR_{b'}\mu = R_{bb'}\mu$ holds only if $\lambda_b=b^y$ for some constant y. It would be more

appropriate to call R_b an "effective coupling transformation" (Ravndal 1976).

Mathematics of R_b

The connection of R_b to critical behaviour is made on studying fixed points μ^* of R_b defined by

$$R_b \mu^* = \mu^* \tag{1.4.6}$$

For μ near μ^* we write $\mu=\mu^*+\delta\mu$ where $\delta\mu$ is small. Then

$$\delta\mu' = R_b^{\ell}\, \delta\mu \tag{1.4.7}$$

If $O(\delta\mu^2)$ terms are ignored $R_b{}^{\ell}$ is a linear operator and in principle we can determine its eigenvalues and eigenvectors. Denoting the eigenvalues of $R_b{}^{\ell}$ by b^{y_j} and the eigenvectors by e_j, we have

$$\delta\mu' = \sum_j t_j\, b^{y_j} e_j \tag{1.4.8}$$

where the t_j are the coefficients in the expansion of $\delta\mu$ in the eigenvectors. Now simplicity arises if for example we suppose $y_1, y_2 > 0$ (all other y_j's < 0) and b is large, then

$$\delta\mu' = t_1 b^{y_1} e_1 + t_2 b^{y_2} e_2 + O(b^{y_3}, \ldots) \tag{1.4.9}$$

If $t_1=t_2=0$, $R_b{}^{\ell}\delta\mu \to 0$ as b increases and so $\mu \to \mu^*$. The subspace $t_1=t_2=0$ defines the critical surface of μ^*, the set of all points pushed to the fixed point by R_b. This is just standard mathematics

of fixed-point analysis.

Physics of R_b

The physics in all this enters as follows. Consider a ferromagnet at temperature T in a magnetic field h. Its parameter space, denoted $\mu(T,h)$, contains couplings which are smooth functions of T and h since they describe local properties of blocks. The crucial assumption linking critical phenomena to R_b is that $\mu(T=T_c,h=0)$ is a point on the critical surface. Then for T close to T_c and h close to 0, the smoothness assumption means that t_1, the distance to the critical surface along the temperature eigenvector e_1, is proportional to $(T-T_c)$, while t_2, the distance to the critical surface along the field eigenvector e_2, is proportional to h. Hence we have

$$\delta\mu' = A(T-T_c)b^{y_t}e_1 + hb^{y_h}e_2 + O(b^{y_3},\ldots) \qquad (1.4.10)$$

Critical exponents are related to the two independent exponents y_t and y_h, properties of the RGT near the fixed point μ^*, as follows.

First, the scale change $\underline{k}'=b\underline{k}$, $s'_L(\underline{k}')=b^{-y}s_L(\underline{k})$ identifies y as the (anomalous) length dimension of $s_L(\underline{k})$. From (1.4.2) we find $s'_L(\underline{x}')=b^{-y+d/2}s_L(\underline{x})$ and so y-d/2 is the length dimension of $s_L(\underline{x})$. In section 1.3 we saw that near criticality M has anomalous dimension $^1/_2(2-d-\eta)$ to get the correct length scaling (1.2.8) of G(x) at T_c. Thus we must choose the special value $y=y^*$ where

$$y^* = \frac{1}{2}(2-\eta) \qquad (1.4.11)$$

to get the correct critical correlation function. Another way of stating this is to say that the fixed point equation (1.4.6) is an eigenvalue equation for eigenvector μ^* and y^* is the special value of y in R_b that admits a solution with eigenvalue 1. The critical exponent η is thus related to the fixed point μ^* of R_b.

In a similar way we see that when $\underline{x}'=\underline{x}/b$ the magnetic field h near criticality must transform to $h'=b^{1/2(2+d-\eta)}h$ in order that the (invariant) magnetic energy $hL^d\sum_x s_L(x)$ may be rewritten $h'L^d\sum_{x'} s_L'(x')$. Comparing with the RGT equation (1.4.10) identifies

$$y_h = \frac{1}{2}(2+d-\eta) \qquad (1.4.12)$$

Finally, the correlation length ξ transforms to $\xi'=\xi/b$ when $\underline{x}'=\underline{x}/b$. Hence from (1.2.7) $t'=b^{1/\nu}t$. Comparing with the RGT equation (1.4.10) identifies

$$y_t = 1/\nu \qquad (1.4.13)$$

The last two equations are exact analogues of the identifications (1.3.9), (1.3.10) of the exponents u,v describing the Kadanoff transformation via (1.3.3),(1.3.4). The exponents $y_3,y_4,\ldots < 0$ of Wilson's RG transformation then describe corrections to Widom scaling, induced by the "irrelevant" eigenvectors $e_3,e_4,\ldots$ (or "marginal" if $y_i=0$).

Scaling and universality from R_b

All the assertions of the scaling hypothesis concerning the dependence of various quantities on $(T-T_c)$ and on h follow from (1.4.10)-(1.4.13). This can be seen as follows.

The distribution P' is equivalent to the distribution P as far as random variables $s_L(\underline{k})$ with $k < 1/bL$ are concerned. For these variables the RGT just represents a change of variables $s \to s'$, $\mu \to \mu'$ in our description (the parameter space) of the physical system, analogous, say, to a transformation to a rotated co-ordinate system useful in other fields of physics. Such transformations are most useful when the Hamiltonian is invariant or else contains a small symmetry-breaking term which transforms in a simple way. The simple form (1.4.10) for the RGT arises when we look at a ferromagnet near $\mu(T_c,0)$ on large length scales. The symmetry here is scale-invariance. It is attained at $\mu(T_c,0)$.

Now we can view (1.4.10) in an active way, as a law of corresponding states which sets up a correspondence between a ferromagnet with couplings μ and the same ferromagnet with different couplings μ' as measured in the same parameter space co-ordinate system. From such a correspondence we can construct the dependence of various quantities on the parameters μ.

For example, the correspondence for magnetisation $M(\mu(T,h))$ takes the form

$$M(\mu(T,h)) = b^{\frac{1}{2}(2-d-\eta)} M(R_b \mu(T,h))$$

$$= b^{\frac{1}{2}(2-d-\eta)} M(\mu^* + A(T-T_c) b^{1/\nu} e_1 + h b^{y_h} e_2 + \dots) \qquad (1.4.14)$$

For $T=T_c$ and $h=0$ we set $b=h^{-1/y_h}$ and as h tends to zero we obtain M

$\sim h^{1/\delta}$ with

$$\delta = \frac{d+2-\eta}{d-2+\eta} \qquad (1.4.15)$$

For $h=0$ and $T=T_c$ we set $b=t^{-\nu}$ and for small $T-T_c$ we obtain $M \sim t^{\beta}$

with

$$\beta = \frac{1}{2}\nu (d-2+\eta) \qquad (1.4.16)$$

(1.4.15),(1.4.16) are consistent with the scaling laws (1.2.12)-(1.2.15).

Indeed, by writing (1.4.10) as

$$\delta\mu' = (b/\xi)^{1/\nu} e_1 + h b^{y_h} e_2 + O(b^{y_3}, \dots) \qquad (1.4.17)$$

we now see explicitly that the dependence of quantities on $(T-T_c)$, via the correspondence $\mu' \leftrightarrow \mu$, is controlled by the simple behaviour of the correlation length $\xi'=\xi/b$ under a change of length scale, as advocated by the scaling hypothesis.

Finally, universality appears naturally within the RG framework. Many different systems at criticality are deemed to be represented by

points on the critical surface, all of which are therefore pushed to the same fixed point μ^* by R_b. Since critical exponents are related to properties of R_b near μ^*, all of these materials share the same critical exponents.

Beyond the universal nature of exponents it becomes clear, however, that the amplitudes of the various asymptotic quantities governing behaviour at the critical point are not universal. Nevertheless, we find as many relations between the amplitudes as between the exponents so that in many cases there are only two of these non-universal amplitudes that are independent. We should stress "universality modulo two scale factors" or "two-scale-factor universality" in qualifying the universality of our description of critical behaviour. Appearing first as a conjecture (Stauffer *et al* 1972), this notion is now understood also within the RG approach which describes the critical behaviour in terms of (usually) two relevant quantities and allows explicit construction of the amplitude relations (see Amit (1984) for example). We will meet examples of non-universal amplitudes in later chapters.

As well as providing an understanding of scaling and universality, Wilson's RG provides a tool for calculating exponent values. However it is very difficult in practice to implement exactly the definition (1.4.5) for R_b and various approximation schemes are usually introduced. One successful perturbative scheme is the ϵ-expansion, outlined in section 1.5 and applied in section 2.3 to a model field theory of critical behaviour in $d=2+\epsilon$ dimensions. A non-perturbative approximation called Wilson's approximate recursion formula will be discussed in section 2.4 and applied in section 2.5

to the XY model in three dimensions.

1.5 Renormalised field theory and critical phenomena

This final review section is a very short discussion of the field theoretic techniques adopted in chapter 2. A detailed discussion can be found in Amit (1984) for example. Without formal definitions etc., all we are going to do here is to introduce the Hamiltonian functional $\mathcal{H}[\underline{\phi}]$ and motivate its relevance to the description of critical behaviour on physical grounds. Following an outline of how the RG à la quantum field theory may be used to control perturbative calculations near the critical point, we will expose the connection with Wilson's RG in critical phenomena. This will set the scene for the perturbative calculation described in section 2.3 which we control using the dimensional regularisation and minimal subtraction scheme of t'Hooft and Veltman (1972).

Field representations of H

To illustrate the ideas, our starting point is the classical Heisenberg model, with an O(n)-symmetric interaction, described by the (zero-field) Hamiltonian

$$H = -\sum_{ij} V_{ij}\, \underline{S}_i \cdot \underline{S}_j \qquad (1.5.1)$$

in which the $\{\underline{S}_i\}$ are unit n-component vectors sitting at the sites i of an infinite d-dimensional lattice; V_{ij} is a short-range positive translationally invariant interaction. n=1 is the Ising model of uniaxial magnets, liquid-gas systems or of binary alloys; n=2 is the XY model of magnets with an easy plane or of superfluid ^{4}He; n=3

describes isotropic ferromagnetism. This model has a phase transition above two dimensions (above one dimension if n=1).

Motivated by the existence of powerful well-developed tools in field theory, one may choose to work with a continuous spin density $\underline{\Phi}(x)$ rather than lattice spins $\underline{S}_i$ ($\underline{x}$ is here abbreviated to x). The lattice structure is ignored to a large extent; its only remnant lies in providing a natural momentum cut-off Λ for the Fourier decomposition of the field $\underline{\Phi}(x)$

$$\underline{\phi}(x) = \int_0^{\Lambda} d^d k \; e^{i k.x} \; \underline{\phi}(k) \qquad (1.5.2)$$

where Λ is of the order of (lattice spacing)$^{-1}$ and $\int_0^{\Lambda} d^d k$ means $\int_{0<k<\Lambda} \frac{d^d k}{(2\pi)^d}$. $\underline{\Phi}(x)$ might be constructed from the $\underline{S}_i$ by coarse-graining over a few lattice spacings. It is here allowed to range from $-\infty$ to $+\infty$ in magnitude.

One possible continuous representation of the Hamiltonian (1.5.1) is given by the Landau expansion

$$\mathcal{H}[\underline{\phi}] = \int d^d x \left\{ \frac{1}{2}(\nabla\phi)^2 + \frac{1}{2} r \phi^2 + \frac{1}{4!} g \phi^4 + \cdots \right\} \qquad (1.5.3)$$

where $(\nabla\phi)^2 = \sum_{i=1}^{d} \sum_{\alpha=1}^{n} (\partial_i \phi_\alpha)^2$, $\phi^2 = \sum_{\alpha=1}^{n} (\phi_\alpha)^2$, $\phi^4 = (\phi^2)^2$ and the dots include terms like ϕ^6, $\phi^2(\nabla\phi)^2$, $(\nabla\phi)^4$, etc. which are to be neglected. (1.5.3) can be derived by an exact Gaussian transformation of (1.5.1) (Hubbard 1972). However, as far as critical behaviour is concerned, the form of (1.5.3) and the neglect of the dots can be motivated by physical considerations as follows.

The lattice Hamiltonian (1.5.1) is invariant under the action of the O(n) group so we construct the field Hamiltonian by including all terms consistent with this symmetry; we get the expansion (1.5.3) in powers of the field and its derivatives. In the critical region $\underline{\phi}(x)$ is small and slowly varying so we keep only the lowest non-trivial powers. The derivative term $^1/_2(\nabla\phi)^2$ mimics the interaction V_{ij} which acts to align the spins (- the factor $^1/_2$ is arbitrary since we can rescale $\underline{\phi}$ without changing the physics). The potential energy density $V(\phi) = {}^1/_2 r\phi^2 + {}^1/_{4!}g\phi^4$ mimics the local potential seen by a coarse-grained spin $\underline{\phi}(x)$ and acts to constrain its magnitude (- the temperature dependence enters through $r(T) \propto (T-T_C)$ whose sign controls the structure of the minima of $V(\phi)$).

Ultimately, neglected terms (representing shorter-range fluctuations and 6-spin, 8-spin etc. interactions of the lattice spins) must be shown to be irrelevant in the RG sense - they represent interactions whose coupling constants tend to zero under the action of R_b. It is the irrelevance of short-range fluctuations to critical behaviour that also motivates the neglect of the lattice structure when the correlation length $\xi >>$ (lattice spacing). We will use the representation (1.5.3) to discuss renormalised field theory. (1.5.3) is an expansion of $\mathcal{H}$ about the disordered state for $T > T_C$. In section 2.3 another equivalent field representation of (1.5:1) called the non-linear σ model will be introduced, which is an expansion of $\mathcal{H}$ about the completely ordered ground state at T=0.

Perturbative calculations

Given a field Hamiltonian $\mathcal{H}[\underline{\phi}]$, quantities of interest such as the correlation functions can be calculated as functional integrals weighted by the Boltzmann probability $\exp(-\mathcal{H})$:

$$G^{(N)}_{\alpha_1 \cdots \alpha_N}(x_1 \cdots x_N) \equiv \langle \phi_{\alpha_1}(x_1) \cdots \phi_{\alpha_N}(x_N) \rangle = \frac{\int D\underline{\phi}\ \phi_{\alpha_1}(x_1) \cdots \phi_{\alpha_N}(x_N)\ e^{-\mathcal{H}[\underline{\phi}]}}{Z} \quad (1.5.4a)$$

where Z is the partition function

$$Z = \int D\underline{\phi}\ e^{-\mathcal{H}[\underline{\phi}]} \quad (1.5.4b)$$

Here $\int D\underline{\phi}$ denotes the functional integral over all field configurations $\underline{\phi}(x)$. Integrals such as (1.5.4) can be evaluated perturbatively by expanding $\exp(-g/4!\,\phi^4)$ in powers of g, using standard Feynman graph techniques to keep track of the terms generated. The rules relating graphs to algebraic expressions are detailed in Amit (1984). Here we only illustrate by example.

Taking n=1, the field propagator is

$G^{(2)}(x,y)$ = 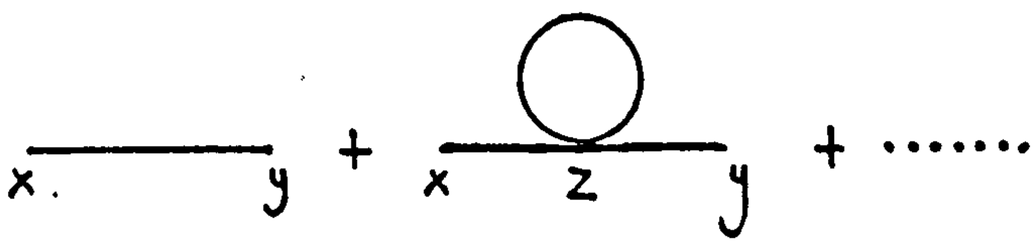 + ...

$$= G_0(x,y) - \frac{g}{4!} \cdot 12 \int d^d z\ G_0(x,z)\, G_0(z,z)\, G_0(z,y) + o(g^2) \quad (1.5.5a)$$

or, in momentum space,

$$G^{(2)}(k) = \quad + \quad + \cdots\cdots$$

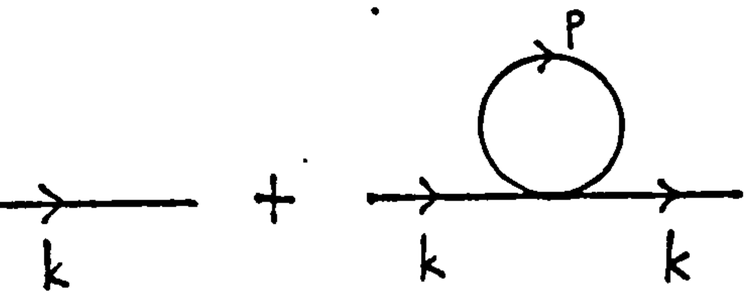

$$= G_0(k) - \frac{g}{4!}.12\, G_0^2(k) \int_0^{\Lambda} d^d p\; G_0(p) + o(g^2) \qquad (1.5.5b)$$

Here $G_0(x,y)$ is the free-field propagator (for the classical or mean-field theory g=0) which is calculable exactly from (1.5.4) as a Gaussian integral. We find that

$$G_0(x,y) = \int_0^{\Lambda} d^d k\; e^{i k.(x-y)} G_0(k) \quad , \quad G_0(k) = \frac{1}{k^2 + r} \qquad (1.5.6)$$

Note that all momentum integrals are cut off by Λ, which appears as the natural momentum scale for all dimensional parameters in $\mathcal{H}$. Naive dimensional analysis shows that

$$[\phi] = \Lambda^{\frac{1}{2}(d-2)} \quad , \quad [r] = \Lambda^2 \quad , \quad [g] = \Lambda^{4-d} \qquad (1.5.7)$$

We find that the expansion of physical quantities near the critical point in powers of g is accompanied by the dimensionless ratios $(\Lambda/r^{1/2})^{4-d}$ or $(\Lambda/q)^{4-d}$. Clearly, d=4 plays a special role. If d < 4 these ratios become large in the critical region; perturbation theory breaks down and the classical theory is invalid. If d > 4 the opposite is true.

Perturbative approach to R_b

Wilson and Kogut (1974) and Wallace and Zia (1978) discuss the implementation of the momentum-shell renormalisation procedure R_b in field theory. Under Kadanoff blocking, the cut-off Λ in (1.5.2)

becomes Λ/b, restored to Λ after rescaling the momenta. The integration of $\exp(-\mathcal{H})$ over the field components $\underline{\phi}(k)$ with $\Lambda/b < k < \Lambda$ can be done perturbatively, in the spirit of (1.5.5). A new Hamiltonian of the form (1.5.3) is calculated and recursion formulae are derived for the parameters r and g. To first order O(g), no new couplings are generated. A non-trivial fixed point (r^*,g^*) of $O(\varepsilon)$ can then be found, where $\varepsilon=4-d$, and a fixed-point analysis as outlined in section 1.4 yields estimates of critical exponents to $O(\varepsilon)$. When $\varepsilon < 0$ the only physical fixed point (with $g^* \geq 0$) is the trivial one $(r^*,g^*)=(0,0)$. The special role of d=4, which we noted above, now becomes apparent in the RG language of fixed points. It is the dimension at (and above) which the exponents take on the classical (mean-field) values associated with the trivial fixed-point $(r^*,g^*)=(0,0)$.

Technically, generating an ε-expansion in this way is not very efficient. For example, at $O(\varepsilon^2)$ a ϕ^6 coupling is generated and the calculation becomes correspondingly more involved. However, this approach has been used in many practical applications (see e.g. Aharony 1976) and forms a bridge between the block-spin approach to renormalisation and the more powerful field theoretic approach, which we discuss now.

Renormalised field theory method

This method makes contact with the RG as first used in quantum field theory (QFT). The field formalism of statistical physics outlined by (1.5.2) *et seq* is very similar to QFT. The former enables a systematic treatment of thermal fluctuations, the latter of quantum fluctuations. In QFT, where one normally works in d=4, we have an

action instead of a Hamiltonian and Green's functions instead of correlation functions. When n=1, (1.5.3) is equivalent to a (Euclidean) $g\phi^4$ model of interacting bosons with (bare) mass $m = r^{1/2}$. We can apply Feynman graph techniques to calculate physical quantities in both these contexts.

However, one important difference is that no natural cut-off Λ exists in QFT. Consequently we should set $\Lambda = \infty$ in QFT. But then the factors $\ln(\Lambda/m)$ or $\ln(\Lambda/q)$ that are found to accompany the expansion of Green's functions in powers of the coupling g are infinite. As we said in section 1.1, the renormalisation group was invented to cope with these ultra-violet (large-momentum) divergences.

To do this, one makes the d=4 theory finite by (for example) putting in a fictitious cut-off Λ by hand. This step is called regularisation. The ultra-violet divergences as $\Lambda\to\infty$ are then absorbed into the definitions of (renormalised) physical parameters m_R and g_R (as well as a new field ϕ_R) such that quantities expressed in terms of m_R, g_R are finite, order by order in perturbation theory, as $\Lambda\to\infty$. This step is the renormalisation. The limit $\Lambda\to\infty$ may now be taken safely. The physical coupling g_R can be defined as the effective coupling at some momentum scale μ. What is important here is that, in describing the physical theory, one is free to choose the momentum scale μ at which g_R is defined.

What relevance has this procedure to critical phenomena? We recall that for $d < 4$, perturbative calculations about the classical theory break down as one encounters the infra-red divergences due to

long-wavelength fluctuations at criticality. Technically, the problem arises because although Λ is the natural momentum scale in the theory, it is far removed from the momentum scales of interest. One encounters the (large) ratios $(\Lambda/r^{1/2})^{4-d}$ or $(\Lambda/q)^{4-d}$ as $r \to 0$ $(T \to T_c)$ and $q \to 0$ with Λ fixed. In QFT where d=4 one encounters $\ln(\Lambda/m)$ or $\ln(\Lambda/q)$ as $\Lambda \to \infty$ with m and q fixed. The analogy is appealing. In perturbation theory we can tame the infra-red divergences of critical phenomena by taming the $\Lambda \to \infty$ limit à la QFT i.e. we renormalise the theory so that it is finite for all $d \leqslant 4$ as $\Lambda \to \infty$, even though we are not really obliged to set $\Lambda = \infty$. $\varepsilon = 4-d$ emerges as a necessary expansion parameter to force the infra-red divergences to appear as expansions in powers of $\varepsilon \ln(\Lambda/r^{1/2})$ or $\varepsilon \ln(\Lambda/q)$ whence they can be dealt with order by order. Calculations then become meaningful via a double expansion in g and ε.

Having done this, we get a controllable perturbation expansion written in terms of the renormalised parameters r_R and $g_R(\mu)$. By choosing μ such that $r_R^{1/2}, q << \mu << \Lambda$, we can eliminate the unphysical strong cut-off dependence (corrections are written in terms of μ/Λ) and μ becomes the natural momentum scale of the renormalised theory. The dimensionless coupling $u_R = \mu^{d-4} g_R$ is the effective coupling at the momentum scale μ. Choosing a different 'momentum scale μ' at which to renormalise the theory corresponds to a RG transformation in the spirit of Wilson's. To effect this, we can parameterise the momentum scale like $\mu = e^{-\tau}\mu_o$; as $\tau \to \infty$ then $\mu \to 0$ and we get the effective coupling on the large length scales in which we are interested.

The critical behaviour of the system is governed by the fixed points u_R^* of this procedure (Brezin *et al* 1976, Amit 1984), which are given by the solutions of

$$\mu\left(\frac{d}{d\mu} u_R\right)\Big|_u = 0 \qquad (1.5.8)$$

analogous to the recursion relations constructed from R_b. The fixed point of interest is the solution approached by $u_R(\mu)$ as $\mu \to 0$ (the "infra-red stable" one). When (1.5.8) is satisfied, the scaling behaviour of correlation functions, critical exponents etc. can be extracted from the renormalisation group equation (see Brezin *et al* 1976, Amit 1984) describing the differential behaviour with respect to μ of the renormalised theory. This version of the RG is computationally more powerful than the perturbative approach to Wilson's R_b - e.g. the equation for g_R does not depend on the ϕ^6 coupling. Finally, in renormalised perturbation theory, universality manifests itself in the independence of the asymptotic behaviour near u_R^* on the initial value of the bare coupling g (within its domain of attraction), and on the particular scheme adopted for renormalising the bare theory.

As an alternative to the cut-off regularisation scheme outlined above, we can use the powerful dimensional regularisation and minimal subtraction scheme of t'Hooft and Veltman (1972), in which integrals are simpler to do because the cut-off Λ is set to ∞ at the beginning. We adopt this scheme in section 2.3; technical details are presented in the context of the calculation there.

1.6 Preview of Chapters 2-4

The rest of this thesis is about various problems involving scale-invariance, to which we can apply the foregoing ideas and techniques. The title is "Configurational studies of scaling phenomena" because the main approach has been to study scaling properties of the patterns that underlie - or show themselves explicitly in - these problems.

In chapter 2 we study the universal scaling properties of configurations of O(n)-invariant block-spins at the critical point of a ferromagnet. These configurations reflect the universal patterns of short-range order (s.r.o.) that underlie observed critical behaviour - "short" on a macroscopic scale, that is - and the aim of our study is to determine their nature.

The behaviour of block-spin configurations is characterised by the probability density function (p.d.f.) for a single block-spin. By exploiting the field theoretic techniques outlined in section 1.5, we obtain the critical scaling properties of this p.d.f. for $n > 2$ and $d=2+\epsilon$ within a perturbative calculation for small ϵ. Then we focus attention on the d=3 XY model (n=2). Wilson (1971b) obtained a non-perturbative approximation to the renormalisation group transformation R_2. Following the work of Bruce (1981) on Ising-like systems, we use this approximation to calculate the p.d.f. at the d=3 XY transition. We then carry out a Monte-Carlo simulation of this model which supports the results of the calculation. We discuss the implications of these results for the nature of the patterns of s.r.o.

Chapter 3 is devoted to a study of scaling in the problem of percolation. Here scaling properties at the percolation threshold are discussed naturally in terms of the underlying cluster geometry. We address a recent controversy regarding the mean number of clusters in d=2, whose currently-accepted scaling behaviour has been challenged by Jug (1984).

Using a specially written fast parallel cluster-counting algorithm, we carry out a numerical study of the mean number of clusters in bond percolation on square lattices and in site percolation on triangular lattices of various sizes up to linear size L=32. Then a finite-size scaling analysis of the data yields evidence in support of the currently-accepted scaling behaviour, as expressed by the critical exponents α_p and ν_p for percolation. Further evidence is obtained from our numerical results for critical amplitudes, which are in excellent agreement with a prediction of the currently-accepted theory, derived using arguments of finite-size scaling and two-scale-factor universality.

Several phenomena, associated with processes of growth and aggregation, lead to the formation of patterns with interesting scaling properties. In chapter 4 we examine a simple model of random epidemic growth first studied by Richardson (1973) who called it G[p]. The parameter p measures the virulence of the epidemic.

From numerical simulations of this model, we find that the growth is characterised by two independent scales, describing the dynamic and static scaling properties of the epidemic interface. The parameter p controls the size of the scaling region. Then we note

that our results are in close agreement with the predictions of a Langevin equation, proposed by Kardar *et al* (1986) as a phenomenological description of a growing interface, and which these authors note can be solved exactly within a dynamical RG treatment for the case d=2 which we have simulated. We discuss the physical content of this equation and thus identify the essential large-distance, long-time physics of the model G[p]. Universal scaling properties of the surface are then understood in terms of the ideas we have set out in chapter 1.

CHAPTER 2

SCALING OF O(N)-INVARIANT BLOCK-SPIN DISTRIBUTIONS

This chapter presents a study of the universal scaling properties of probability distributions for block-spins near a critical point. These distributions carry information about the universal patterns of short-range order (s.r.o.) that underlie observable critical behaviour - "short" on a macroscopic scale, that is - and the aim of our study is to determine their nature. Here we will be working with the O(n)-symmetric model of ferromagnetism introduced in section 1.5.

Section 2.1 explains the motivation for our study more fully and sets up the notation. In section 2.2, in a direct extension of the configurational description of scaling in Ising-like systems (Bruce 1981), we formulate the scaling theory of O(n)-invariant block-spin distributions. A perturbative calculation in section 2.3 for $n > 2$ in $d=2+\varepsilon$ yields an explicit scaling form for the universal block-spin distribution at the critical point T_c of $O(\varepsilon)$. We interpret the result and extend the calculation of the first two non-trivial moments to $O(\varepsilon^2)$. The limitations of such a calculation are discussed.

In section 2.4, following Bruce (1981), an approximate non-perturbative renormalisation group (RG) recursion formula is derived for the block-spin distribution, and is applied to the d=3 XY model (n=2) in section 2.5. Its fixed-point solution is

non-Gaussian, indicating the presence of non-trivial patterns of s.r.o. at criticality, but it does not reveal their nature. A Monte-Carlo simulation of this model is reported in section 2.6, which reproduces the result of the previous section remarkably well. We conclude that a future investigation should consider some angular description of the spin configurations. Section 2.7 summarises our study and discusses the possible role played by topological excitations at the d=3 XY transition.

2.1 Introduction to block-spin distributions

In chapter 1 we saw how scaling and universality play central roles in the successful description of critical phenomena. The RG provides the mathematical framework in which these ideas appear naturally, as properties of a RG transformation near its fixed point.

A deeper physical understanding of scaling and universality begins with the realisation that the critical point is not characterised by the behaviour of local co-ordinates (spins) - seen at length scales comparable with the lattice spacing - but rather by the collective behaviour of large aggregates (block-spins) of local co-ordinates - seen at length scales L>>lattice spacing. One might then postulate that the universal aspects of critical point singularities are reflections of universal aspects of the underlying collective co-ordinate configurations, and that scale-invariance at criticality is a reflection of a (statistical) self-similarity within such coarse-grained pictures.

To formulate this idea mathematically, we describe the local spins using the field representation $\underline{\Phi}(\underline{x})$ introduced in section 1.5 and then describe the collective critical behaviour by a coarse-grained field configuration $\underline{\Phi}_L(\underline{x})$, where L is the spatial resolution to which we have coarse-grained.

In chapter 1, in the context of lattice spins, we met two qualitatively similar definitions of coarse-grained co-ordinates. Following Kadanoff, as in (1.3.6), we may define

$$\underline{\phi}_L(\underline{x}) = a_L \int_{V(L)} d\underline{y}\ \underline{\phi}(\underline{y}) \qquad (2.1.1)$$

where V(L) is a hyperspherical block of radius L centred on the point $\underline{x}$, and a_L is a scale factor left arbitrary for the moment. If we choose $a_L = V(L)^{-1}$ then $\underline{\Phi}_L(\underline{x})$ is just the instantaneous value of the local spin field spatially averaged over the block V(L).

Alternatively, following Wilson as in (1.4.1), we may choose to define

$$\underline{\phi}_\Lambda(\underline{x}) = a_\Lambda \int_0^\Lambda d^d k\ e^{i\underline{k}.\underline{x}}\ \underline{\phi}(\underline{k}) \qquad (2.1.2)$$

where a_Λ is another scale factor, the set $\{\underline{\Phi}(\underline{k}),\ |\underline{k}|<\Lambda_o\}$ are Fourier components of the local spin field $\underline{\Phi}(\underline{x})$, and the integral is over the hyperspherical Brillouin zone of radius Λ. As already noted in section 1.4, the two representations are physically similar if we identify $\Lambda \sim 1/L$ (Bruce 1981). Definition (2.1.1) is adopted in section (2.3) where calculations are done in configuration space. Definition (2.1.2) is adopted for the derivation of the RG recursion

formula described in section 2.4.

Now the statistical behaviour of $\underline{\Phi}_\Lambda$ (or of $\underline{\Phi}_L$) may be characterised by the probability density function (p.d.f.) $P_\Lambda(\underline{\Phi})$ (or $P_L(\underline{\Phi})$), by which we mean the joint p.d.f. $P_\Lambda(\phi_1,.....,\phi_n)$ of components of a single block-spin $\underline{\Phi}_\Lambda$. Alternatively, exploiting the O(n) symmetry of the spin interactions, one can instead consider $P_\Lambda(\phi^2)$ where $\phi^2 = \sum_{\alpha=1}^{n} (\phi_\alpha)^2$. In the symmetric phase $T > T_C$ where the O(n) symmetry is manifest, $P_\Lambda(\underline{\Phi})$ is a function of $|\underline{\Phi}|$ alone and these two distributions are related via

$$P_\Lambda(\phi^2) = \frac{1}{2} S_n (\phi^2)^{\frac{n-2}{2}} P_\Lambda(\underline{\phi}) \qquad (2.1.3)$$

where $S_n = 2\pi^{n/2}/\Gamma(n/2)$ is the surface area of the unit sphere in n dimensions. Even for $T<T_C$, $P_\Lambda(\phi^2)$ is useful because it can be meaningfully compared to the distributions $P_\Lambda^{(V)}(\phi^2)$ in finite systems of volume V for which there is no spontaneous magnetisation M but where the symmetrised moment $\langle|\underline{\Phi}_\Lambda|\rangle \to M$ as $V\to\infty$. The universal features we wish to study are expected to emerge in these distributions when Λ^{-1} and ξ are large.

It is useful to introduce the dimensionless ratio of moments

$$G_\Lambda = 1 - \frac{1}{2} n \left[\frac{\langle (\phi_\Lambda^2)^2 \rangle}{\langle \phi_\Lambda^2 \rangle^2} - 1 \right] \qquad (2.1.4)$$

G_Λ ranges from 0 to 1 according to whether the symmetric distribution $P_\Lambda(\phi^2)$ lies in the "Gaussian" (disordered) regime

$$P_\Lambda(\phi^2) = \frac{1}{2} S_n (\phi^2)^{\frac{n-2}{2}} (2\pi)^{-\frac{n}{2}} e^{-\frac{1}{2}\phi^2} \qquad (2.1.5a)$$

or the "δ-function" (ordered) regime

$$P_\Lambda(\phi^2) = \delta(\phi^2 - 1) \qquad (2.1.5b)$$

and thus effectively characterises the nature of the block-spin amplitude fluctuations. In (2.1.5) we have made specific (and different) choices for the scale factor a_Λ. We will discuss choices for a_Λ in the next section.

Finally, we note some relations between moments of the block-spin p.d.f.'s and thermodynamic observables. It is clear from the block-spin definitions (2.1.1) and (2.1.2) that the moments $\langle \underline{\phi}_\Lambda \rangle$ and $\langle \underline{\phi}_L \rangle$ are simply related to the magnetisation $\underline{M}$ by

$$\langle \underline{\phi}_\Lambda \rangle = a_\Lambda \underline{M} \quad , \quad \forall \Lambda \qquad (2.1.6)$$

and

$$\langle \underline{\phi}_L \rangle = a_L V(L) \underline{M} \quad , \quad \forall L \qquad (2.1.7)$$

Then we note the following connection between the limiting behaviour of the moment $\langle \phi_\Lambda^2 \rangle$ as $\Lambda \to 0$ and the susceptibility of the system. The definition (2.1.2) implies

$$\langle \phi_\Lambda^2 \rangle = \sum_{\alpha=1}^{n} a_\Lambda^2 \int_0^\Lambda d^d k \; G^{(2)}_{\alpha\alpha}(k) \qquad (2.1.8)$$

where the correlation function $G_{\alpha\alpha}^{(2)}(k)$ is defined by (1.5.4) in Fourier space, and we have used translational invariance to do one momentum integration. Restricting our attention to $T > T_c$, the

zero-field isotropic susceptibility χ is given by the fluctuation theorem

$$\chi = \sum_{\alpha=1}^{n} G^{(2)}_{\alpha\alpha}(k=0) \qquad (2.1.9)$$

Consequently, in (2.1.8) we expand $G_{\alpha\alpha}{}^{(2)}(k)$ for small k and, providing Λ is small, we may keep only the leading term k=0 to get the relation

$$\lim_{\Lambda\to 0} \langle \phi_\Lambda^2 \rangle = q_\Lambda^2 \frac{S_d}{(2\pi)^d} \frac{\Lambda^d}{d} \chi \qquad (2.1.10)$$

The analogous result for $\langle \phi_L{}^2 \rangle$ is simply

$$\lim_{L\to\infty} \langle \phi_L^2 \rangle = q_L^2 \, S_d \, \frac{L^d}{d} \chi \qquad (2.1.11)$$

We are going to use these results in the following section.

2.2 Scaling theory

Here we discuss the scaling behaviour of the distributions and their moments near criticality. To express the idea, discussed in section 2.1, regarding the scaling and universal aspects of the coarse-grained configurations $\underline{\phi}_\Lambda(\underline{x})$ when Λ^{-1} and ξ are large, we write the following scaling form for $P_\Lambda(\underline{\phi})$ as Λ^{-1} and $\xi \to \infty$.

$$P_\Lambda(\underline{\phi}) = c_\Lambda^n \, \tilde{P}^{(\pm)}(c_\Lambda \underline{\phi}, \Lambda^{-1}/\xi) \qquad (2.2.1a)$$

$$c_\Lambda = a_0 \, a_\Lambda^{-1} \, \Lambda^\theta \qquad (2.2.1b)$$

in which scaling arises when we choose a power-law form for a_Λ. a_0 is a non-universal constant included to take account of the non-universality of the scale of spin co-ordinates. θ is related to the critical exponent η (see (2.2.4) below). $\tilde{p}^{(\pm)}(\underline{z},\Lambda^{-1}/\xi)$ is a universal p.d.f. for $\underline{z}$ - the superscripts $(\pm)$ refer to the cases $T \to T_c^{\pm}$ respectively. It is written as a function of Λ^{-1}/ξ ($\sim L/\xi$) to take account of the non-universality of the scale of space co-ordinates - we mean that, for assemblies within the same universality class, configurations are statistically similar only when their correlation lengths are equal as measured on the scale of their respective block sizes. We recall the idea of "universality modulo two scale factors" mentioned in section 1.4.

We may take (2.2.1) as a scaling ansatz for coarse-grained configurations near criticality. It is equivalent to scaling assumptions for the multi-spin correlation functions $G_{\alpha_1 \ldots \alpha_N}^{(N)}(x_1,\ldots,x_N)$ which enter the moments of $P_\Lambda(\underline{\phi})$ as in (2.1.8), and therefore its universal structure can be justified from RG arguments (Bruce 1981). Using (2.2.1) it is easy to show that the following scaling forms hold for the moments $\langle(\phi_\Lambda{}^\alpha)^m\rangle$ and the ratio G_Λ

$$\langle (\phi_\Lambda^\alpha)^m \rangle = C_\Lambda^{-m} \tilde{f}^{(\pm)}(\Lambda^{-1}/\xi) \qquad (2.2.2)$$

$$G_\Lambda = \tilde{G}^{(\pm)}(\Lambda^{-1}/\xi) \qquad (2.2.3)$$

where $\tilde{f}^{(\pm)}{}_m$ and $\tilde{G}^{(\pm)}$ are universal functions. When $T>T_c$, by matching the asymptotic form of (2.2.2) for $m = 2$, $\Lambda \to 0$ to the result (2.1.10), in which we put $\chi \sim \xi^{2-\eta}$ for large ξ, we identify

the exponent θ of (2.2.1b) as

$$\theta = \frac{1}{2}(2-d+\eta) \tag{2.2.4}$$

When $T<T_c$ and $n > 1$, the zero-field susceptibility (longitudinal or transverse) is infinite (Brezin and Wallace 1973) so we cannot exploit the relation equivalent to (2.1.10) for the connected moment. Instead, we exploit (2.1.6) in which $M \sim \xi^{1/2(2-d-\eta)}$ for large ξ, to recover the same identification (2.2.4) for θ when $T<T_c$.

We now discuss choices for the scale factor a_Λ, until now left arbitrary. Near T_c, for the purposes of deriving a RG recursion formula for $P_\Lambda(\underline{\Phi})$ in section 2.4, it will be convenient to choose

$$a_\Lambda = \Lambda^{\frac{1}{2}(2-d-\eta)} \tag{2.2.5}$$

since we will have $c_\Lambda=a_0$, independent of Λ, and then $P_\Lambda(\underline{\Phi})$ takes the simpler form

$$P_\Lambda(\underline{\phi}) = a_0^n \, \tilde{P}^{(\pm)}(a_0\underline{\phi}\,, \Lambda^{-1}/\xi) \tag{2.2.6}$$

in which the dependence on Λ enters only via the ratio Λ^{-1}/ξ. The moments (2.2.2) then become functions of Λ^{-1}/ξ alone, universal up to the arbitrary choice for the constant a_0 (- which may be taken in order that $\langle\phi_\Lambda^2\rangle=n$, for example). Hence as $\xi\to\infty$, P_Λ tends to a universal fixed-point distribution P^* independent of Λ, which characterises the universal configurations of short-range order at the critical point. In this limit, $G_\Lambda\to G^*$, a universal constant.

To illuminate this choice, note that the scaling form for $P_L(\underline{\Phi})$ analogous to (2.2.1a) may be written with the replacements $c_\Lambda \to c_L = a_o a_L^{-1} L^{\bar{\theta}}$ and $\Lambda^{-1} \to L$. Via (2.1.7) and (2.1.11), this leads to the identification $\bar{\theta} = -{}^1/_2(2+d-\eta)$. When expressed in terms of a_L, the choice (2.2.5) therefore becomes

$$a_L = L^{-\frac{1}{2}(2+d-\eta)} \tag{2.2.7}$$

Then the definition (2.1.1) for $\underline{\phi}_L$ is entirely consistent with the definition of the Kadanoff block-spin via (1.3.6),(1.3.10) and with the special choice (1.4.11) for y^* required for convergence of the Hamiltonian to a fixed point under Wilson's transformation R_b.

In other contexts (when we do not know a priori the value of η, for example) we may choose $a_L = V(L)^{-1} \sim L^{-d}$ which leads to the scaling form

$$P_L(\underline{\phi}) = (b_o L^{\beta/\nu})^n \tilde{P}^{(\pm)}(b_o L^{\beta/\nu} \underline{\phi}, L/\xi) \tag{2.2.8}$$

This choice then allows the determination of the exponent ratio $\beta/\nu = {}^1/_2(d-2+\eta)$ via the large-L dependence of moments of $P_L(\underline{\Phi})$ as $L/\xi \to 0$ (Binder 1981).

Finally, from (2.2.8) and the relation (2.1.3), the equivalent scaling form for the symmetric distribution $P_L(\phi^2)$ follows directly when $T > T_c$. A similar scaling form for $T < T_c$ can also be argued from (2.2.8). The result may then be written

$$P_L(\phi^2) = c_o L^{2\beta/\nu} \tilde{P}^{(\pm)}(c_o L^{2\beta/\nu} \phi^2, L/\xi) \tag{2.2.9}$$

We shall obtain such a scaling form explicitly as the result of the calculation described in the next section.

2.3 A perturbative calculation for $n > 2$ and $d = 2 + \varepsilon$

When $n > 2$ and dimension $d > 2$, the O(n)-symmetric spin system with Hamiltonian (1.5.1) spontaneously magnetises in the temperature range $0<T<T_c(d)$ where $T_c(d) \to 0$ as $d \to 2$ (Mermin and Wagner 1966). Close to two dimensions - we write $d=2+\varepsilon$ - we can develop an ε-expansion for critical properties as an expansion in powers of T that leads to a $T_c=O(\varepsilon)$ (Brezin and Zinn-Justin 1976). We are going to do this here to $O(\varepsilon)$ for the O(n)-symmetric block-spin p.d.f. $P_L(\phi^2)$ and to $O(\varepsilon^2)$ for the ratio of moments G_L (cf. equation (2.1.4)), in an attempt to describe critical coarse-grained configurations in low dimensions. The reason for choosing $P_L(\phi^2)$ in preference to $P_L(\underline{\phi})$ is a technical point which will become apparent when we discuss infra-red divergences in perturbation theory.

Since our calculations will be done in configuration space, we start with the block-spin $\underline{\phi}_L$ defined by (2.1.1), and calculate the block-spin p.d.f. $P_L(\phi^2)$ via

$$P_L(\phi^2) = \int_{-\infty}^{+\infty} \frac{dh}{2\pi} e^{-ih\phi^2} \tilde{P}_L(h) \qquad (2.3.1)$$

in which the characteristic function $\tilde{P}_L(h) = \langle e^{ih\phi_L^2} \rangle$ has an expansion in cumulants of the block-spin p.d.f.:

$$\tilde{P}_L(h) = \exp\left[\sum_{k=1}^{\infty} \frac{(ih)^k}{k!} C_k \right] \qquad (2.3.2)$$

C_k denotes the cumulant $\langle(\phi_L{}^2)^k\rangle_c$ which is given in terms of the unconnected moments $\mu_k=\langle(\phi_L{}^2)^k\rangle$ by

$$\frac{C_k}{k!} = \sum_{q=1}^{k} \frac{(-1)^q}{q} \sum_{k_1\cdots k_q=1}{}' \prod_{i=1}^{q} \frac{\mu_{k_i}}{k_i!} \qquad (2.3.3)$$

where $\sum'$ indicates a sum restricted to terms with $\sum_{i=1}^{q} k_i=k$. From (2.1.1), μ_k is given in terms of the local field $\underline{\phi}$ by

$$\mu_k = V(L)^{-2k}\left(\prod_{i=1}^{k}\int_{V(L)} d\underline{x}_i \int_{V(L)} d\underline{y}_i\right)\left\langle \prod_{i=1}^{k} \underline{\phi}(x_i)\cdot\underline{\phi}(y_i)\right\rangle \qquad (2.3.4)$$

where we have chosen the scale factor a_L to be $V(L)^{-1}$; as discussed in section 2.2, this will lead to the explicit appearance of β/ν in the scaling form for $P_L(\phi^2)$ (cf. (2.2.9)). Then we proceed by calculating the local field average $\langle\ldots\ldots\rangle$ as an expansion in powers of T.

Non-linear σ-model

In order to carry out this expansion, we use a field representation of the lattice model (1.5.1) called the non-linear σ-model (see Amit (1984) for a general discussion) whose partition function $Z[\underline{\phi}]$ and Hamiltonian $\mathcal{H}[\underline{\phi}]$ are given by

$$Z[\underline{\phi}] \sim \int D\underline{\phi}\ \delta(\phi^2-1)\ \exp(-\mathcal{H}) \qquad (2.3.5a)$$

$$\mathcal{H}[\underline{\phi}] = \frac{1}{T}\int d^dx \left\{\frac{1}{2}(\nabla\phi)^2 + \ldots\ldots\right\} \qquad (2.3.5b)$$

(2.3.5b) can be derived as the long-distance; low-temperature limit of (1.5.1) (Brezin and Zinn-Justin 1976). As in the ϕ^4 representation, the term $^1/_2(\nabla\phi)^2$ mimics the interaction V_{ij} and the

dots refer to irrelevant (in the RG sense) higher-order derivatives; the local potential $V(\underline{\phi})$ is replaced by the O(n)-invariant constraint $\phi^2=1$ to express the belief that at low temperatures, fluctuations in phase play a more important role than fluctuations in amplitude in the destruction of long-range order. The temperature appears explicitly in (2.3.5b), allowing the expansion in powers of T to proceed as a standard loop expansion (Amit 1984).

Low-temperature expansion

In the ordered phase the lattice spins $\underline{S}_i$ fluctuate around the direction of spontaneous magnetisation and at low temperatures these fluctuations are small. It is then natural to write the vector $\underline{\phi}$ as $(\underline{\pi},\sigma)$, where the (n-1)-component vector $\underline{\pi}$ represents the fluctuations transverse to the direction of spontaneous magnetisation $\langle\sigma\rangle$, and to expand in powers of $\underline{\pi}$ (Migdal 1975, Polyakov 1975, Brezin and Zinn-Justin 1976).

First, the field σ is integrated out of (2.3.5) using the constraint $\sigma=\sqrt{1-\pi^2}$. Next, we rescale $\underline{\pi}\to T^{1/2}\underline{\pi}$, so that now

$$\underline{\phi} = \left(T^{\frac{1}{2}}\underline{\pi},\ \sqrt{1-T\pi^2}\right) \qquad (2.3.6)$$

Finally, we expand the partition function in powers of $T\pi^2$. To O(T) the result is

$$Z[\underline{\phi}] \sim \int D\underline{\pi}\ \exp(-\mathcal{H}) \qquad (2.3.7a)$$

$$\mathcal{H}[\underline{\phi}] = \int d^dx \left\{ \tfrac{1}{2}(\nabla\pi)^2 + \tfrac{1}{2}T\left(\underline{\pi}.\nabla\underline{\pi}\right)^2 + O(T^2)\right\} \qquad (2.3.7b)$$

Note that we have discarded the factor $(1-\pi^2)^{-1/2}$ which appears with $\int D\underline{\pi}$ to make the O(n)-invariant measure $\int D\underline{\phi}$. This will be discussed shortly. Using (2.3.7) we calculate the local field average in (2.3.4) by a standard loop expansion in the interaction of O(T).

UV divergences, IR finiteness

At and above two dimensions, we encounter ultra-violet (UV) divergences when we do this, unless we retain a cut-off Λ. But, as outlined in section 1.5, their elimination by renormalisation is a powerful way to analyse the critical behaviour near T_c, where effectively $\Lambda=\infty$ at the momentum scales of interest. Brezin and Zinn-Justin (1976) adopt the cut-off regularisation.

It is computationally less cumbersome, however, if we adopt the dimensional regularisation and minimal subtraction scheme (t'Hooft and Veltman 1972). Since the renormalisation calculations for the non-linear σ-model are presented and discussed in the papers by McKane and Stone (1980) and Amit and Kotliar (1980), we outline the scheme for the present calculation only very briefly.

In dimensional regularisation, the cut-off Λ is set to ∞ and a regularisation is provided by choosing a low enough dimension where integrals are UV convergent (i.e. $d < 2$). Then one analytically continues to the values of d of interest (i.e. $d > 2$). The UV divergences as $\varepsilon \to 0$ appear as ε-poles.

To see this in action in the present problem, we calculate μ_k of (2.3.4) to lowest order in T. Using (2.3.6), the local field average in (2.3.4) is expanded in powers of $T\pi^2$ to generate averages of

$\underline{\pi}$-fields. With the free $\underline{\pi}$-propagator for (2.3.7b)

$$G_o(x-y) = \int_o^\infty d^d k \quad \frac{e^{ik.(x-y)}}{k^2} \tag{2.3.8}$$

we find

$$\mu_k = V(L)^{-2} \int_{V(L)} d\underline{x} \int_{V(L)} d\underline{y} \quad \lambda_k(T; x-y) \tag{2.3.9}$$

in which

$$\lambda_k(T; x-y) = 1 + k(n-1)T\left[G_o(x-y) - G_o(0)\right] + o(T^2) \tag{2.3.10}$$

In this simple calculation we have included no interactions. As emphasised by McKane and Stone (1980), the calculation of configuration-space correlation functions to $O(T^\ell)$ is achieved by evaluating only $(\ell-1)$-loop graphs.

The subtracted propagator $G_o(x-y)-G_o(0)$ is UV divergent for $d > 2$. In dimensions $d < 2$ in which it is convergent it has value

$$G_o(x-y) - G_o(0) = \frac{S_d^{-1}}{\varepsilon |x-y|^\varepsilon} \tag{2.3.11}$$

We then take the RHS as the analytic continuation of the LHS to all ε. The UV divergence as $\varepsilon \to 0$ appears as a simple ε-pole.

The minimal subtraction scheme eliminates this pole as follows. When the $|x-y|^{-\varepsilon}$ in (2.3.11) is expanded in powers of $\varepsilon \ln|x-y|$ and the renormalised quantities $\lambda_k{}^R$ and (dimensionless) T_R are defined at momentum scale μ by

$$\lambda_k^R(T_R;\mu(x-y)) = Z_2^{-k}\,\lambda_k(T;x-y) \tag{2.3.12a}$$

$$T_R = \mu^{\varepsilon} Z_1^{-1} T \tag{2.3.12b}$$

we choose $Z_1(T_R,\varepsilon)$ and $Z_2(T_R,\varepsilon)$ to eliminate all poles on the RHS of (2.3.12a) at each order in T_R.

The choices (McKane and Stone 1980)

$$Z_1 = 1 + O(T_R) \tag{2.3.13a}$$

$$Z_2 = 1 + \frac{(n-1)T_R}{\varepsilon} + O(T_R^2) \tag{2.3.13b}$$

accomplish this to $O(T_R)$, giving the finite expression

$$\lambda_k^R(T_R;\mu(x-y)) = 1 - k(n-1)T_R \ln\mu|x-y| + O(\varepsilon T_R, T_R^2, \varepsilon^2) \tag{2.3.14}$$

as a double expansion in T_R and ε.

At this point we remark that the factor $(1-\pi^2)^{-1/2}$ that should appear in the measure of (2.3.7a) can be exponentiated into a term in $\mathcal{H}[\underline{\phi}]$ (see Amit 1984) proportional to the quadratically-divergent integral

$$\int_0^\infty d^dk = \int_0^1 d^dk + \int_1^\infty d^dk \tag{2.3.15}$$

The second term on the RHS, when evaluated in $d < 0$ and continued to $d > 0$, cancels the first term, so the factor $(1-\pi^2)^{-1/2}$ can be discarded in dimensional regularisation.

We also remark that since we are expanding about a state of broken O(n) symmetry, we expect (Goldstone 1961) additional IR divergences to arise from the massless $\underline{\pi}$-propagator (2.3.8) - in statistical physics language, $\underline{\pi}$ represents spin-wave fluctuations at low temperatures and zero-mass corresponds to their infinite susceptibility below T_c. Note however that the expression (2.3.10) for $\lambda_k(T;x-y)$ is actually IR finite even for $d < 2$ because it is the subtracted propagator $G_o(x-y)-G_o(0)$ that appear's in the perturbation series. This persists to higher orders, as we shall see, and is a consequence of Elitzur's theorem (Elitzur 1979) which states that O(n)-invariant quantities are IR finite, order by order in perturbation theory. It is for this reason that we focus our efforts on the symmetric p.d.f. $P_L(\phi^2)$; the calculation of $P_L(\underline{\phi})$ encounters IR divergences unless an extra ad hoc IR regulator is retained throughout the calculation. (Brezin and Zinn-Justin 1976).

One-loop expressions

In order to locate the critical temperature T_c to $O(\epsilon)$ we need to renormalise the theory to $O(T^2)$ (one loop). The extension of (2.3.10) to $O(T^2)$ is straightforward. The 4-point interaction of O(T) in (2.3.7b) is now to be included. Figure (2.1) shows the graphs which appear to this order with the corresponding algebraic expressions. We have neglected quadratically-divergent graphs in the manner of equation (2.3.15)..

Evaluating the graphs, we find

$$\mu_k = V(L)^{-4}\left(\prod_{i=1}^{2}\int_{V(L)} d\underline{x}_i \int_{V(L)} d\underline{y}_i\right) \Lambda_k(T; x_1 \cdots y_2) \qquad (2.3.16)$$

$(n-1)G_o(x_1-y_1)$

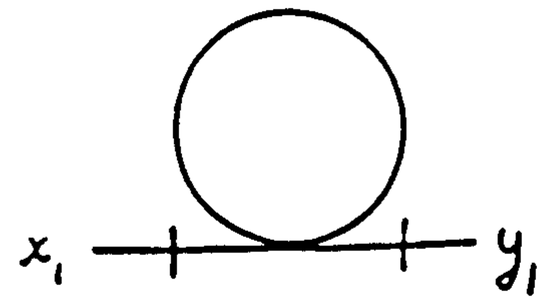

$(-1/2T)2(n-1)G_o(x_1-y_1)G_o(0)$

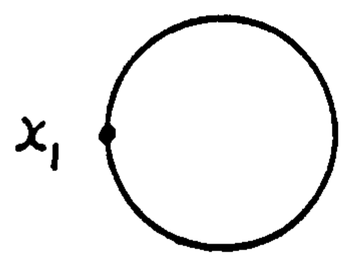

$(n-1)G_o(0)$

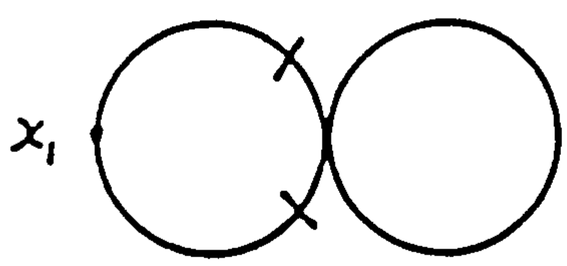

$(-1/2T)2(n-1)G_o(0)^2$

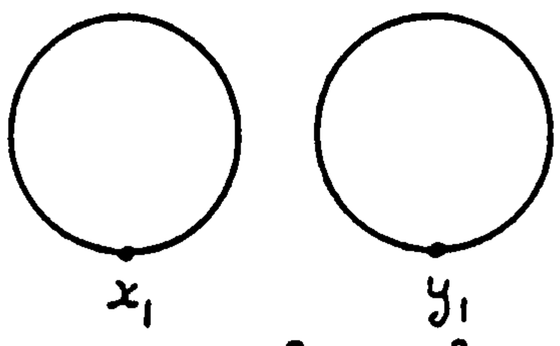

$(n-1)^2G_o(0)^2$

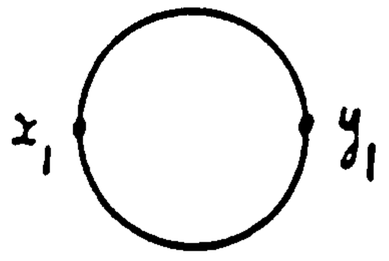

$2(n-1)G_o(x_1-y_1)^2$

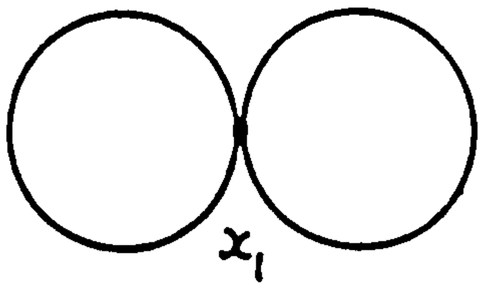

$[(n-1)^2+2(n-1)]G_o(0)^2$

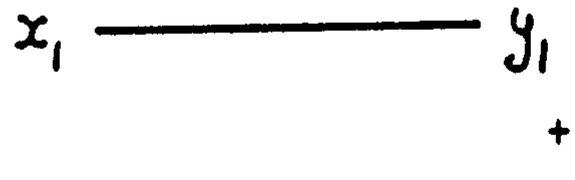

+ 2 perms.

$(n-1)^2G_o(x_1-y_1)G_o(x_2-y_2)$
$+(n-1)G_o(x_1-x_2)G_o(y_1-y_2)$
$+(n-1)G_o(x_1-y_2)G_o(x_2-y_1)$

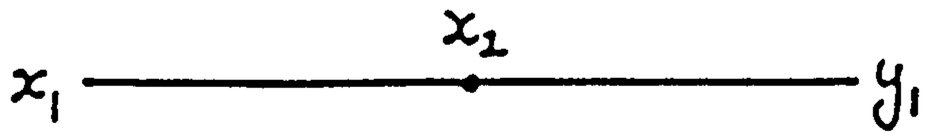

$2(n-1)G_o(x_1-x_2)G_o(x_2-y_1)$

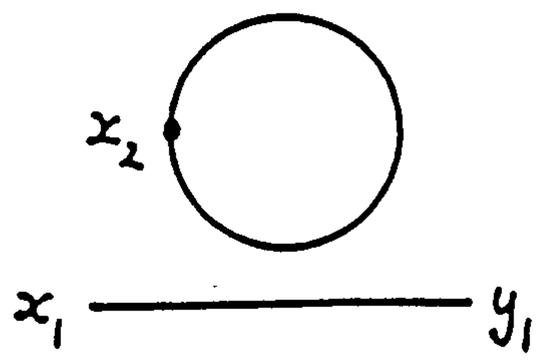

$(n-1)^2G_o(x_1-y_1)G_o(0)$

FIGURE (2.1). Graphs contributing to $\Lambda_k(T;x_1,x_2,y_1,y_2)$ at one loop [$O(T^2)$] and corresponding algebraic expressions; a slashed line is a field derivative at the O(T) interaction vertex.

in which

$$\Lambda_k(T; x_1 \cdots y_2) = 1 + k(n-1)T\,\tilde{G}_0(x_1-y_1) + \tfrac{1}{2}k(n-1)T^2\,\tilde{G}_0(x_1-y_1)^2 + \binom{k}{2}(n-1)^2T^2\,\tilde{G}_0(x_1-y_1)\tilde{G}_0(x_2-y_2) + \tfrac{1}{2}\binom{k}{2}(n-1)T^2\left[\tilde{G}_0(x_1-x_2)+\tilde{G}_0(y_1-y_2)-\tilde{G}_0(x_2-y_1)-\tilde{G}_0(x_1-y_2)\right]^2 + O(T^3) \qquad (2.3.17)$$

where $\tilde{G}_0(x-y)$ denotes the subtracted propagator $G_0(x-y)-G_0(0)$. As advertised, this expression is manifestly IR finite. It is of course UV divergent for $d > 2$. Renormalisation of Λ_k proceeds as for its lowest order version λ_k. The extension of (2.3.13) to next order is (McKane and Stone 1980)

$$Z_1 = 1 + (n-2)\frac{T_R}{\varepsilon} + O(T_R^2) \qquad (2.3.18a)$$

$$Z_2 = 1 + (n-1)\frac{T_R}{\varepsilon} + (n-1)(n-\tfrac{3}{2})\frac{T_R^2}{\varepsilon^2} + O(T_R^3) \qquad (2.3.18b)$$

yielding the finite expression

$$\Lambda_k^R(T_R; \mu x_1 \cdots \mu y_2) = 1 - k(n-1)T_R \ln\mu|x_1-y_1| + \tfrac{1}{2}k(n-1)(T_R^2+\varepsilon T_R)\ln^2\mu|x_1-y_1| + \binom{k}{2}(n-1)^2T_R^2\ln\mu|x_1-y_1|\ln\mu|x_2-y_2| + \tfrac{1}{2}\binom{k}{2}(n-1)T_R^2\left[\ln\mu|x_1-x_2|+\ln\mu|y_1-y_2|-\ln\mu|x_2-y_1|-\ln\mu|x_1-y_2|\right]^2 + O(T_R^3, T_R^2\varepsilon, T_R\varepsilon^2, \varepsilon^3) \qquad (2.3.19)$$

The critical temperature T_c in $d=2+\varepsilon$ dimensions is identified with the fixed point coupling T_R^*. In analogy with (1.5.8), it is given by the solution of

$$\mu\left(\frac{d}{d\mu}\, T_R(T,\mu)\right)\Big|_T = 0 \qquad (2.3.20)$$

The non-trivial solution is actually IR unstable - in contrast to the remarks in section 1.5 - but here the difference is because the coupling constant is the temperature, which is naturally a relevant variable (Amit 1984). From (2.3.12b) and (2.3.18a) one finds

$$T_c = \frac{\varepsilon}{n-2} + O(\varepsilon^2) \qquad (2.3.21)$$

The results

It is now possible to derive an explicit form for $P_L^*(\phi^2)$ to $O(\varepsilon)$. From (2.3.3), (2.3.9) and the $O(T_R)$ expression (2.3.14) we obtain the renormalised cumulants C_k to $O(T_R)$. Then, on substituting in the value of the critical temperature T_c from (2.3.21), we obtain the cumulants at criticality to $O(\varepsilon)$. The result is

$$\frac{C_k}{k!} = \begin{cases} 1 - \left(\frac{n-1}{n-2}\right)\varepsilon\, V(L)^{-2} \int_{V(L)} d\underline{x} \int_{V(L)} d\underline{y}\ \ln\mu|x-y| + O(\varepsilon^2) \ , & k=1 \\ O(\varepsilon^2) \ , & k>1 \end{cases} \qquad (2.3.22)$$

Recall that V(L) is the volume of a d-dimensional spherical block of radius L. To the order we are working we may perform the integration over the block in d=2. Hence from (2.3.1) and (2.3.2) we find the fixed-point p.d.f. $P_L^*(\phi^2)$ to $O(\varepsilon)$. The result is

$$P_L(\phi^2) = \delta(\phi^2 - A^2) \tag{2.3.23}$$

where

$$A^2 = 1 - \left(\frac{n-1}{n-2}\right)\varepsilon\left[\ln\mu L - \frac{1}{4}\right] + O(\varepsilon^2) \tag{2.3.24}$$

For large block-size L, the logarithm diverges; following the remarks of section 1.5, we can resum into scaling form the perturbation series (2.3.24), or equivalently (2.3.14) for k=1 and $T_R=T_c$, by integrating the renormalisation group equation (RGE) for $\lambda_1{}^R(T_R;\mu x)$ at the fixed point of the coupling constant, here at T_c (Brezin *et al* 1976, Amit 1984). To see this happening, we construct the RGE by differentiating (2.3.12a) with respect to μ and using the independence of $\lambda_1(T;x)$ on μ. We get

$$\left[\mu\frac{\partial}{\partial\mu} + \beta(T_R)\frac{\partial}{\partial T_R} + \gamma(T_R)\right]\lambda_1^R(T_R(\mu);\mu x) = 0 \tag{2.3.25}$$

where

$$\beta(T_R) = \mu\frac{d}{d\mu}T_R(T,\mu)\Big|_T \tag{2.3.26}$$

and

$$\gamma(T_R) = \mu\frac{d}{d\mu}\ln Z_2\Big|_T \tag{2.3.27}$$

From (2.3.20) we have $\beta(T_R^*)=0$ by definition; from (2.3.13b),(2.3.21) we find

$$\gamma^* \equiv \gamma(T_R^*) = \left(\frac{n-1}{n-2}\right)\varepsilon + O(\varepsilon^2) \tag{2.3.28}$$

With suitable normalisation, the solution of the RGE (2.3.25) at T_c can then be found:

$$\lambda_1^R(T_c;x) = \frac{1}{|x|^{\gamma^*}}, \quad x \to \infty \qquad (2.3.29)$$

Since $\lambda_1^R(T_R;x)$ is just the O(n)-invariant local field propagator $<\underline{\Phi}(x).\underline{\Phi}(0)>$, we recall (1.2.8) to recognise

$$d-2+\eta = \gamma^* \qquad (2.3.30)$$

Proceeding as before, the above analysis amounts to the re-exponentiation

$$A^2 = c_0^{-1} L^{-2\beta/\nu}, \quad L \to \infty \qquad (2.3.31)$$

where c_0 is a non-universal constant (which depends on the spherical geometry we chose for V(L)) and

$$2\beta/\nu = (d-2+\eta) = \left(\frac{n-1}{n-2}\right)\varepsilon + O(\varepsilon^2) \qquad (2.3.32)$$

In this way we are able to write the fixed point p.d.f. $P_L^*(\phi^2)$ to lowest order explicitly in a scaling form

$$P_L^*(\phi^2) = c_0 L^{2\beta/\nu}\, \delta(c_0 L^{2\beta/\nu}\phi^2 - 1) \qquad (2.3.33)$$

that, from (2.2.9) with $\xi \to \infty$, we expect it to display.

The δ-function profile of (2.3.33) signifies that at $O(\varepsilon)$ the major agent restoring the symmetry at T_c is the fluctuating phase

rather than the amplitude (viz. (2.1.5b)). The scaling with L would indicate the presence of some self-similar structure within the block (cf. nesting of droplets in low-dimensional Ising systems (Bruce and Wallace 1983)). However, the interpretation is not clear because $P_L(\phi^2)$ contains no information on the nature of phase fluctuations.

How does $P_L^*(\phi^2)$ evolve as ε increases?. As $\varepsilon \to 2$ we expect it to evolve into the "Gaussian" regime (viz. (2.1.5a)) characterising the s.r.o. at the Gaussian fixed point of the usual ϕ^4 theory. In order to see the commencement of this evolution from the above analysis we have to go one order higher in ε.

In (2.3.22), the presence of cumulants C_k with $k > 1$ at this order prevents the construction of $P_L^*(\phi^2)$ in closed form. However, one may calculate the moment ratio G^* which characterises $P_L^*(\phi^2)$ in the manner we discussed in section 2.1. We require T_c to $O(\varepsilon^2)$; the result of a two-loop calculation (Amit and Kotliar 1980) gives

$$T_c = \frac{\varepsilon}{n-2} - \frac{\varepsilon^2}{(n-2)^2} + O(\varepsilon^3) \qquad (2.3.34)$$

Then at T_c and for k=1 and k=2, we write the result (2.3.19) to $O(\varepsilon^2)$; from (2.3.16) we construct the moments $\mu_1=\langle\phi_L{}^2\rangle$ and $\mu_2=\langle\phi_L{}^4\rangle$ and then we calculate G^* to $O(\varepsilon^2)$ from the definition (2.1.4).

After some algebra - mostly the integrations over the block V(L) - we obtain the result

$$G^* = 1 - \left(\frac{1+4\pi^2}{48}\right) \frac{n(n-1)}{(n-2)^2} \varepsilon^2 + O(\varepsilon^3) \qquad (2.3.35)$$

As a check on the calculation, it is possible to verify that, analogous to (2.3.31), μ_1 exponentiates correctly to the scaling form $\mu_1 \sim L^{-2\beta/\nu}$ with

$$2\beta/\nu = \left(\frac{n-1}{n-2}\right)\varepsilon - \frac{(n-1)}{(n-2)^2} \varepsilon^2 + O(\varepsilon^3) \qquad (2.3.36)$$

Similarly, we note that $\mu_2 \sim L^{-4\beta/\nu}$ or equivalently G^* is independent of L.

The result (2.3.35) describes the evolution of G^* from 1 for small ε. The prefactor containing $4\pi^2$ is specific to the choice of a hyperspherical block V(L). In general G^* will depend to some degree on the geometry of the block, although it will be independent of the type of lattice underlying the continuous representation (2.3.5b).

At this order, beyond the provision of results displaying an explicit dependence of $P_L^*(\phi^2)$ on dimension d, one must not ask too much of the non-linear σ-model in regard to accurate numerical predictions for the interesting case d=3. For that, one would require at least one higher order and an interpolation with the results from an ε=4-d expansion. However, one may question whether perturbation theory really captures the nature of spin configurations at T_c, given that it allows the $\underline{\pi}$-field to take on all values in the range $(-\infty,+\infty)$ - the functional integral in (2.3.7a) should really be restricted to the range $|\underline{\pi}| \varepsilon (0,1)$. Thus, perturbation theory knows nothing about the global topology of the system and we must look for some non-perturbative information to determine $P_L^*(\phi^2)$ more fully.

2.4 Non-perturbative recursion formula for block-spin distributions

In order to escape the confines of perturbation theory in $d=2+\epsilon$ dimensions, one can try to look for non-perturbative approaches to the study of $P_\Lambda(\underline{\phi})$.

In this section we are going to derive an approximate, non-perturbative RG recursion formula relating $P_{\Lambda/2}$ to P_Λ. This formula follows as a simple extension to O(n) systems of the formula, due to Bruce (1981), for Ising systems (n=1); the level of approximation is that of Wilson's approximate recursion formula (ARF) for $\mathcal{H}_\Lambda$ (Wilson 1971b), whose result we exploit on the way. We will derive Wilson's formula first.

Wilson's ARF

Consider the block-spin co-ordinate $\underline{\phi}_\Lambda(x)$ defined in the Fourier representation (2.1.2), whose behaviour is described by an effective Hamiltonian $\mathcal{H}_\Lambda$. It will be convenient to choose the scale factor a_Λ of (2.2.5). Wilson's ARF is a non-perturbative approximation to the transformation R_2, defined in section 1.4, relating $\mathcal{H}_{\Lambda/2}$ to $\mathcal{H}_\Lambda$.

To simplify notation we write

$$\underline{\phi}_\ell = \underline{\phi}_\Lambda = \underline{\phi}_{\Lambda_0/2^\ell} \qquad (2.4.1)$$

and denote by $\mathcal{H}_\ell$ the effective Hamiltonian for $\underline{\phi}_\ell$. We start with a Hamiltonian of the form

$$\mathcal{H}_\ell[\underline{\phi}_\ell] = \Omega^{-1}\int d^dx \left\{ \frac{1}{2}c(\nabla\phi_\ell)^2 + V_\ell(\underline{\phi}_\ell) \right\} \qquad (2.4.2)$$

O(n) symmetry implies that V_ℓ is a function only of $\phi_\ell{}^2$. V_ℓ is equivalent to an infinite number of couplings (e.g. via the coefficients in its Taylor series in $\phi_\ell{}^2$); this is the non-perturbative feature. Ω and c are constants which we will choose later on.

In the spirit of the definition (1.4.5) of R_b (b=2), we split $\underline{\phi}_\ell$ into two parts

$$\underline{\phi}_\ell = \underline{\phi}^< + \underline{\phi}^> \qquad (2.4.3)$$

- where $\underline{\phi}^<$ and $\underline{\phi}^>$ contain the fluctuations with momenta $k<\Lambda/2$ and $\Lambda/2<k<\Lambda$ respectively - and we integrate over the field $\underline{\phi}^>$ to obtain an effective Hamiltonian $\mathcal{H}'$ for $\underline{\phi}^<$ i.e.

$$e^{-\mathcal{H}'[\underline{\phi}^<]} = \int \mathcal{D}\underline{\phi}^> \; e^{-\mathcal{H}_\ell[\underline{\phi}^< + \underline{\phi}^>]} \qquad (2.4.4)$$

Explicitly, we will then have

$$\mathcal{H}'[\underline{\phi}^<] = \Omega^{-1}\int d^dx \left\{ \frac{1}{2}c(\nabla\phi^<)^2 \right\} + F[\underline{\phi}^<] \qquad (2.4.5)$$

in which

$$F[\underline{\phi}^<] = -\ell n \left(\frac{I_1[\underline{\phi}^<]}{I_1[0]} \right) \qquad (2.4.6)$$

where

$$I_1[\underline{\phi}^<] = \int D\underline{\phi}^> \exp\left(-\Omega^{-1}\int d^dx \left\{ \tfrac{1}{2}c\,(\nabla\phi^>)^2 + V_\ell(\underline{\phi}^< + \underline{\phi}^>)\right\}\right) \quad (2.4.7)$$

In (2.4.6) we have normalised F(0) to zero in order to discard the $\underline{\phi}^<$-independent terms in $\mathcal{H}'$.

To get any further we have to make some approximations in (2.4.7). We will introduce Wilson's "phase cell" approximations, discussed in detail by Ma (1976). À la Kadanoff blocking, we imagine dividing the system into blocks of side $\sim 2/\Lambda$. Fluctuations within any block are due primarily to $\underline{\phi}^>(x)$, so the first approximation is that $\underline{\phi}^<(x)$ is constant over a block.

Further, we suppose the high momentum part of $\underline{\phi}(x)$ can be written

$$\underline{\phi}^>(x) = \sum_z \underline{\phi}_z W_z(x) \quad (2.4.8)$$

where the z's locate the centres of the blocks. $W_z(x)$ is non-zero only inside the block centred at z; it is the most localised wave-packet that can be constructed by superposing the Fourier component plane waves of $\underline{\phi}^>$. Since there is no overlap of the $W_z(x)$'s between different z's, we write a statement of orthogonality

$$\int d^dx\, W_z(x)\, W_{z'}(x) = \Omega\,\delta_{zz'} \quad (2.4.9)$$

in which the normalisation Ω is to be chosen as the volume of a block. The functional integration in (2.4.7) then decouples into independent integrals

$$\int D\underline{\phi}^> = \prod_z \left(\int d\underline{\phi}_z\, \Omega^{n/2}\right) \quad (2.4.10)$$

From a similar orthogonality of $\underline{\Phi}^{>}(x)$ with respect to $\underline{\Phi}^{<}(x)$ (constant over the block z) we also find

$$\int d^d x \; W_2(x) \;=\; 0 \qquad (2.4.11)$$

The final approximation is to ignore the variation of $|W_z(x)|$ over its corresponding block. Then (2.4.9),(2.4.11) imply that $W_z(x)=+1$ over one half of the block and $W_z(x)=-1$ over the other half.

By choosing the constant c to be

$$c \;=\; 2\Omega \left[\int d^d x \; (\nabla W_2(x))^2 \right]^{-1} \qquad (2.4.12)$$

one finds that the above approximations allow the integral I_1 of (2.4.7) to be written

$$I_1[\underline{\phi}^{<}] = \prod_{z} \int d\underline{\phi}_z \; \Omega^{n/2} \; e^{-\phi_z^2 - \frac{1}{2}\left[V_\ell(\underline{\phi}^{<}+\underline{\phi}_z)+V_\ell(\underline{\phi}^{<}-\underline{\phi}_z)\right]} \qquad (2.4.13)$$

On substituting this into (2.4.6) and rewriting $\sum_z$ as $\Omega^{-1}\int d^d x$, one can incorporate $F[\underline{\Phi}^{<}]$ as an effective potential inside the space-integral in (2.4.5) i.e.

$$\mathcal{H}'[\underline{\phi}^{<}] = \Omega^{-1} \int d^d x \; \left\{ \tfrac{1}{2} c (\nabla \phi^{<})^2 + V'(\underline{\phi}^{<}) \right\} \qquad (2.4.14)$$

where

$$V'(\underline{\phi}) \;=\; -\ln \left(\frac{I(\underline{\phi})}{I(0)} \right) \qquad (2.4.15)$$

and

$$I[\underline{\phi}] = \int d\underline{y}\ e^{-y^2 - \frac{1}{2}\left[V_\ell(\underline{\phi}+\underline{y}) + V_\ell(\underline{\phi}-\underline{y})\right]} \qquad (2.4.16)$$

To complete the RG transformation, we rescale $\underline{x}$ and $\underline{\Phi}^<$ according to the scale transformation (see section 1.4)

$$\underline{x}' = \underline{x}/2 \qquad (2.4.17a)$$

$$\underline{\phi}' = 2^{-\frac{1}{2}(2-d-\eta)}\,\underline{\phi}^< \equiv \alpha^{-1}\underline{\phi}^< \qquad (2.4.17b)$$

With our choice of scale factor $a\Lambda$, $\underline{\Phi}'$ is just the block-spin co-ordinate $\underline{\Phi}_{\ell+1}$ and we find - dropping the prime on $\underline{x}$ - the effective Hamiltonian

$$\mathcal{H}_{\ell+1}[\underline{\phi}_{\ell+1}] = \Omega^{-1}\int d^dx\ \left\{\frac{1}{2}c'(\nabla\phi_{\ell+1})^2 + V_{\ell+1}(\underline{\phi}_{\ell+1})\right\} \qquad (2.4.18)$$

where

$$c' = c\,2^{-\eta} \qquad (2.4.19)$$

and

$$V_{\ell+1}(\underline{\phi}) = -2^d \ln\left(\frac{I(\alpha\underline{\phi})}{I(0)}\right) \qquad (2.4.20)$$

with I given by (2.4.16).

In order to recast $\mathcal{H}_{\ell+1}$ into the same form as $\mathcal{H}_\ell$ (equation (2.4.2)) - and thus to find a fixed point of R_2 - it is clear from (2.4.19) that we must set

$$\eta = 0 \tag{2.4.21}$$

an approximation which is not too severe, since in the dimension of interest, d=3, η is generally small (section 1.2). Then (2.4.20), Wilson's ARF, constitutes the result of one iteration of R_2, within the approximations we have introduced.

Recursion formula for p.d.f.

Now let $P_\ell(\underline{\phi})$ denote the joint p.d.f. for the components of a single block-spin $\underline{\phi}_\ell$. We derive a recursion formula for P_ℓ. Following Bruce (1981), we write the self-consistency equation

$$P_\ell(\underline{\phi}) = \int d\underline{\phi}^< \int d\underline{\phi}^> \; P^<(\underline{\phi}^<) P_c(\underline{\phi}^<, \underline{\phi}^>) \delta(\underline{\phi} - \underline{\phi}^< - \underline{\phi}^>) \tag{2.4.22}$$

in which $P^<$ is the p.d.f. for $\underline{\phi}^<$ and P_c is the conditional p.d.f. that given its first argument $\underline{\phi}^<$, its second argument lies in the infinitesmal hypercube bounded by $\underline{\phi}^>$ and $\underline{\phi}^> + \underline{d\phi}^>$, thus satisfying the normalisation condition

$$\int d\underline{\phi}^> \; P_c(\underline{\phi}^<, \underline{\phi}^>) = 1 \tag{2.4.23}$$

($\int \underline{d\phi}$ denotes the integration $\prod_\alpha \int d\phi_\alpha$). Inserting (2.4.17b) into (2.4.22) and performing the integration over $\underline{\phi}^>$ yields the recursion formula

$$P_\ell(\underline{\phi}) = \int d\underline{y} \; P_{\ell+1}(\underline{y}) \, P_c(\alpha \underline{y}, \underline{\phi} - \alpha \underline{y}) \tag{2.4.24}$$

Within the approximations of Wilson's ARF, one can work out the kernel P_c in terms of the potentials V_ℓ, $V_{\ell+1}$. It is easy to show

that, for a given field $\underline{\phi}^<$, the Boltzmann probability $\exp(-\mathcal{H}_\ell)$ factorises into a product over the blocks z, i.e.

$$e^{-\mathcal{H}_\ell}\Big|_{\{\underline{\phi}^<(x)\}} = \text{Constant} \times \prod_z e^{-\phi_z^2 - \frac{1}{2}\left[V_\ell(\underline{\phi}^< + \underline{\phi}_z) + V_\ell(\underline{\phi}^< - \underline{\phi}_z)\right]} \tag{2.4.25}$$

where the constant depends on $\underline{\phi}^<$. O(n) symmetry and the approximation $|W_z(x)|=1$ imply

$$P_c(\underline{\phi}^<, \underline{\phi}^>) = P_c(\underline{\phi}^<, W_z \underline{\phi}_z) = P_c(\underline{\phi}^<, \underline{\phi}_z) \tag{2.4.26}$$

for the single-block conditional p.d.f., so that

$$P_c(\underline{\phi}^<, \underline{\phi}^>) = p_0\, e^{-(\phi^>)^2 - \frac{1}{2}\left[V_\ell(\underline{\phi}^< + \underline{\phi}^>) + V_\ell(\underline{\phi}^< - \underline{\phi}^>)\right]} \tag{2.4.27}$$

From the normalisation condition (2.4.23) and Wilson's ARF (2.4.20), the constant p_0 is found to be

$$p_0 = \frac{e^{2^{-d} V_{\ell+1}(\alpha^{-1}\underline{\phi}^<)}}{\int d\underline{y}\; e^{-y^2 - V_\ell(y)}} \tag{2.4.28}$$

For $T=T_c$, in the limit $\ell\to\infty$ (large block-size), V_ℓ tends to a fixed point V^* which can be determined by iterating (2.4.20). Correspondingly, as asserted in section 2.2, P_ℓ tends to P^*, independent of the block-size. It is the fixed point solution of (2.4.24):

$$P^*(\underline{\phi}) = \int d\underline{y}\; P^*(\underline{y})\, P_c^*(\alpha\underline{y}, \underline{\phi} - \alpha\underline{y}) \tag{2.4.29}$$

in which P_c^* is the limiting form of (2.4.27),(2.4.28) given by

$$P_c^*(\underline{u},\underline{v}) = \frac{e^{2^{-d}V^*(\alpha^{-1}\underline{u}) - v^2 - \frac{1}{2}\left[V^*(\underline{u}+\underline{v}) + V^*(\underline{u}-\underline{v})\right]}}{\int d\underline{y}\; e^{-y^2 - V^*(\underline{y})}} \qquad (2.4.30)$$

The approximations inherent in (2.4.30) are essentially uncontrollable. However, we note the success with which Wilson's ARF accounts for critical point exponents in d=3 (Wilson and Kogut 1974), and remark on the very close agreement between estimates of $P^*(\phi)$ for the d=3 Ising model from the recursion formula (Bruce 1981) and Monte Carlo studies (Binder 1981). It seems reasonable to expect fairly reliable results from (2.4.29),(2.4.30) in three dimensions.

2.5 d=3 XY model: recursion formula study

We proceed now to discuss the application of the recursion formula to a study of the classical d=3 XY model at criticality. The XY model is a model of magnets with an easy plane, and is also thought to describe superfluid helium. It is the first member (n=2) of the class of O(n) spin systems we have been considering. We are going to calculate the fixed-point form $P^*(\underline{\phi})$ of the joint p.d.f. $P_\ell(\underline{\phi})$ for a two-component block-spin $\underline{\phi}_\ell=(\phi_\ell{}^x,\phi_\ell{}^y)$ defined by equations (2.1.2),(2.4.1).

We saw how to do this in the previous section. We find the fixed-point potential V^* by iterating equation (2.4.20), in which, under the approximation $\eta=0$, we put $\alpha=2^{-1/2}$ in three dimensions. Then we solve equation (2.4.29) for $P^*(\underline{\phi})$ with the kernel P_c^* specified by (2.4.30).

First we must specify a suitable starting potential $V_0(\underline{\phi})$. To study the critical behaviour we can, by equation (1.5.3), choose

$$V_0(\phi) = r_0 \phi^2 + \frac{1}{2}(\phi^2)^2 \qquad (2.5.1)$$

where r_0 is an analytic function of T. The factor $1/2$ is arbitrarily chosen; results should be independent of this choice.

The fixed-point of the recursion formula for V_ℓ is obtained by locating the critical value r_{0c} of the parameter r_0, such that, after a few iterations, the sequence of potentials V_ℓ is sufficiently stable over, say, ℓ' iterations. If $r_0 > r_{0c}$, the sequence tends first to V^* but eventually escapes into the Gaussian regime dominated by the term $r\phi^2$. If $r_0 < r_{0c}$, the sequence starts similarly but is then found to oscillate badly for large ℓ. The closer r_0 is to r_{0c}, the larger is ℓ' and the better is V_ℓ an approximation to V^* for large ℓ.

Numerical studies of the recursion formula for the d=3 XY model were first performed by Grover (1972). The calculations here are very similar. By O(n) symmetry, we need only keep track of V_ℓ as a function of $z \equiv |\underline{\phi}|$. The recursion formula is rewritten

$$V_{\ell+1}(z) = -2^d \ln\left(\frac{J(z)}{J(0)}\right) \qquad (2.5.2)$$

where

$$J(z) = \int_0^\infty u\,du \int_0^\pi d\vartheta \exp\left(-u^2 - \frac{1}{2}z^2 + \sqrt{2}\,zu\cos\vartheta - \frac{1}{2}V_\ell(u)\right)$$

$$\times \exp\left(-\frac{1}{2}V_\ell\left(\sqrt{u^2 + 2z^2 - 2\sqrt{2}\,zu\cos\vartheta}\,\right)\right) \qquad (2.5.3)$$

The integrations were performed numerically in double precision by Simpson's rule, varying u from 0 to 4.0 in steps of 0.1, and θ from

0 to π in steps of $\pi/32$. $V_\ell(z)$ was calculated in double precision on a uniformly-spaced mesh of 41 points from z=0 to z=4.0 with spacing 0.1; linear interpolation was used between mesh points and a z^6-extrapolation was assumed for z > 4.0. This procedure was sufficient for three significant figure accuracy in V^*.

Using r_{OC}=-2.3290414.... resulted in a value of $V_\ell(1.5)$ that was stable to within one part in 10^5 over the iterates from ℓ=14 to ℓ=21. The iterate ℓ=17 was used as an estimate of $V^*(z)$, and is shown in figure (2.2).

As a check, the thermal eigenvalue $\lambda=2^{y_t}$ was estimated from the deviations $\delta V_\ell(z)=V_\ell(z)-V^*(z)$ into the Gaussian phase, induced by temperature deviations $\delta r=r_O-r_{OC} \sim 10^{-12}$ above the critical surface $r_O=r_{OC}$. For small deviations we expect the linearised recursion formula to yield the exponentially-growing solution (Wilson 1971b)

$$\delta V_\ell = \delta r \, \lambda^\ell \, q(z) \qquad (2.5.4)$$

where the eigenfunction q(z) is independent of ℓ and r_O. The expression

$$\lambda_\ell = \frac{\delta V_{\ell+1}(1.5)}{\delta V_\ell(1.5)} \qquad (2.5.5)$$

then yielded the estimate

$$\lambda = 2.930 \qquad (2.5.6)$$

stable in the last decimal place over the two iterations ℓ=18 and

FIGURE (2.2). Fixed-point potential

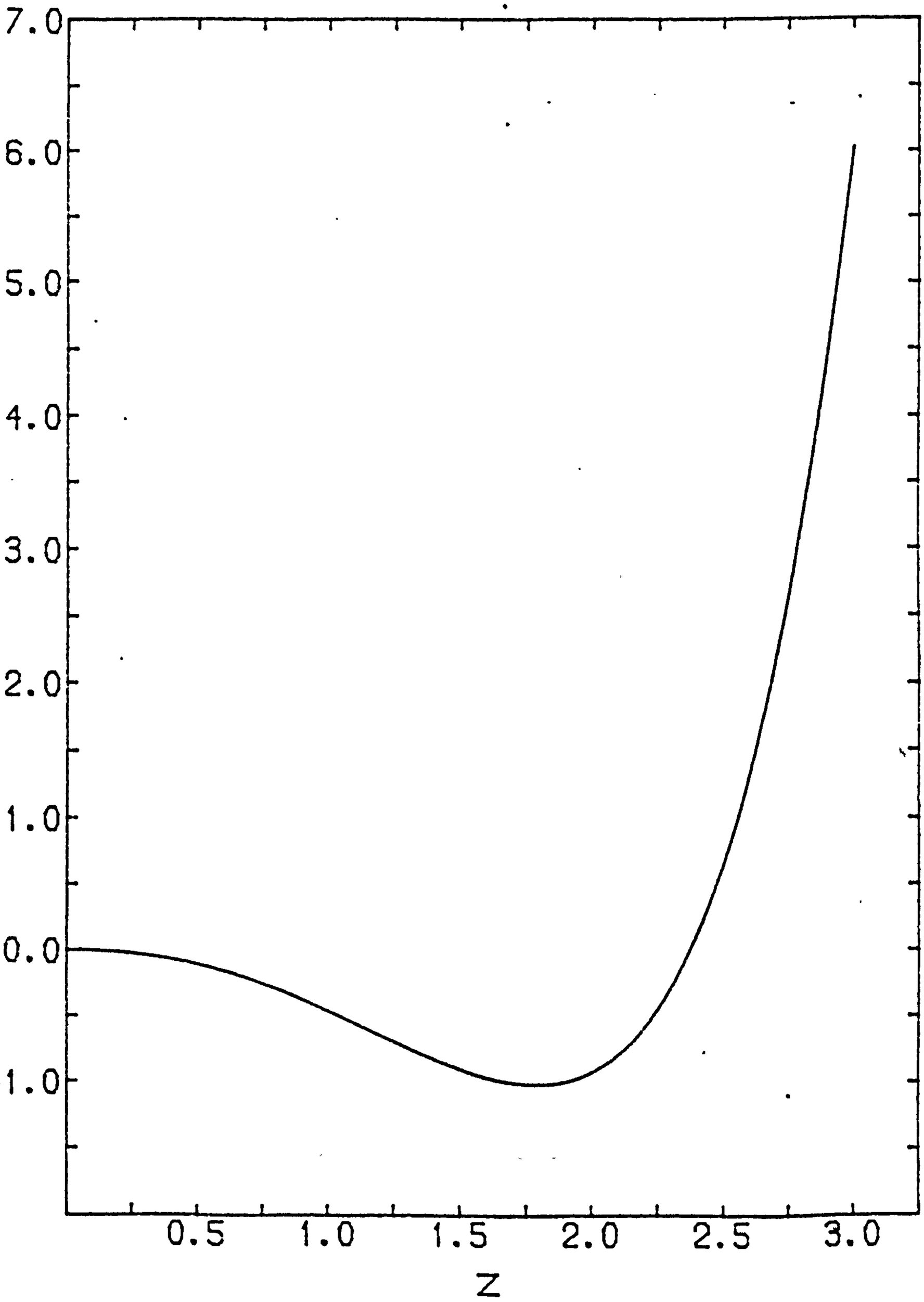

FIGURE (2.3). $P^*(\Phi_x)$

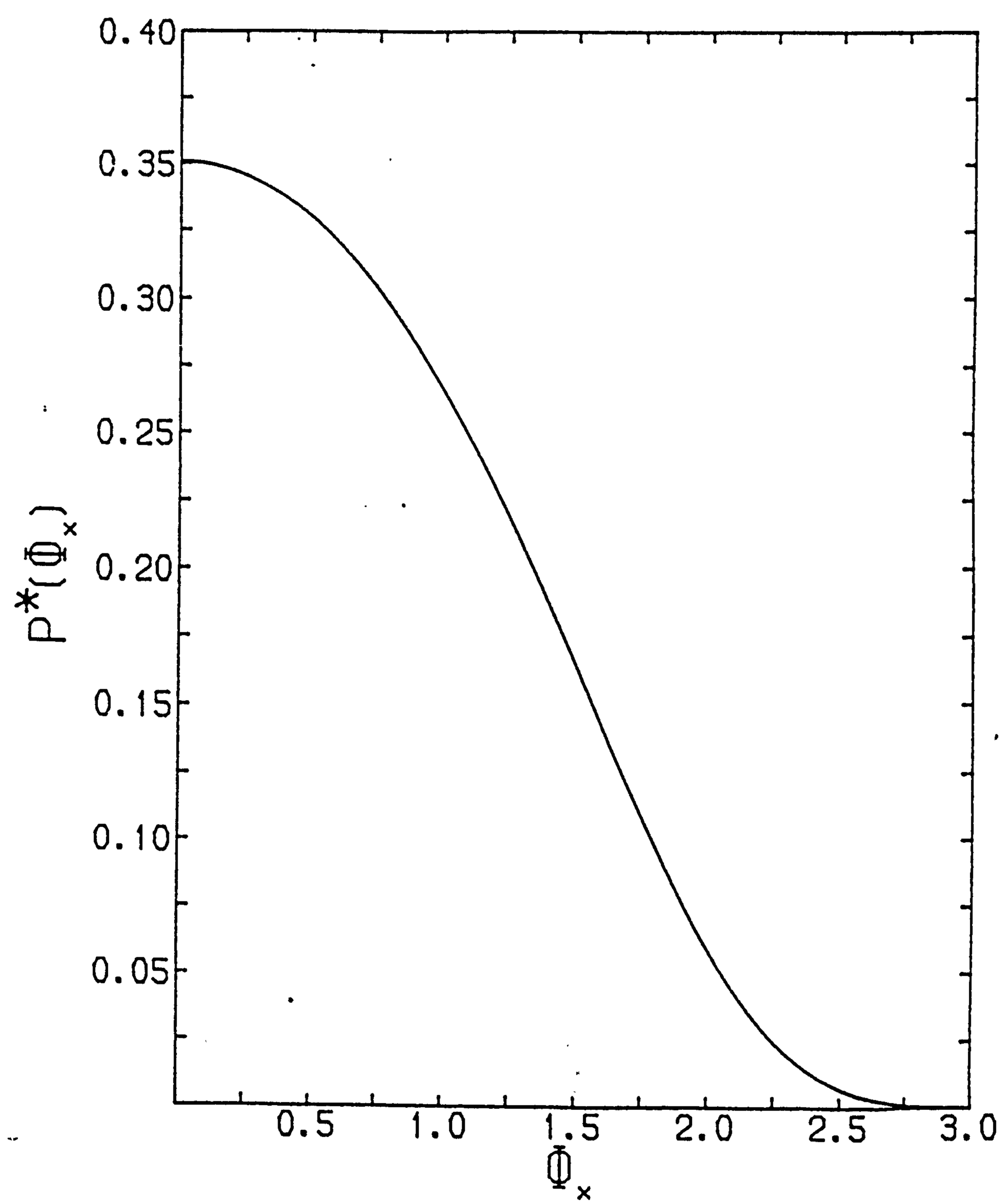

FIGURE (2.4). $P^*(\Phi^2)$

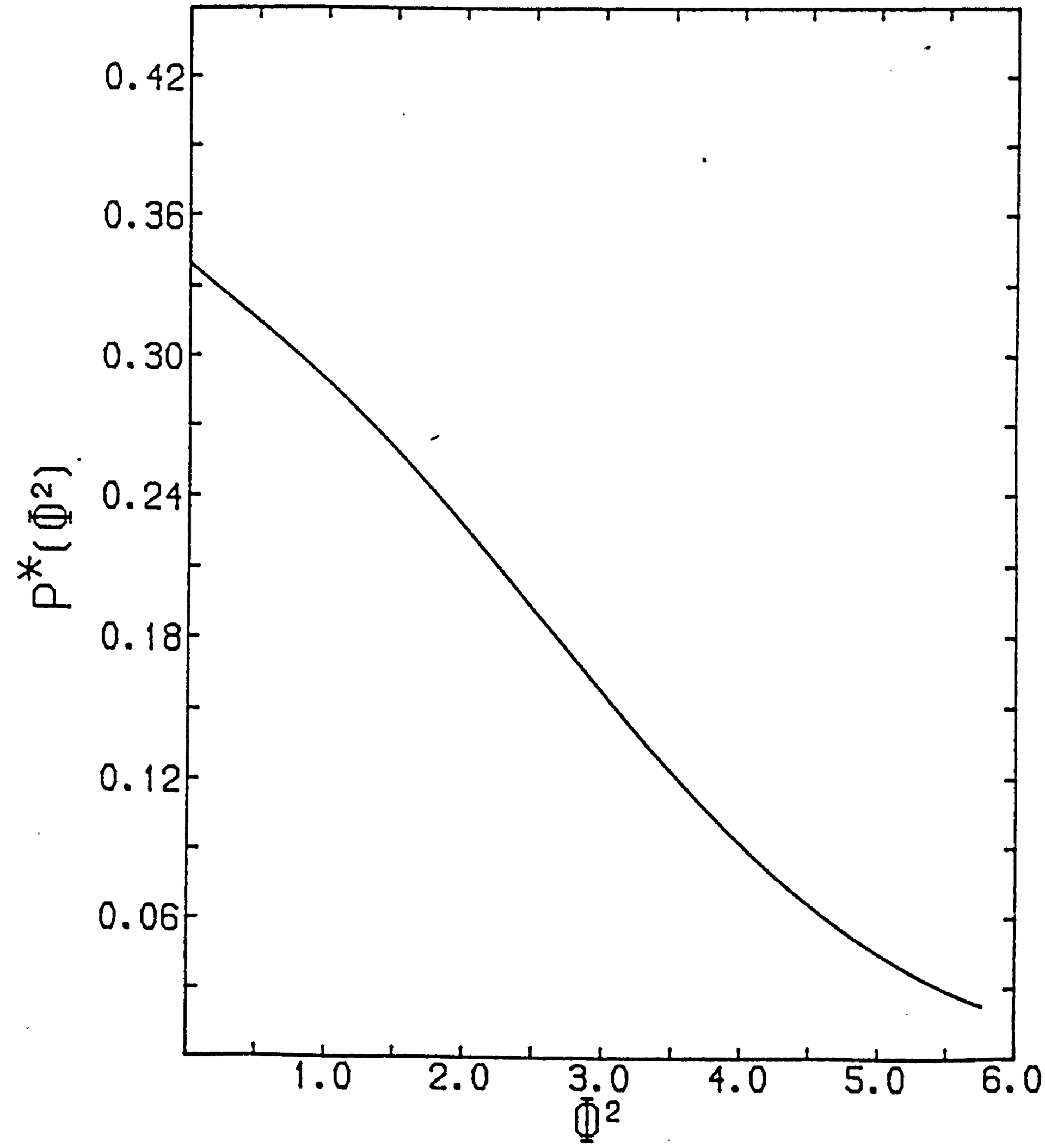

ℓ=19, and in close agreement with the value 2.931 obtained by Grover (1972).

By numerically integrating eqn. (2.4.29) we have obtained $P^*(\underline{\phi})$ as a function of $z=|\underline{\phi}|$. From $P^*(z)$ we have constructed the p.d.f. $P^*(\phi_x)$ by integrating over ϕ_y, and the p.d.f. $P^*(\phi^2)$ by using eqn. (2.1.3) with n=2. The resulting distributions are shown in figures (2.3) and (2.4), in which we have chosen to scale the spin co-ordinate such that $<\phi_x{}^2>=1$ and $<\phi^2>=2$, respectively.

The quantity G^*, defined by eqn. (2.1.4), for the fixed point p.d.f. is a universal number and it has value

$$G^* \approx 0.434 \qquad (2.5.7)$$

Hence the distribution is non-Gaussian, signifying the presence of non-trivial, universal patterns of short-range order (s.r.o.) at criticality, but it reveals no interesting structure. It suggests that the s.r.o. at the d=3 XY transition resides in some angular distribution of the spins, to which $P^*(z)$ is insensitive.

2.6 d=3 XY model: Monte Carlo study

The Monte Carlo study discussed here was initiated as an independent check on the form of $P^*(\phi^2)$ derived in the previous section via the recursion formula (figure (2.4)). It serves as a direct investigation of whatever short-range order there is at criticality. The principal aim was not to estimate critical exponents.

As with the work of the previous section, this work has two parts. First, we locate the critical temperature T_c. Then we sample the distribution . $P_L(\phi^2)$ at T_c for various block-sizes L. Before describing these parts in detail, we outline briefly the Monte Carlo method which was implemented as an algorithm on the highly parallel ICL Distributed Array Processor (DAP) at Edinburgh. See, for example, Flanders *et al* (1977) for a general description of the DAP. The features important to this study will be mentioned in context.

Monte Carlo (MC) method

Reviews of MC techniques are found in Binder (1979) and Mouritsen (1984). The basic task is to estimate numerically the phase space integrals in the configurational average of some interesting observable $O(\phi)$ of the system in equilibrium

$$\langle o(\phi) \rangle = \frac{\int D\phi \; o(\phi) \; e^{-\mathcal{H}[\phi]}}{\int D\phi \; e^{-\mathcal{H}[\phi]}} \qquad (2.6.1)$$

In the MC or importance sampling method, the solution is to set up an algorithm which randomly samples configurations ϕ in phase space with probability $p_{eq}(\phi) = e^{-\mathcal{H}[\phi]}$ reflecting the size of their contribution to the integrals in (2.6.1). Since these configurations are then correctly weighted, an estimate of (2.6.1) is given by the sample average

$$\langle o(\phi) \rangle \simeq \frac{1}{M} \sum_{i=1}^{M} o(\phi_i) \qquad (2.6.2)$$

over a large number M of sampled configurations.

The correct weight $p_{eq}(\phi)$ is achieved as follows. From an initial configuration ϕ_0, a Markov sequence $\phi_1,\phi_2,.....\phi_n$ can be generated by specifying the Markov transition probability $W(i\to j)$ for the transition from ϕ_i to ϕ_j. If $p_n(\phi)$ is the probability of getting ϕ after n steps, and if $W(i\to j)$ satisfies detailed balancing i.e.

$$W(i\to j)\, p_{eq}(\phi_i) = W(j\to i)\, p_{eq}(\phi_j) \qquad (2.6.3)$$

then it can be shown that

$$p_n(\phi) \longrightarrow p_{eq}(\phi) \quad \forall \phi \quad as \quad n\longrightarrow \infty \qquad (2.6.4)$$

thus fulfilling our aim when n is large enough.

Metropolis algorithm

The commonest realisation of such a $W(i\to j)$, and the one we adopt here, occurs as the Metropolis algorithm (Metropolis *et al* 1953). For the d=3 XY model it goes as follows. The Hamiltonian we use is

$$\mathcal{H}(\{\underline{S}\}) = -K \sum_{<rr'>} \underline{S}(r).\,\underline{S}(r') \qquad (2.6.5)$$

where $\{\underline{S}\}$ is a configuration of two-component unit vectors, K is the (reduced) coupling and the sum is over pairs of nearest-neighbour sites of a simple cubic lattice with cyclic boundary conditions imposed at all edges. Then we

(1) generate an initial configuration of spins $\{\underline{S}\}_i$

(2) generate a trial configuration $\{\underline{S}\}_{i+1}$ by, say,

randomly "hitting" one of the spins in $\{\underline{S}\}_i$.

(3) calculate the resultant energy change $\Delta\mathcal{H}$

$$= \mathcal{H}(\{\underline{S}\}_{i+1}) - \mathcal{H}(\{\underline{S}\}_i)$$

(4) take $W(i \to i+1) = 1$ if $\Delta\mathcal{H} < 0$

$$= e^{-\Delta\mathcal{H}} \quad \text{if} \quad \Delta\mathcal{H} > 0$$

and accept $\{\underline{S}\}_{i+1}$ accordingly.

(5) go to (2)

Step (2) is realised by choosing an angle θ from the uniform distribution on $(0,2\pi)$ and then setting the trial spin to $(\cos\theta,\sin\theta)$. This procedure ensures that the spins in $\{\underline{S}\}_{i+1}$ remain of unit length. Although the spin representation $\{\theta\}$ is half as costly in computer space as the spin representation $\{\underline{S}\}$, it turns out to be more than twice as costly in computer time at step (3) where it is cheaper to calculate $\Delta\mathcal{H}$ directly in terms of the XY spin components. Savings in time prove to be the more valuable so we use $\{\underline{S}\}$. We note that a random number $r\varepsilon[0,1]$ is required in step (4) when $\Delta\mathcal{H} > 0$; when $r < e^{-\Delta\mathcal{H}}$ the trial spin is accepted.

Time efficiency is increased on the DAP by updating several spins simultaneously, provided that none of them are coupled through the Hamiltonian (2.6.5). In addition, for lattices of linear size $N < 64$, we enhance space and time efficiency by storing and updating $(64/N)^2$ configurations simultaneously.

The application of the cycle of steps (2)-(5) once for each and every lattice site constitutes one lattice sweep. For a 64^3 lattice of XY spins, the DAP algorithm executes 1.961 lattice sweeps per second i.e. 0.514 million spin update trials per second. This is to

be compared with 42 million spin update trials per second for the simulation of the Ising model on the same size lattice and on the same machine (Reddaway *et al* 1985); the latter simulation uses logical variables and operations only, so the comparison is not so unfavourable.

Two problems are inherent to the MC method. They are those of reaching thermal equilibrium, particularly in the critical region due to "critical slowing down", and sampling a sufficient number of (statistically independent) configurations so that averages have small statistical error. With the special features of the DAP, it is possible to overcome these problems simply by running for long times.

A third problem is the finite size of the system whose bulk features are being simulated. In the task of locating T_c, this may be turned to advantage by the use of finite-size scaling (see e.g. Barber 1983).

Locating T_c

Initially, simulations at various couplings K were performed on lattices of linear size N = 2,4,8,16,32 and 64. The quantities monitored were the absolute magnetisation $\langle|\underline{\phi}|\rangle_N$ and the moments $\langle\phi^2\rangle_N$ and $\langle\phi^4\rangle_N$, where $\underline{\phi}$ is the instantaneous magnetisation per spin. From an initially "cold" configuration, 10000 lattice sweeps were performed before taking data, sufficient to allow the system to equilibrate. Thereafter, data were taken every 50th lattice sweep to reduce the statistical correlation between sampled configurations.

Figure (2.5) shows the coupling dependence of the magnetisation $M_N(K)=<|\underline{\phi}|>_N$, and figure (2.6) shows that of the symmetrised susceptibility χ_N, defined by

$$\chi_N = N^3 K \left(<\phi^2>_N - <|\underline{\phi}|>_N^2 \right) \qquad (2.6.6)$$

obtained from relatively short runs. These curves are intended to provide only an indication of the location of the transition point. Figure (2.5) displays the classic finite-size effect of rounding-off at a continuous phase transition in the vicinity of K=0.45. An "eyeball" estimate from the position of the peaks in figure (2.6) yields $K_c=0.454$

With longer runs, a reasonably accurate estimate of K_c was obtained from a study of the cumulant ratio $\tilde{G}_N$ defined by

$$\tilde{G}_N = 2 - \frac{<\phi^4>_N}{<\phi^2>_N^2} \qquad (2.6.7)$$

This $\tilde{G}_N$ pertains to lattices of linear size N, and is analogous to - though distinct from - ratio G_Λ defined by (2.1.4) for sub-blocks of side $\sim 1/\Lambda$. Finite-size scaling arguments (Binder 1981) then show that as $N \to \infty$, $\tilde{G}_N \to 1$ for $K>K_c$, $\tilde{G}_N \to 0$ for $K<K_c$ and $\tilde{G}_N \to \tilde{G}^*$ for $K=K_c$, where $\tilde{G}^*$ is a non-zero, universal constant independent of N (though dependent on the lattice boundary conditions) and distinct from the G^* for sub-blocks in which we are ultimately interested. K_c is then located at the non-trivial point of intersection of the curves $\tilde{G}_N(K)$ for large N, which we have plotted in figure (2.7). An extrapolation of the intersections for consecutive pairs of curves yields the estimate $K_c=0.4535 \pm 0.0005$, at which $\tilde{G}^* \approx 0.76$. This

FIGURE (2.5). Magnetisation vs. coupling

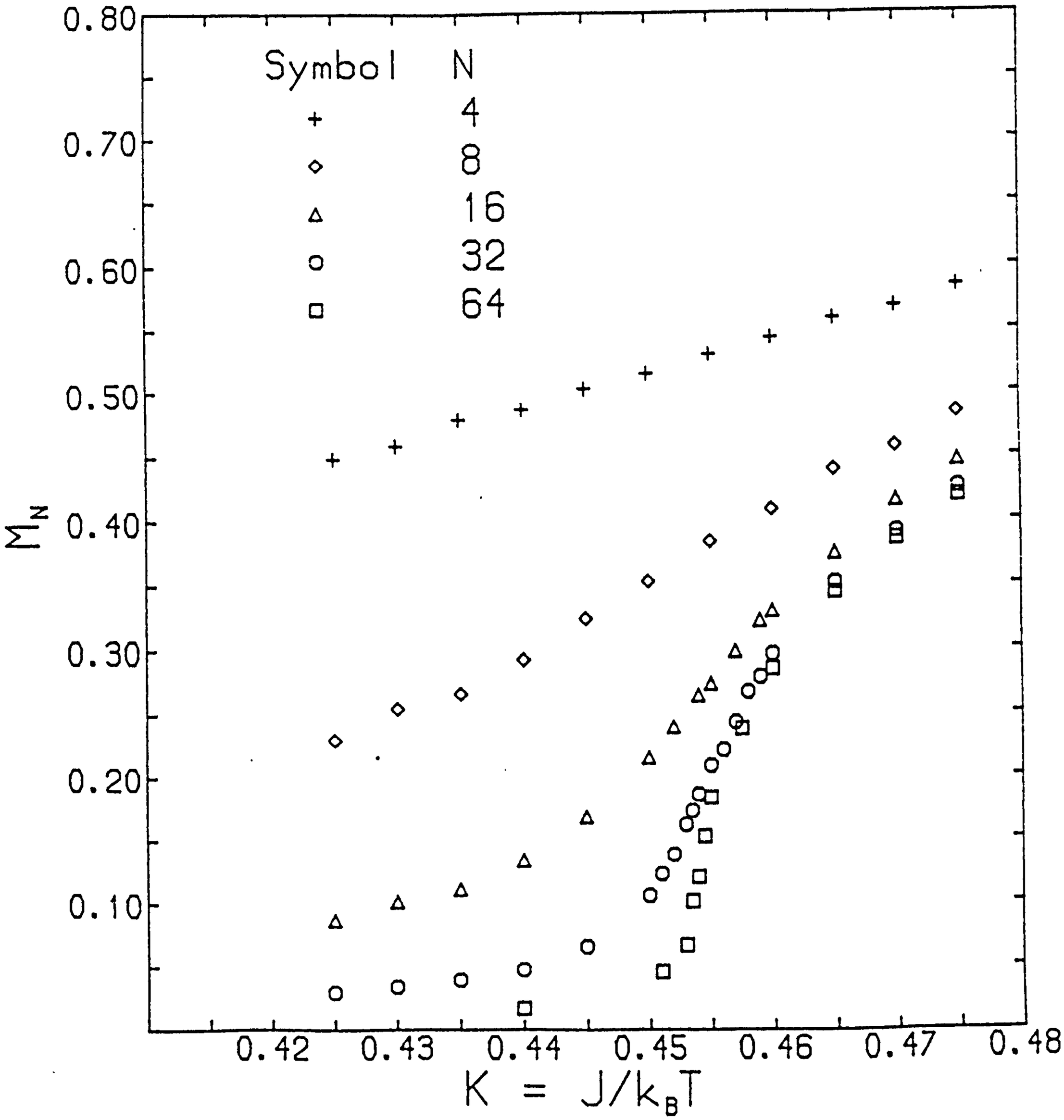

FIGURE (2.6). Susceptibility vs. coupling

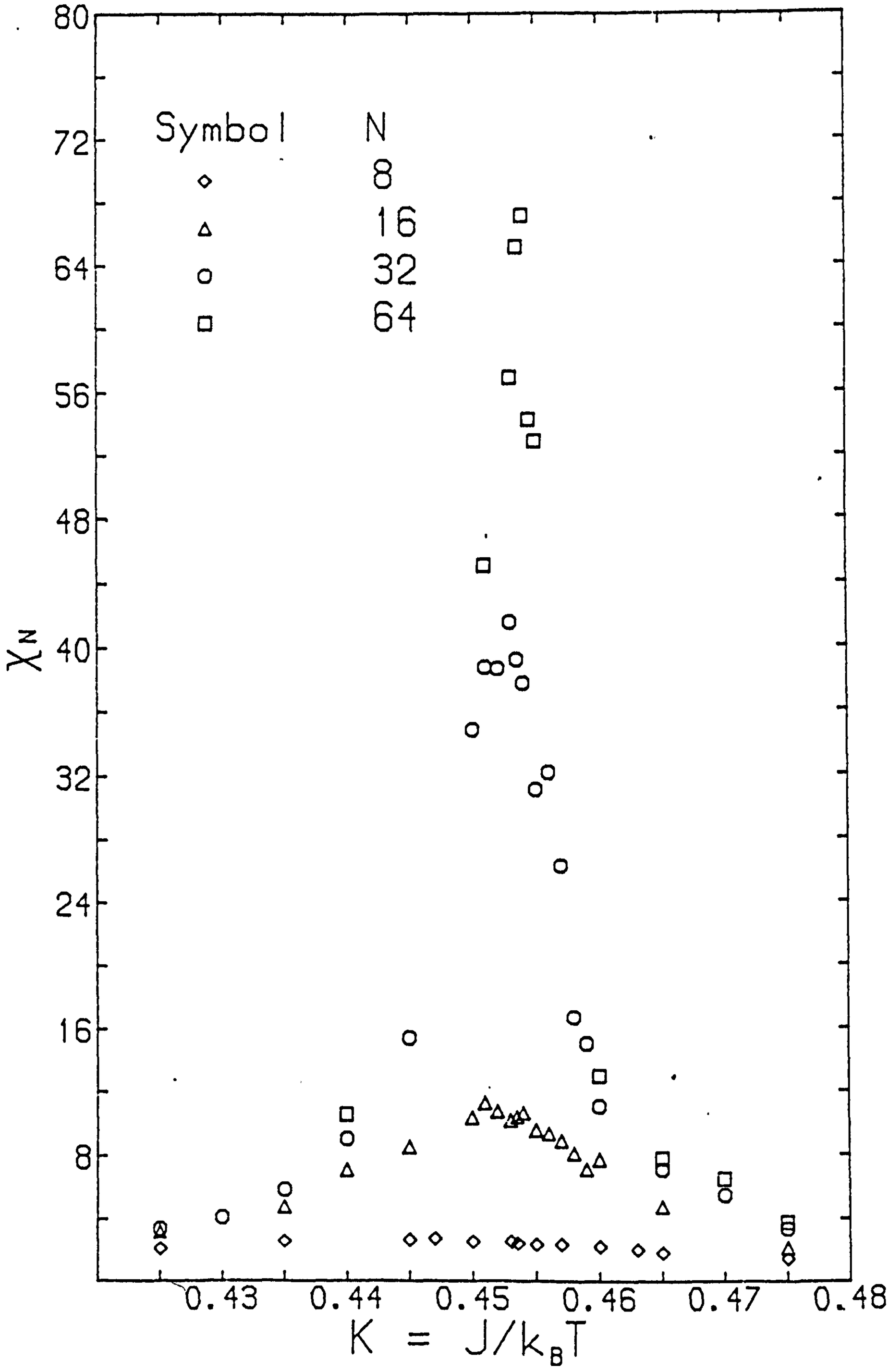

FIGURE (2.7). Cumulant ratio vs. coupling

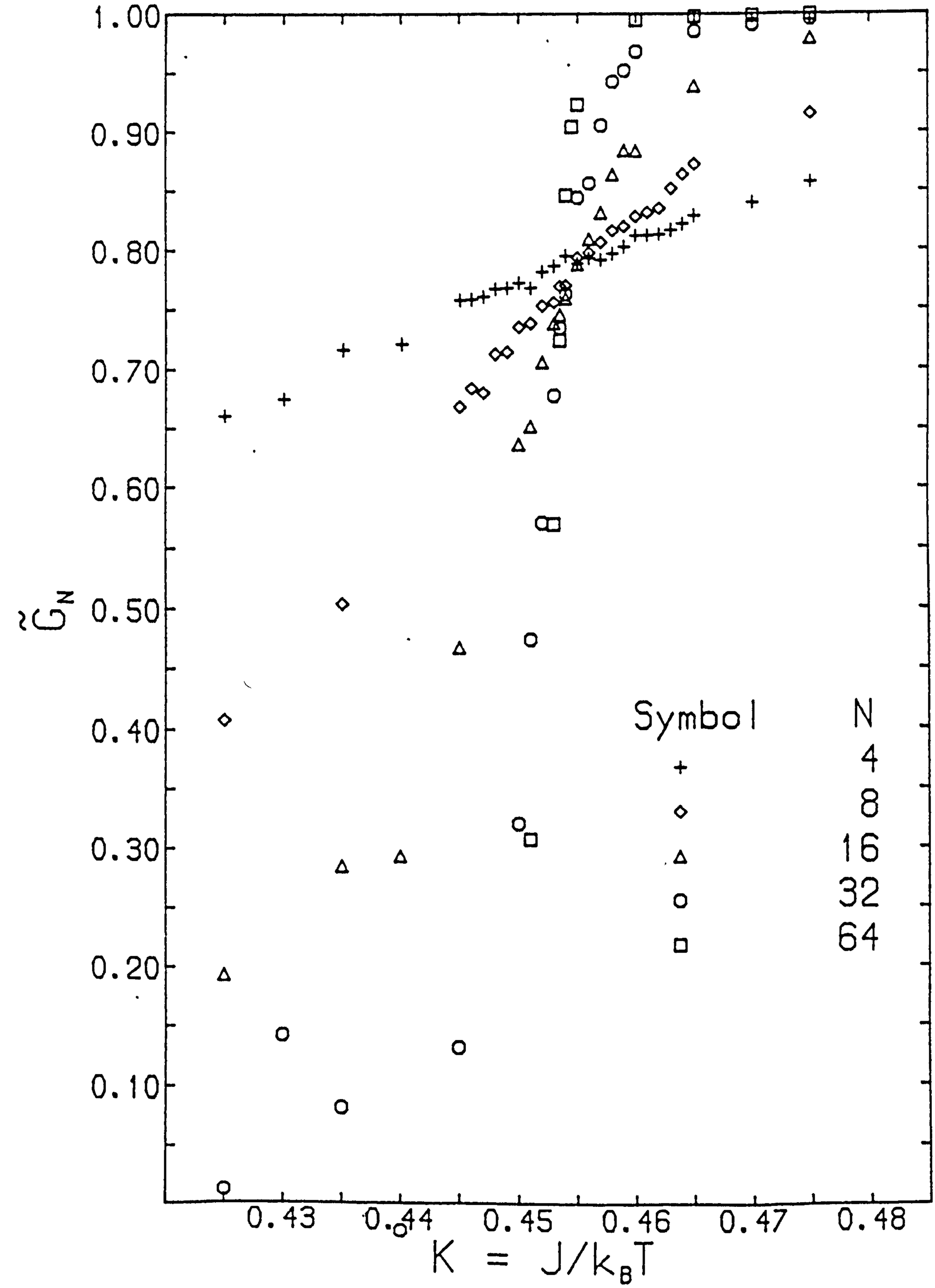

estimate of K_c is consistent with the value $K_c=0.454 \pm 0.001$ obtained from the analysis of high-temperature series (Ferer *et al* 1973).

Block-spin distributions

Subsequent simulations were performed on a N=64 lattice at $K_c=0.4535$ and sub-block spins $\underline{\Phi}_L$ of side L=4,8 and 16 were sampled from equilibrated configurations. Here, $\underline{\Phi}_L$ is constructed from cubic sub-blocks of volume $V(L)=L^3$ i.e.

$$\underline{\phi}_L = V(L)^{-1} \sum_{r \in V(L)} \underline{S}(r) \qquad (2.6.8)$$

Ideally, one seeks a value of L in the regimes $1 << L << \xi$ and $L << N$. The first two inequalities ensure that $P_L(\underline{\Phi})$ attains its universal form $P^*(\underline{\Phi})$ while the last inequality suppresses the finite-size effects of the host lattice (in particular, its cyclic boundary conditions).

$P_L(\phi_x)$ and $P_L(\phi^2)$ were constructed from 5000 samples of $\underline{\Phi}_L$ for each L. The results are shown in figures (2.8) and (2.9), where a direct comparison is made with the corresponding results - dotted curves - for $P^*(\phi_x)$ and $P^*(\phi^2)$ obtained from the recursion formula (i.e. figures (2.3) and (2.4)). The distributions for each L have been scaled so that $<\phi_x^2>_L=1$ and $<\phi^2>_L=2$, consistent with figures (2.3) and (2.4). On doing this, we note first the collapse of distributions onto a single curve independent of L. This is a result of scaling; from the variation of the required scale factors with L, we can estimate the exponent ratio $2\beta/\nu=1+\eta$ in d=3, as we indicated in section (2.2) on scaling theory. A simple power-law fit to the

FIGURE (2.8). $P_L(\Phi_x)$

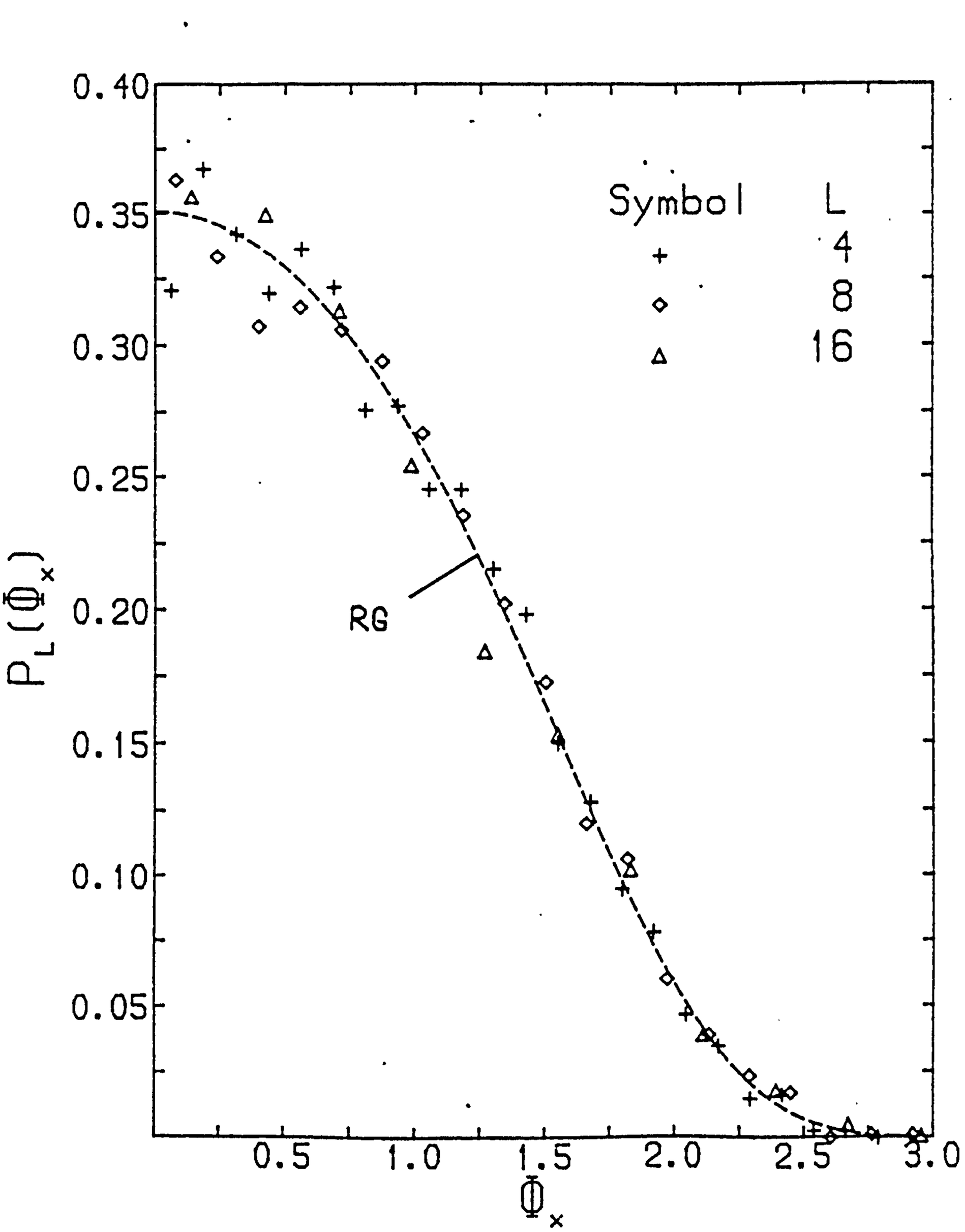

FIGURE (2.9). $P_L(\Phi^2)$

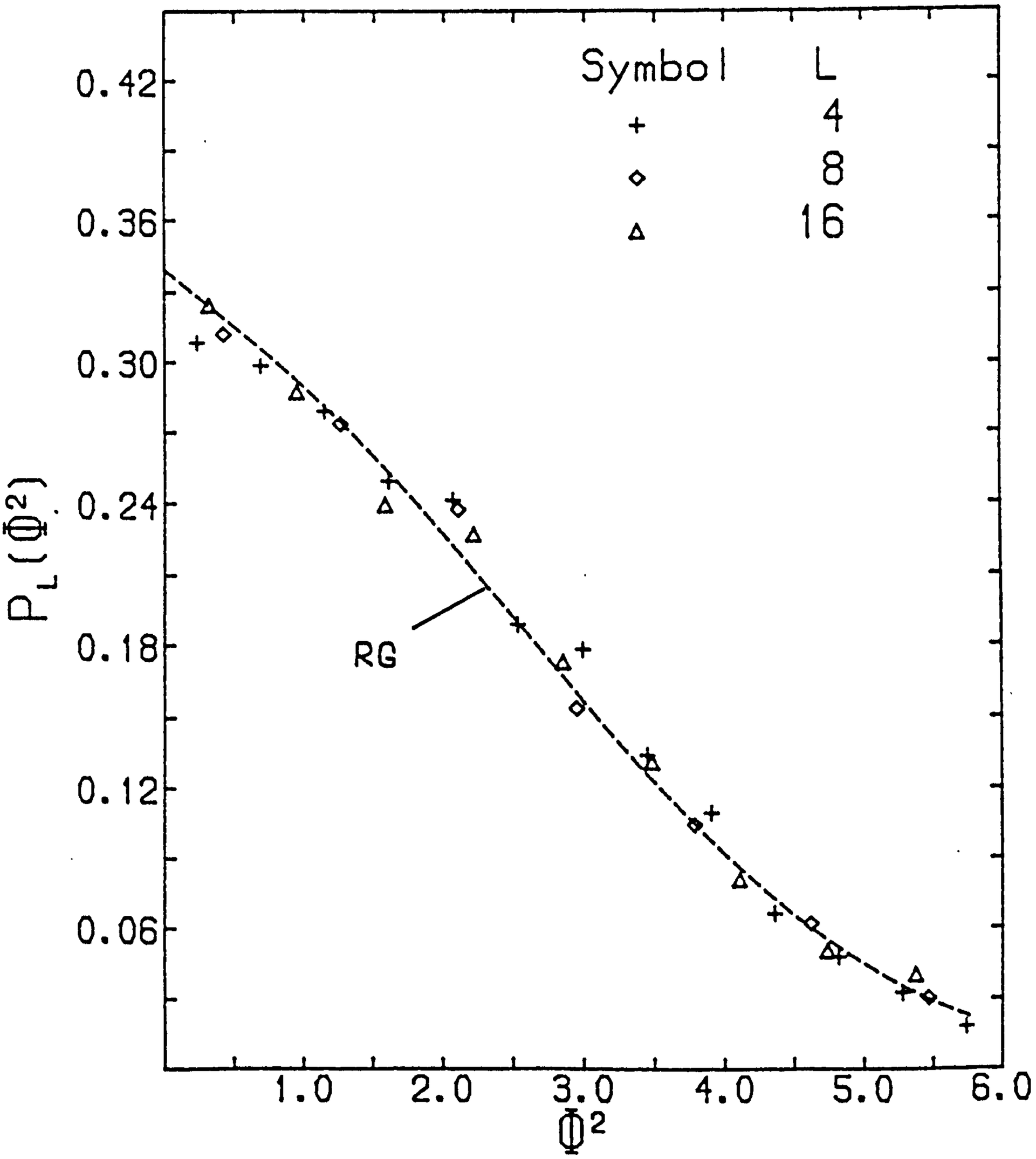

TABLE (2.1). THe sub-block cumulant ratio G_L on a 64^3 lattice at K_c=0.4535, for various values of L. For L large compared to unity but small compared to 64, we expect $G_L \to G^*$ independent of L.

L	G_L
4	0.48 ± 0.01
8	0.45 ± 0.01
16	0.45 ± 0.02

data for L=8 and L=16 yields the value

$$\eta = 0.09 \pm 0.05 \qquad (2.6.9)$$

which is just within error bars of the estimate $\eta = 0.04 \pm 0.01$ from high-temperature series (Ferer *et al* 1973).

Then we note the close agreement between the scaled curves and the recursion formula results. From the data of table (2.1), we obtain an estimate of the sub-block moment ratio at criticality:

$$G^* = 0.45 \pm 0.02 \qquad (2.6.10)$$

which is in excellent agreement with the fixed-point value $G^* \approx 0.434$ obtained from the recursion formula; given the recursion formula approximation that $\eta=0$, together with the small value of η in (2.6.9), we should not find this altogether surprising.

Therefore we conclude that, in accordance with the expectations raised at the end of section 2.4, the result for $P^*(\underline{\phi})$ obtained in section 2.5 from the approximate recursion formula (2.4.29) is a faithful reflection of the universal coarse-grained spin configurations at the d=3 XY transition. Our suggestion at the conclusion of section 2.5, that the non-trivial aspects of the short-range order at criticality may reside in some angular distribution of the spins, then merits further investigation. We discuss the prospects for one such distribution in the concluding section that follows.

2.7 Conclusions and future prospects

In this chapter we have studied the critical properties of the O(n)-symmetric Heisenberg model of ferromagnetism, in terms of spin configurations $\underline{\Phi}_L$ that have been coarse-grained over length scale L.

In a direct extension of the configurational description of scaling in Ising-like systems (Bruce 1981), we have described the universal, scaling aspects of our system near criticality in a scaling theory for the probability distribution $P_L(\underline{\Phi})$ when L and the correlation length ξ are large (see e.g. (2.2.8)). Thus, the underlying patterns of short-range order (s.r.o.) themselves have universal characteristics near criticality, and the aim of our study has been to identify their nature from $P_L(\underline{\Phi})$.

In Section 2.3, we obtained an explicit form for the critical distribution $P^*_L(\phi^2)$, within the confines of a renormalised perturbation calculation for $n > 2$ and $d=2+\epsilon$, to lowest order in ϵ. The δ-function profile (2.3.33) signifies that at $O(\epsilon)$, fluctuations in phase are more important than fluctuations in amplitude in the restoration of symmetry at T_c. As $\epsilon \to 0$ then $T_c \to 0$ and the δ-profile is easily interpreted as characteristic of a critical system at its lower critical dimension. Bruce (1981) obtained the equivalent result for the d=1 Ising model: at $T_c(=0)$ block-spins have only two possible states, either "up" or "down", as characterised by a symmetric double δ-function profile for the Ising block-spin p.d.f.

The evolution of $P^*_L(\phi^2)$ as d increases was followed to one higher order in ε, at which interactions are included, in a calculation of the fixed-point moment ratio G^*. The result (2.3.35) characterises the smearing-out at $O(\varepsilon^2)$ of the δ-function profile at $O(\varepsilon)$. The spin-wave excitations with which the low-temperature expansion was developed cross over to critical modes at T_c. As to their nature, we noted that our calculation ignores the compactness of the O(n) symmetry (i.e. spins are really constrained to lie on an n-dimensional sphere); it is questionable, therefore, whether perturbation theory can really capture the nature of spin configurations at T_c.

In Section 2.5 we studied the d=3 XY model. We applied to it an approximate non-perturbative recursion formula, due to Bruce (1981), that relates $P_L(\Phi)$ to $P_{2L}(\Phi)$. The fixed-point $P^*(\Phi)$ of this formula has a non-Gaussian profile - figures (2.3),(2.4) - signifying the presence of non-trivial patterns of s.r.o. at criticality, but it does not reveal their nature. In Section 2.6 a Monte-Carlo simulation of the model reproduced this result surprisingly well - figures (2.8),(2.9). We concluded that a future investigation should consider some angular description of the spin configurations.

One intriguing description has already been discussed by Savit (1978,1980). Again, we have to consider global topology. The d=3 XY model has topological excitations which are closed vortex strings, or vortex strings which terminate on the boundary of the system. Vortex strings exist naturally on the dual lattice - their strength measures the number of revolutions the XY angles perform round a closed circuit on the original lattice. In its application to ^4He, these

strings represent vortices in bulk superfluid. Their appearance in the d=3 XY model can be made explicit via the Villain approximation (Villain 1975) followed by a duality transformation (Savit 1978,1980). The approximation is exact for the description of those strings which have strength less than or equal to one (Janke and Kleinert 1986). We shall not present details of the vortex loop representation here, but we shall mention its possible implications for the study we have undertaken.

Savit (1980) has argued that the usual order-disorder transition of the d=3 XY model may be associated with a transition involving the vortex loops. The picture, drawn qualitatively using energy-entropy arguments, is that at low temperatures there is only a low density of loops with small perimeters, in addition to the usual spin wave excitations. As we raise the temperature the density and size of loops increases, and at $T=T_c$ a phase transition occurs signalled by the appearance of configurations which are dense with vortex loops of all sizes. Above T_c we have a condensate of loops.

The implication that the vortex loop representation plays an important role at T_c has been substantiated in part by Janke and Kleinert (1986), who have shown from MC simulations of the Villain and XY models on 16^3 lattices that, in the case of the d=3 XY model, the Villain approximation is particularly accurate for temperatures at T_c and above (in contrast to the low temperatures for which it is usually derived). They conclude that in this temperature range the system is dominated by vortex loops of strengh 0, ± 1.

If this picture then is essentially correct, it provides an appealing description of scale-invariance at T_c in terms of a self-similar "alphabet soup" of (predominantly strength-one) loops on all length scales. We could not hope to have revealed this soup in the distribution of a cubic block-spin $\underline{\phi}_L$. In our MC simulation it would seem at first sight a considerable problem in pattern recognition to resolve a spin configuration into a configuration of vortex loops. Nevertheless, the above picture might tempt us to formulate a description of the s.r.o. near T_c in terms of a scaling form for the vortex loop size distribution, ultimately to be justified (or not) by a RG analysis of the vortex loop Hamiltonian itself.

CHAPTER 3

FINITE-SIZE SCALING STUDY OF 2D PERCOLATION

3.1 Introduction

So far, we have talked about scaling in the physics of a ferromagnet near its critical point: a problem of thermodynamics. In chapter 1 we saw how scale-invariance at criticality arose from the presence of a single diverging length-scale ξ, and in chapter 2 we studied its interpretation in terms of the underlying configurations (patterns) of spins.

This chapter discusses scaling in the physics of percolation: a problem of geometry (for reviews, see Essam 1980, Deutscher *et al* 1983). Percolation theory studies patterns made from bonds (or sites) on a lattice which are randomly occupied independently with probability p - for simplicity, usually one only considers regular lattices. The discussion of scaling takes place naturally in terms of the underlying configurations of clusters made up of sites connected to each other via occupied bonds (or via the bonds between occupied sites) - specifically it is large clusters that play the dominant role. For small p, the average cluster consists of only a few sites. As p → a critical value p_c, larger clusters appear until, at $p=p_c$, a cluster will form (with probability 1) which spans the entire lattice, thus providing an open pathway for the percolation of, say, some fluid across the lattice. Many analogues of this phenomenon occur in nature: fluid flow through porous rock,

conductivity in random resistor networks, the spread of epidemics.....

Percolation at p_c is an example of a geometric phase transition, from a state of local connectivity to one of macroscopic connectivity. The language of percolation draws heavily on that of thermal phase transitions. There is a characteristic length ξ called the pair-connectedness length, defined in analogy with (1.2.6) by

$$G(r) \sim e^{-r/\xi} , \quad r \to \infty \qquad (3.1.1)$$

where G(r) is the probability that two sites a distance r apart are connected on a finite cluster (we discount the spanning or "infinite" cluster).

As $p \to p_c$, all quantities scale with the length ξ which diverges, in analogy with (1.2.7), like

$$\xi \sim (p_c - p)^{-\nu_p} , \quad p \to p_c^- \qquad (3.1.2)$$

where ν_p is a percolation critical exponent, with a similar expression when $p \to p_c^+$. In terms of the underlying configurations, scale-invariance manifests itself in the self-similar, fractal or "Swiss cheese"-like structure of large clusters near p_c, over length scales up to ξ. Other analogies may be drawn straightforwardly using the relation between bond percolation and the Potts model (Kasteleyn and Fortuin 1969). Scaling relations between exponents are then identical to the ones originally discovered in the context

of magnetism.

In section 3.2 we discuss a recent controversy regarding the cluster "free energy" - the mean number of clusters - in two dimensions (2D), for which the currently-accepted singular behaviour has been challenged by Jug (1984). Following the description in section 3.3 of a fast, parallel algorithm for counting 2D clusters, we present results in section 3.4 of a numerical study of the free energy which we initiated on learning of the above challenge. A finite-size scaling analysis of our data supports the conventional singular behaviour as expressed by critical exponents and critical amplitude ratios. Section 3.5 presents a summary and conclusions.

3.2 A recent controversy regarding the cluster "free energy" in 2D

We are going to focus on the critical behaviour in two dimensions (2D) of the mean number of clusters (divided by the number of lattice sites) $K(p)$, which is like a free energy. Near p_c it has an analytic part and a singular part

$$K(p) = K_a(p) + K_s(p) \qquad (3.2.1)$$

where the analytic part may be expanded around p_c

$$K_a(p) = a + b(p-p_c) + c(p-p_c)^2 + d(p-p_c)^3 + \cdots \qquad (3.2.2)$$

while the singular part has the form

$$K_s(p) = D\,|p-p_c|^{2-\alpha_p} . \qquad (3.2.3)$$

It has been conjectured for 2D percolation that exponent values are known exactly as simple rational fractions, in particular that $\alpha_p=-2/3$ and $\nu_p=4/3$ (consistent with the hyperscaling relation (1.2.15)). This conjecture is a consequence of the (exact) mapping of percolation onto the $q \to 1$ limit of the q-state Potts model (Kasteleyn and Fortuin 1969), which in turn may be mapped onto the 2D Coulomb gas problem, whose critical behaviour may be found - under certain plausible assumptions - exactly (den Nijs 1979, Nienhuis *et al* 1980).

Alternatively, percolation may be identified with the $T \to 0$ limit of the dilute Ising model on the lattice sustaining the percolation process (Elliot *et al* 1960), for which a crossover in critical properties is held to take place as $T \to 0$, $p \to p_c$ (Stephen and Grest 1977, Lubensky 1977,1979). The values of the dilute Ising exponents α_d, ν_d..... are therefore currently accepted to be distinct from their percolation counterparts.

Recently, however, Jug (1985,1986) has presented evidence from numerical work and series expansion studies for his result (Jug 1984) that

$$K_s(p) = D(p-p_c)^2 \ln|\ln|p-p_c|| \qquad (3.2.4)$$

and hence effectively $\alpha_p = 0$, in contrast to (3.2.3). This result was derived for the bond percolation problem from a Grassmann Path Integral (GPI) treatment of the associated bond-diluted Ising model free energy f(T,p). The GPI representation (Samuel 1980) of the pure 2D Ising model allows a perturbative treatment of the effects of

small dilution q=1-p. A RG analysis finds q to be a marginal operator supplying only logarithmic corrections to the pure critical behaviour,' so effectively $\alpha_d=0$ and $\nu_d=1$ (Dotsenko and Dotsenko, 1982). The analysis of Jug (1984) appears to extend the calculation of, α_d to $q_c=1-p_c$; moreover, the numerical evidence of Jug (1985) is also consistent with the value $\nu_p=1$ and hyperscaling, suggesting that no crossover takes place at the percolation threshold T=0, $p=p_c$.

In section 3.4 we will present results of a numerical study (Dewar and Harris 1986), similar to that of Jug (1985), which we initiated (Dewar and Harris 1985) on learning of the above work. Our results are consistent with the "conventional" behaviour of equation (3.2.3). Recently, Adler (1986) has commented on the series expansion evidence of Jug (1985) by noting difficulties with the Padé analysis of $K_s(p)$ in the presence of the analytic background term (3.2.2). Moreover, Kesten (1986) has since noted that the form (3.2.4) *cannot* be correct since he has shown rigorously (Kesten 1983) that for bond or site percolation on the square lattice $K_s(p)$ is twice-continuously differentiable for all p in [0,1], including at p_c. Nevertheless, in the absence of a demonstration of *how* the GPI theory fails at p_c and in view of the supporting numerical evidence, it is important to re-examine the question raised by the result (3.2.4).

3.3 A parallel algorithm for counting clusters in 2D

As a preliminary to the next section, we introduce here the parallel cluster-counting algorithm which we used to study $K_s(p)$. This algorithm, due to CK Harris, counts the total number of clusters of connected sites on various types of 2D lattice. It is very

simple, an example of a "burning" algorithm, and we have implemented it on the ICL DAP machine in which processing elements operate simultaneously at each lattice site (see e.g. Flanders *et al* 1977 for a general description of the DAP). It is very efficient in practice because of its parallelism and because in identifying the connectivity of clusters only Boolean variables and operations are used.

To illustrate it, consider the typical configuration of figure (3.1a) containing three clusters on a 4 × 4 square lattice with planar boundary conditions, which is stored as a Boolean array (TRUE = occupied, FALSE = unoccupied). Iteration of the central steps of the algorithm systematically reduces all clusters to 1-site clusters, each of which augments the cluster total by one and is then removed. The reduction, using Boolean operations only, is performed in parallel across the entire lattice and is depicted in figures (3.1b-d).

The steps are

(1) Identify all occupied sites having no occupied nearest-neighbours to the north and east. There will be four types, shown in figures (3.2a-d). This step identifies the north and east "coasts" of all clusters.

(2) Then for each (a)-type site, count one cluster and remove the site. This step accumulates the cluster total.

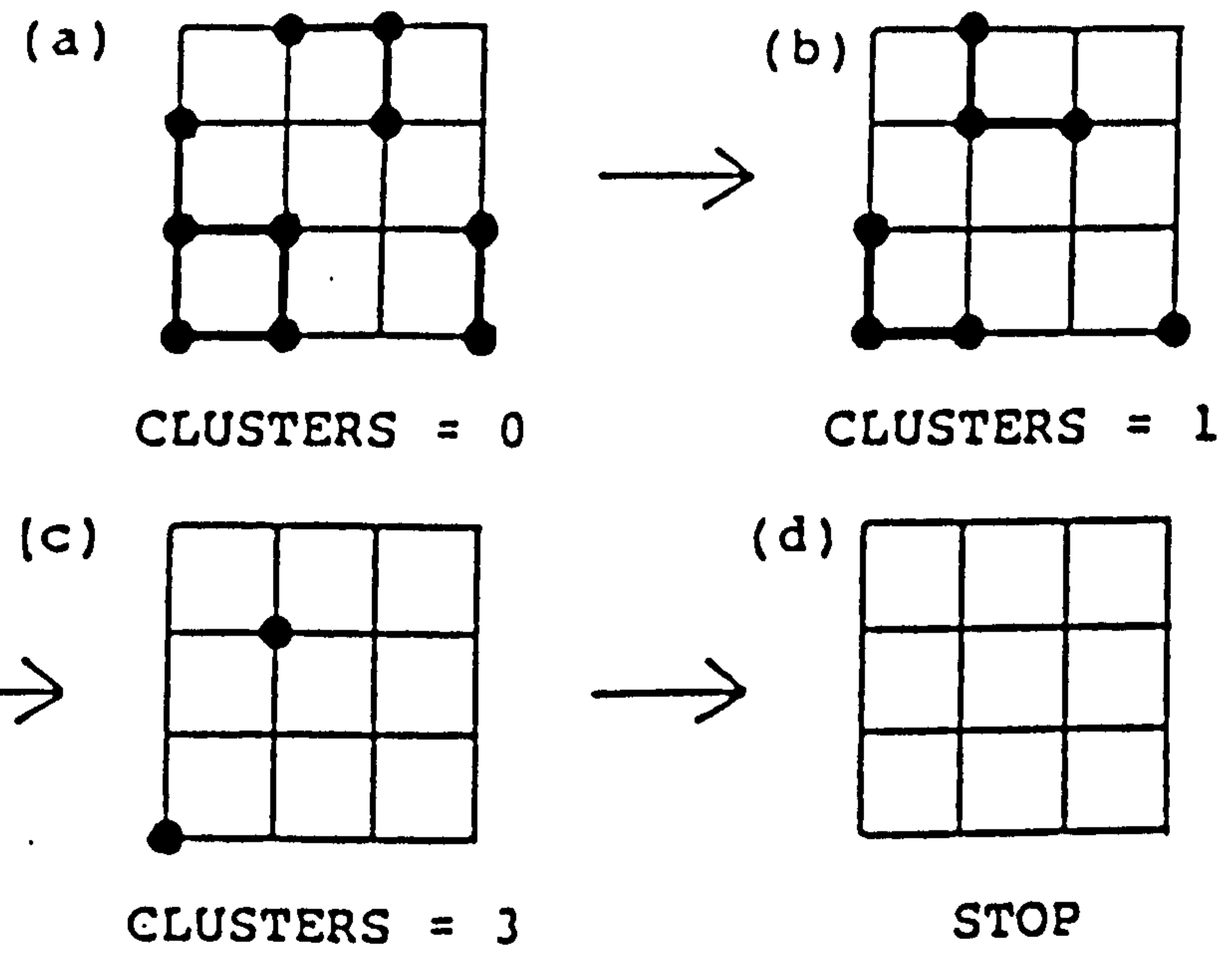

FIGURE (3.1). Illustrating the "burning" algorithm for counting clusters.

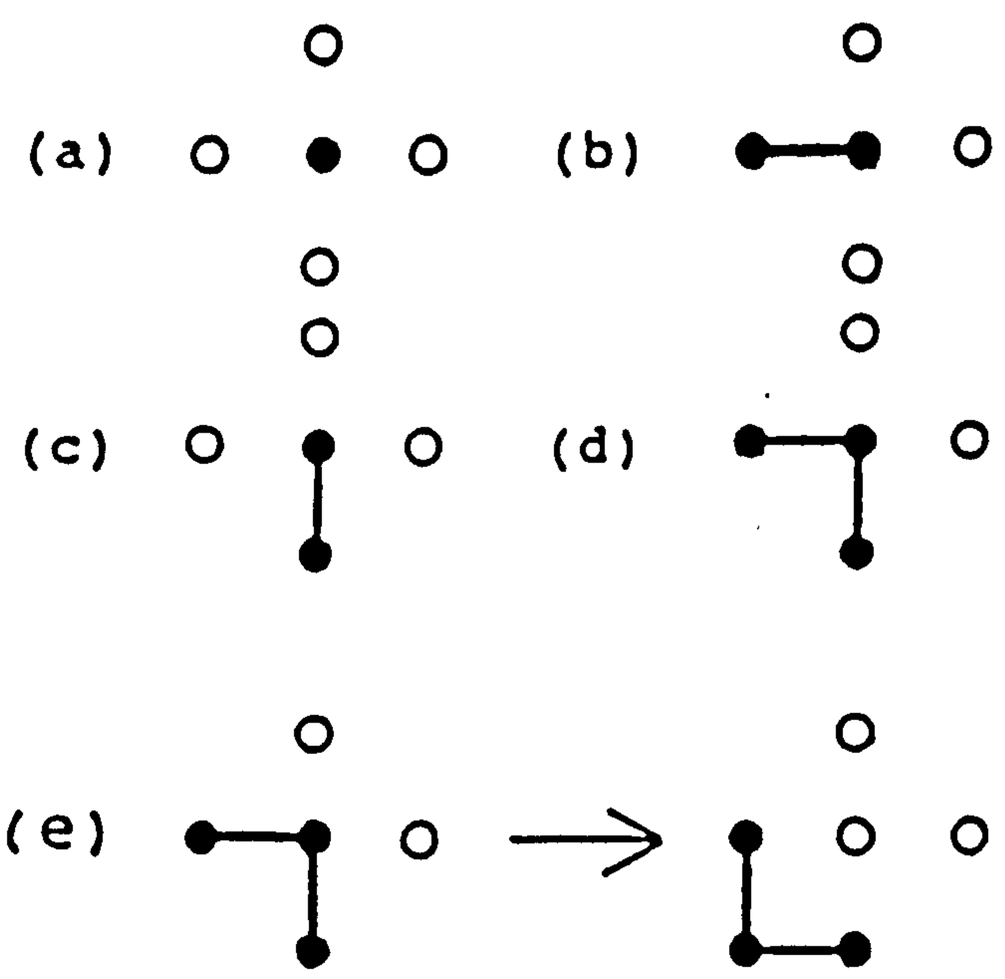

FIGURE (3.2). (a)-(d) Depicting sites with no connections to the to the north and east. (e) Indenting the north-east corners to create new dangling ends.

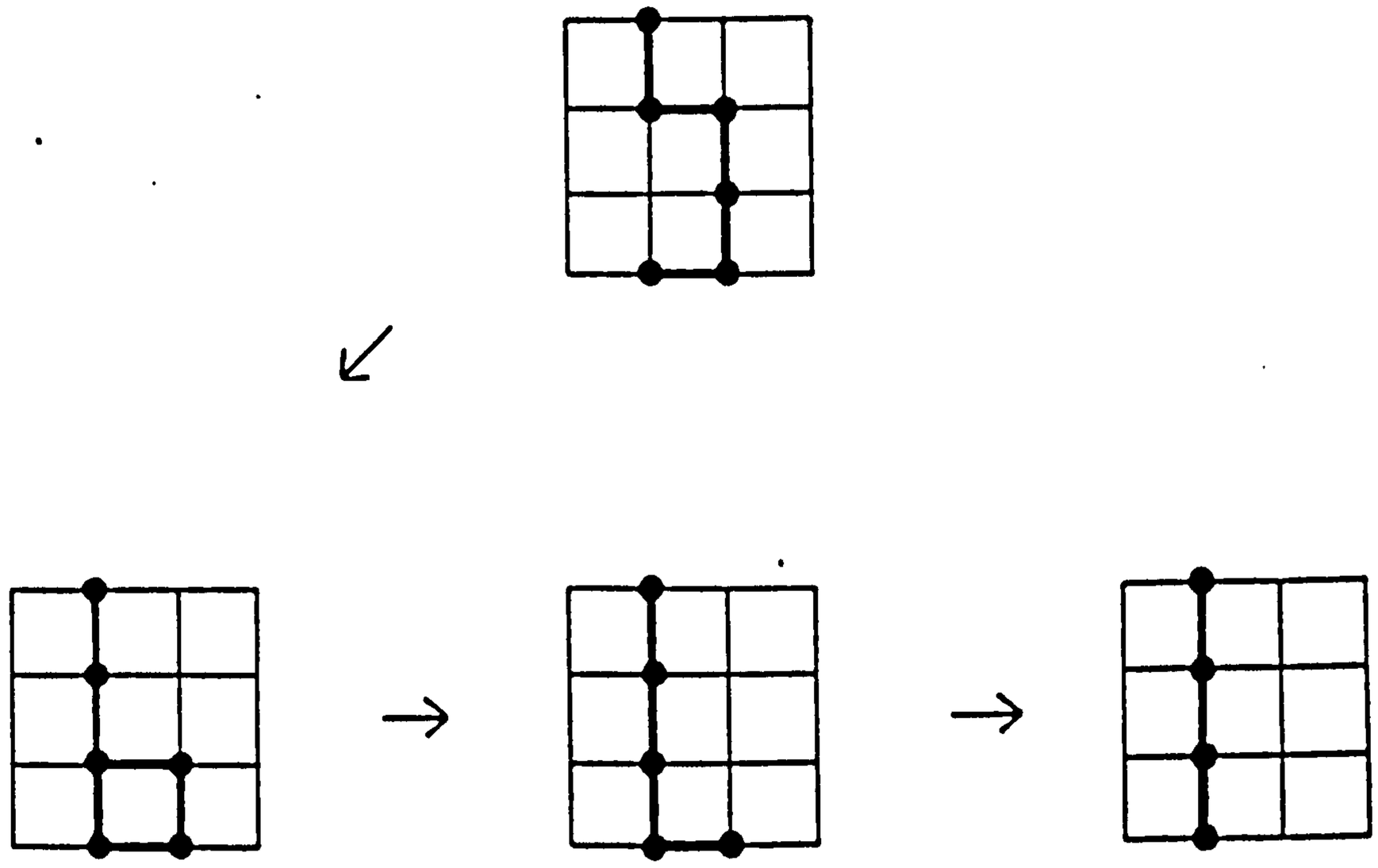

FIGURE (3.3). Reduction of a cyclicly-spanning cluster to a minimal loop.

(3) Now remove all sites of types (b) and (c). This step "burns off" the north- and east-dangling ends.

(4) Finally, replace the (d)-type sites with new occupied sites to the south-west (if not already occupied) as shown in figure (3.2e). This step indents the north-east corners to create new dangling ends. Also, since operations are done in parallel, no two clusters are inadvertantly joined by this step (e.g. see figure (3.2a-b)).

Repeat steps (1)-(4) until no sites remain.

We note that for cyclic boundary conditions, some (cyclicly-spanning) clusters only get reduced to minimal loops wrapped round the lattice, so that the algorithm will not terminate. Figure (3.3) depicts an example. These remaining clusters can be counted, one by one, by a parallelised "ants-in-the-labyrinth" algorithm (Dewar and Harris 1986) - i.e. put an ant on some remaining site; this ant places offspring on each of the nearest-neighbour occupied sites; the offspring multiply likewise until that entire cluster is populated; count one cluster, remove it from the configuration and repeat until no sites remain. The algorithm is easily modified to count both site- and bond-occupied clusters on other regular lattices.

The above analysis is limited to relatively small lattices because the entire configuration must be stored in the computer. For a

lattice of linear size L, the time to analyse a configuration increases as L^2. In practice, on the DAP, we enhanced the efficiency for lattice sizes $L < 64$ by storing and analysing $(64/L)^2$ configurations simultaneously.

For the bond percolation problem at $p_c=0.5$ on a L=32 square lattice with cyclic boundary conditions, the algorithm implemented on the DAP analyses 1.6 million configurations per hour. This performance is to be compared with 70,000 configurations per hour for the same problem on a L=30 lattice using a serial algorithm on the CRAY1 machine (Jug 1985).

3.4 Finite-size scaling study of the "free energy"

Finite-size scaling

Due to the weakness of the singularity in (3.2.3) or (3.2.4), the quantity to look at numerically is $K'''(p)=d^3K(p)/dp^3$. For a lattice of linear size L one then expects a divergence in $K'''(p_c,L)$ as $L\to\infty$.

Finite-size scaling (see e.g.,review by Barber 1983) is a powerful tool for the extraction of useful information in this limit. In the present context it states that on a finite lattice, when L and $\xi(p)$ are large enough, the (singular) bulk quantity $K_s'''(p,\infty)$ is modified to

$$K_s'''(p,L) = K_s'''(p,\infty)\, f(L/\xi_\infty) \qquad (3.4.1)$$

in which ξ_∞ is the bulk pair-connectedness length of (3.1.2). The function f is universal in the sense that it does not depend on the

type of lattice, but it does depend on the shape of the lattice block, on boundary conditions (cyclic, free.....) and on the function $K_s'''(p,\infty)$. Statements such as (3.4.1) can be understood within the framework of the renormalisation group (Brezin 1982).

From the fact that the LHS of (3.4.1) is finite as $p \to p_c$ with L fixed, one deduces immediately the asymptotic form of f(x) as $x \to 0$ required to cancel the divergence of $K_s'''(p,\infty)$ on the RHS. For the divergence derived from (3.2.3) one deduces

$$f(x) \underset{x \to 0}{\longrightarrow} C[\ell] \; x^{(1+\alpha_p)/\nu_p} \qquad (3.4.2)$$

where we remind ourselves that constant $C[\ell]$ depends on the geometry of lattice block ℓ. Hence the quantity $K'''(p_c,L)$ should behave like

$$K'''(p_c,L) = A + B\,L^{(1+\alpha_p)/\nu_p}, \quad L \to \infty \qquad (3.4.3)$$

From (3.2.2) we see that constant A, the analytic part, has bulk value A=6d. Constant B is a critical amplitude which we will later relate to the critical amplitude D in (3.2.3).

If the conjectured exponent values $\alpha_p=-2/3$ and $\nu_p=4/3$ are valid, we expect

$$K'''(p_c,L) = A + B\,L^{1/4}, \quad L \to \infty \qquad (3.4.4)$$

If, however, the GPI result (3.2.4) is valid, we expect

$$K^{III}(p_c, L) = A + B(L)\, L^{1/\nu_p} \quad , \quad L \to \infty \qquad (3.4.5)$$

in which B(L) contains logarithmic corrections; the GPI method has, as yet, no prediction for ν_p, although hyperscaling would imply the value $\nu_p=1$.

Numerical study of the free energy

We will use the notation

G = a configuration of occupied bonds or sites on a lattice of linear size L.

N = total no. of bonds or sites on the lattice.

$N_o(G)$ = no. of occupied bonds or sites in G.

$n_c(G)$ = no. of clusters per site in G.

Now, the average of $n_c(G)$ over M configurations $\{G_i; i=1,...M\}$, sampled during a computer run, is an estimate of K(p,L) and its explicit dependence on p may be exposed by writing

$$K(p,L) \simeq \langle n_c(G) \rangle_{\{G_i\}} = \frac{\sum_{i=1}^{M} p(G_i)\, n_c(G_i)}{\sum_{i=1}^{M} p(G_i)} \qquad (3.4.6)$$

where $p(G_i)$, the probability of sampling G_i, is given by

$$p(G_i) = p^{N_o(G_i)} (1-p)^{N - N_o(G_i)} \qquad (3.4.7)$$

Following Jug (1985), we differentiate (3.4.6) three times w.r.t. p. At $p=p_c=0.5$ (the case we consider here) this yields a fluctuation formula for the quantity of interest:

$$K'''(p_c,L) = 32\{\langle N_o n_c\rangle - \langle N_o\rangle\langle n_c\rangle\} + 64\{\langle N_o^3 n_c\rangle - 3\langle N_o\rangle\langle N_o^2 n_c\rangle$$
$$+ 6\langle N_o\rangle^2\langle N_o n_c\rangle - 3\langle N_o^2\rangle\langle N_o n_c\rangle - 6\langle N_o\rangle^3\langle n_c\rangle \quad (3.4.8)$$
$$+ 6\langle N_o\rangle\langle N_o^2\rangle\langle n_c\rangle - \langle N_o^3\rangle\langle n_c\rangle\}$$

where <.....> stands for an average over the configurations $\{G_i\}$.

Using the "burning" algorithm of section 3.3, $n_c(G)$ was analysed for bond percolation on the square lattice (BSQ) and site percolation on the triangular lattice (ST), each of which has p_c=0.5. Cyclic boundary conditions were chosen - free boundary conditions give a slower rate of convergence to the asymptotic scaling regime in which (3.4.4) and (3.4.5) are valid, due to the excess clusters artificially created by truncation at the lattice edges.

Our results for BSQ and ST for lattice sizes L=8,12,16,24 and 32 are shown in figure (3.4), where they are compared with those of Jug (1985) (BSQ for lattice sizes L=8,12,16,24,30). Our data yields straight line slopes in the log-log plot of 0.28 ± 0.03 (BSQ) and 0.25 ± 0.02 (ST), consistent with the slope 1/4 expected from the "conventional" prediction (3.4.4) - it is understood that constant A=6d has been subtracted off; a duality argument (Sykes and Essam 1964) tells us that for BSQ (ST), d = 0 (1).

Jug's data appears to lie on a straight line of slope 1, consistent with the GPI prediction (3.4.5) together with the value ν_p=1 expected from hyperscaling.

In our analysis, we have adopted the following approach to reduce the considerable fluctuation in the value of $K'''(p_c,L)$ as given by (3.4.8). Consider the mean number of clusters per site $\overline{n_c}(N_o)$ for configurations with a given number of occupied bonds (or sites) N_o.

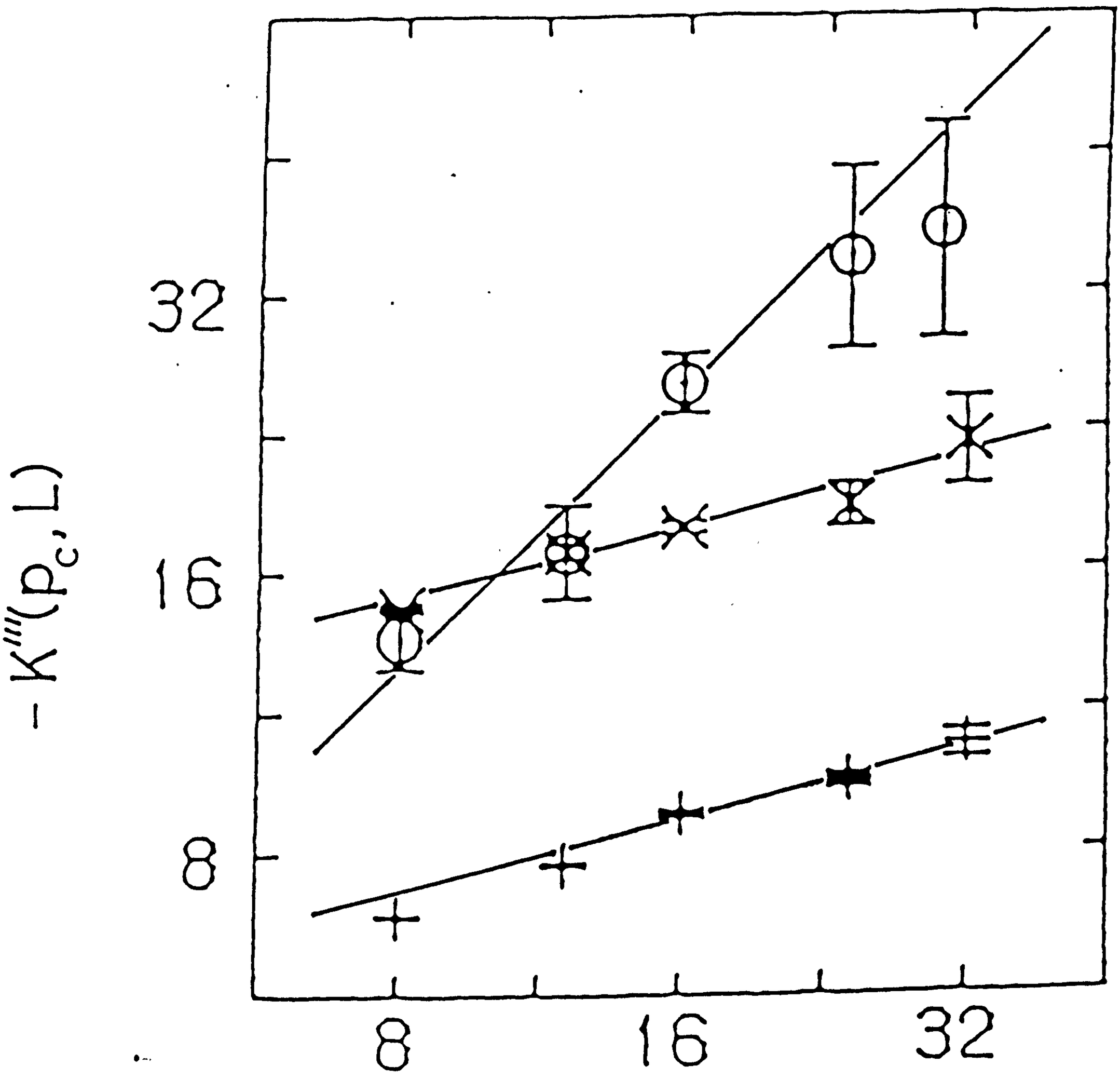

FIGURE (3.4). Divergence of $K'''(p_c,L)$ with L.

× = BSQ, + = ST data of present work; o = BSQ from Jug (1985).

It is easy to show that when $p=p_c$, the Taylor expansion of $\overline{n}_c(N_o)$ about the mean $N_o=Np_c$ is

$$\overline{n}_c(N_o) = a + b\,\frac{(N_o-Np_c)}{N} + c\,\frac{(N_o-Np_c)^2}{N^2} + \cdots\cdots \qquad (3.4.9)$$

where a,b,c are (up to corrections $\sim O(1/L,1/L^2)$) the (bulk) constants appearing in the expansion (3.2.2). They are either known analytically (Sykes and Essam 1964) or estimated from series (Domb and Pearce 1976). They may also be estimated from the numerical simulation itself - using the averages $\langle n_c\rangle$, $\langle(N_o-Np_c)n_c\rangle$, $\langle(N_o-Np_c)^2n_c\rangle$ - as a useful check on the correctness of the algorithm. The results from our BSQ data (a=0.099,b=-0.98,c=4.16) and ST data (a=0.018,b=-0.24,c=1.33) are in excellent agreement with both these references.

Now, when $K'''(p_c,L)$ of (3.4.8) is averaged over a large but finite number M of configurations, the b and c terms in (3.4.9) contribute negligibly to its mean but substantially to its fluctuation. Therefore in the fluctuation formula (3.4.8) we substitute for n_c the decomposition

$$n_c = n_c^* + b\,\frac{(N_o-Np_c)}{N} + c\,\frac{(N_o-Np_c)^2}{N^2} \qquad (3.4.10)$$

then subtract off the contribution arising from the b and c terms. The effect of subtracting off this noise is illustrated in figure (3.5).

In addition we recall from section 3.3 that the "burning" algorithm does not reduce completely certain spanning clusters on

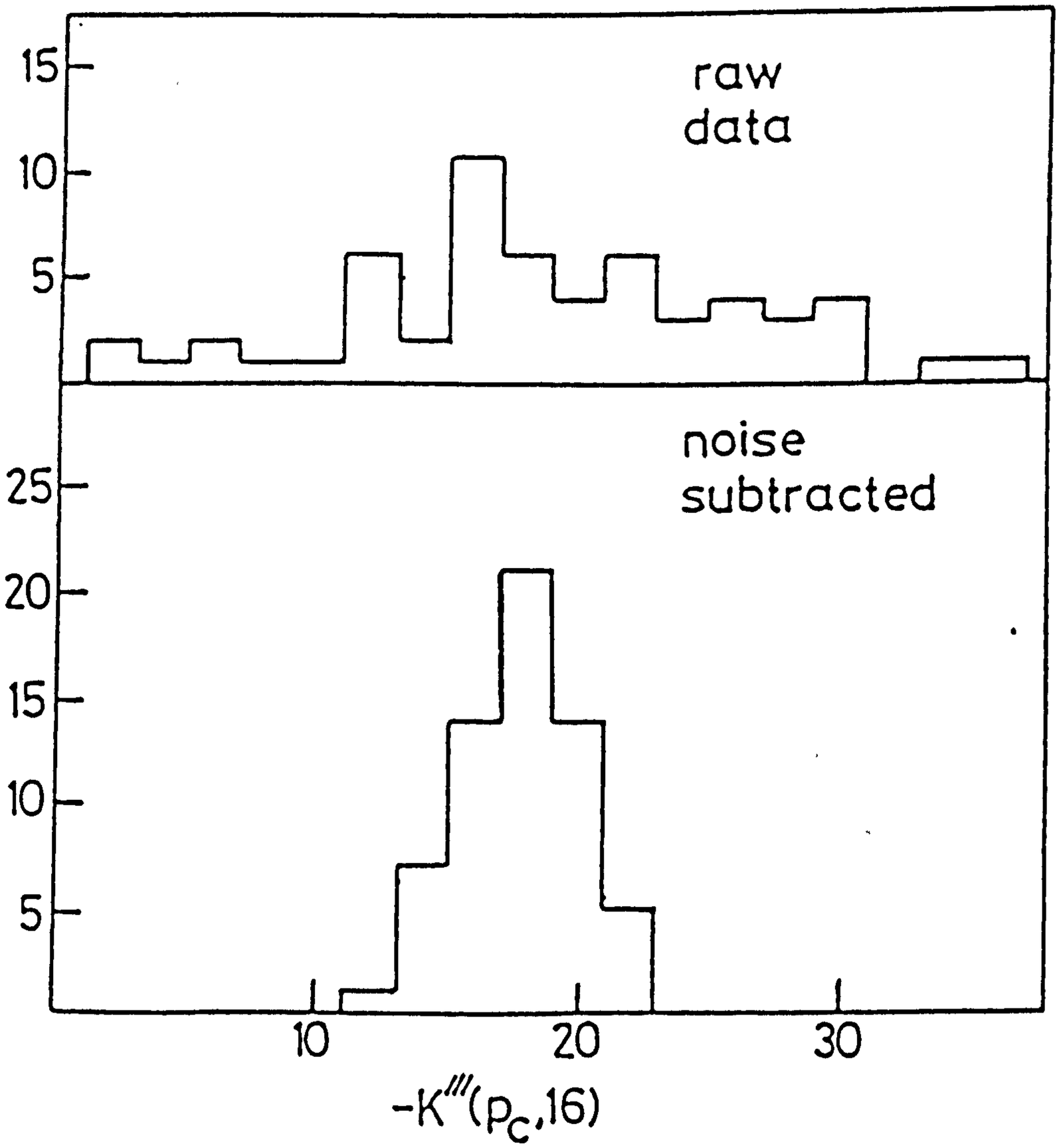

FIGURE(3.5). Effect of noise reduction for $K'''(p_c,16)$, BSQ. 1 box = average over 1638400 configurations, total histogram = 62 boxes.

lattices with cyclic boundary conditions. As we discussed, such remaining clusters can be counted by an "ants-in-the-labyrinth" algorithm, although in practice remaining sites were taken to constitute a single spanning cluster contributing one to the cluster total. We have verified (more details in section 3.5) that the effect of the relatively rare extra spanning clusters on the value of $K'''(p_c,L)$ is negligible on the scale of one standard deviation - there is only one spanning cluster in the bulk at p_c - thus enabling a gain in speed of the algorithm to 2 million configurations per hour for the BSQ problem on a L=32 lattice.

In this way, error bars have been reduced sufficiently to indicate a clear discrepancy between the two sets of BSQ data in figure (3.4).

Critical amplitudes

Figure (3.6) shows the fit of our data to the form $K_s'''(p_c,L)=BL^{1/4}$ (ST data, fit to last four points). Further evidence in support of the conventional theory of 2D percolation is obtained from the resulting amplitude ratio $r \equiv B_s/B_t$ (where the subscripts s and t refer to BSQ and ST respectively):

$$r = 2.09 \pm 0.02 \qquad (3.4.11)$$

A theoretical estimate of r may be obtained as follows, based on the conventional picture and exploiting estimates by Domb and Pearce (1976) for the critical amplitude D in (3.2.3).

Denote $\varepsilon = (p-p_c^x)/p_c^x$ where x refers to the lattice type. From (3.2.3) and hyperscaling, the singular part of the bulk free energy

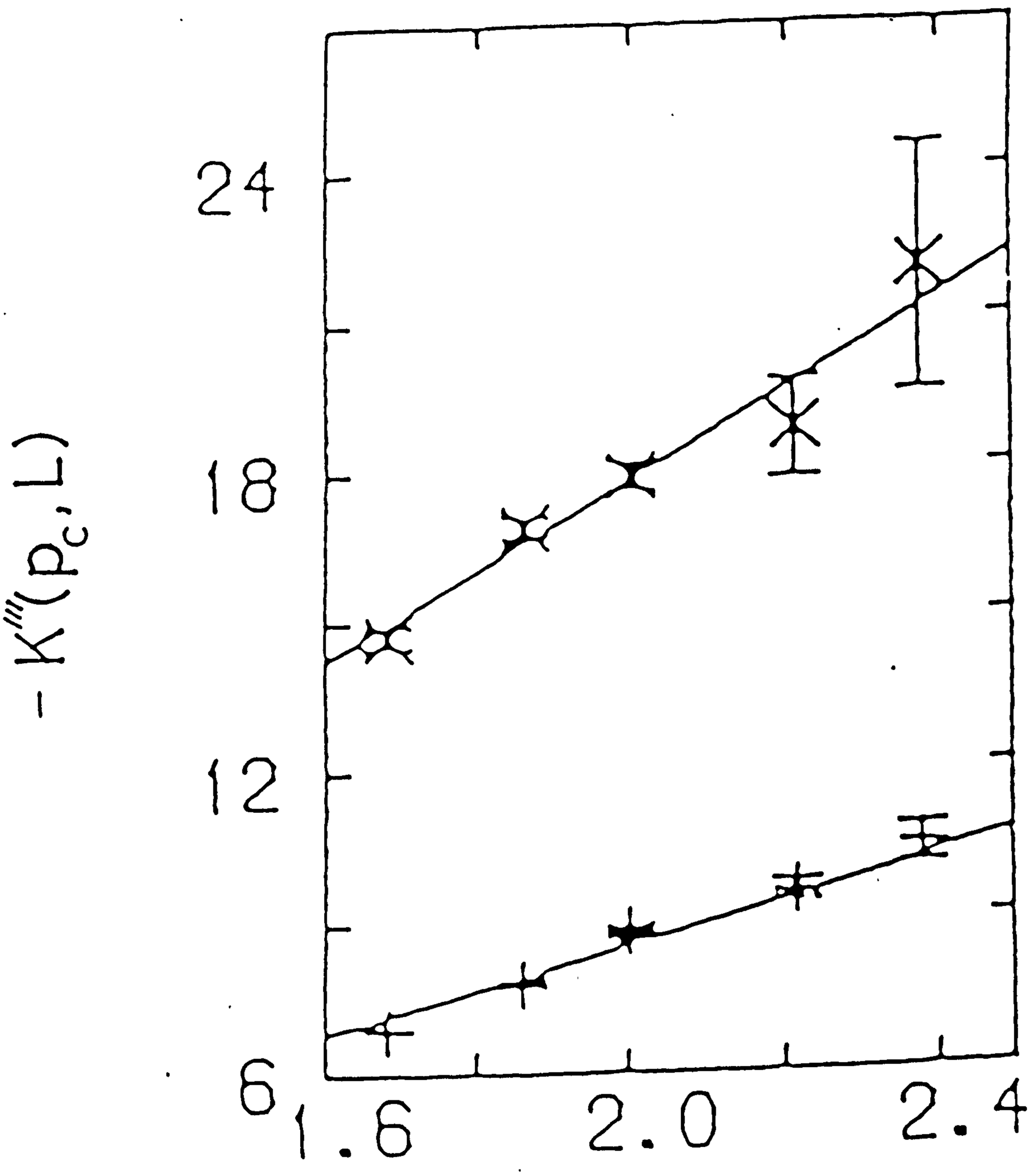

FIGURE (3.6). Fit to $K'''(p_c,L)=BL^{1/4}$.
× = BSQ, + = ST data of present work.

per site has the form

$$K_s(p,\infty) = D_x (p_c^x)^{d\nu_p} (K_o^x \xi_x)^{-d} \qquad (3.4.12)$$

where $\xi_x^{-1} = K_o^x \varepsilon^{\nu_p}$ is the inverse pair-connectedness length. If ρ_x is the density of lattice sites we may also write

$$\therefore K_s(p,\infty) = F \rho_x^{-1} \xi_x^{-d} \qquad (3.4.13)$$

where two-scale-factor universality (Stauffer *et al* 1972) tells us that F, the (singular) free energy of a volume ξ_x^d, is a universal constant independent of lattice type. (3.4.12) and (3.4.13) imply

$$\left(\frac{K_o^x}{K_o^y}\right)^d = \left(\frac{\rho_x D_x}{\rho_y D_y}\right) \cdot \left(\frac{p_c^x}{p_c^y}\right)^{d\nu_p} \qquad (3.4.14)$$

We are interested in $K_s'''(p_c,L)=B_x L^{3/\nu_p-d}$. From (3.4.12) we find

$$K_s'''(p,\infty) = d\nu_p(d\nu_p-1)(d\nu_p-2) D_x (p_c^x)^{d\nu_p-3} (K_o^x \xi_x)^{3/\nu_p - d} \qquad (3.4.15)$$

By inserting (3.4.15) and the asymptotic expression (3.4.2) for f(x) into the finite-size scaling form (3.4.1), and then eliminating K_o^x/K_o^y using (3.4.14), we get

$$\tau = \frac{B_x}{B_y} = \frac{C[x]}{C[y]} \left(\frac{\rho_x}{\rho_y}\right)^{-1} \left(\frac{\rho_x D_x}{\rho_y D_y}\right)^{3/d\nu_p} \qquad (3.4.16)$$

for the ratio of critical amplitudes in finite-size scaling. In the present case, d=2 and $\nu_p=4/3$ conventionally, lattice types x=s and y=t, $\rho_x=1$ and $\rho_y=2/3^{1/2}$, and (Domb and Pearce 1976) $D_x=-8.48(3)$ and $D_y=-4.370(15)$. If we had lattice blocks of the same shape, we would

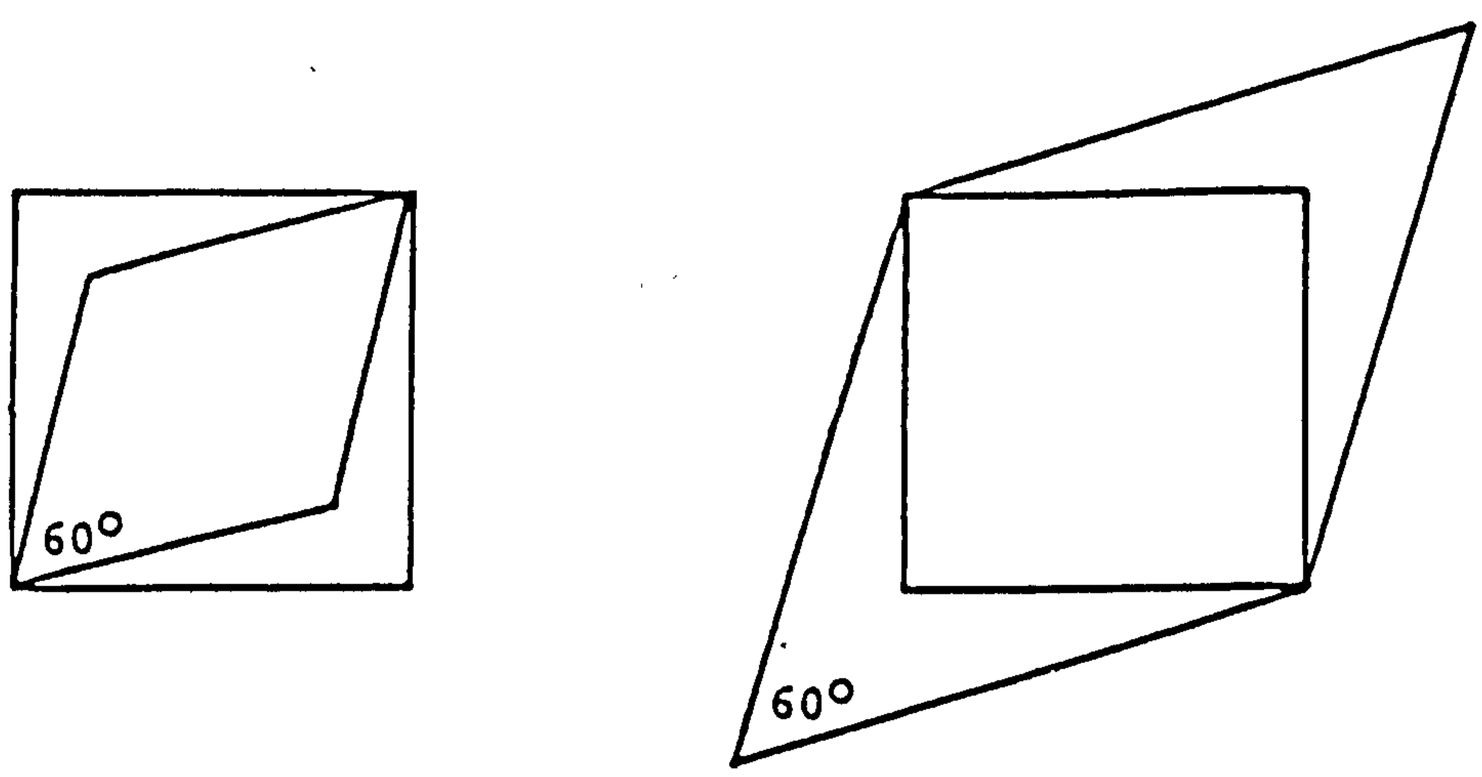

FIGURE (3.7). Block geometry that places bounds on the measured critical amplitude ratio r (Dewar and Harris 1986).

then predict

$$\tau = 2.08 \pm 0.02 \qquad (3.4.17)$$

Such a good agreement with the measured value (3.4.11) may be fortuitous since our lattices had different shapes - they were squares, side L, for BSQ and 60^{o} rhombuses, side L, for ST. By considering the inequalities between the free energies of lattice blocks with the geometries depicted in figure (3.7), one can show straightforwardly (Dewar and Harris 1986) that for our lattices, r is bounded above and below like

$$1.97 \pm 0.02 \leq \tau \leq 2.26 \pm 0.02 \qquad (3.4.18)$$

Even if we are not to attach too much significance to (3.4.17), the fact that our measured value of r lies comfortably within these bounds strongly suggests we have reached the asymptotic scaling regime with the lattice sizes that we used, where a picture emerges consistent with the conventional theory of 2D percolation.

3.5 Conclusions

Following a recent controversy, we have presented numerical evidence for the validity of the conventional picture of the cluster "free energy" K(p) at $p=p_c$.

Two important questions remain to be answered. First, what is the reason for the discrepancy between the two sets of BSQ data which are depicted in figure (3.4) and which attempt to estimate precisely the

same quantity? Second, in view of the analytic statement by Kesten (1986), why does the GPI theory fail at $p=p_c$?

Following numerous program checks, we are unable to answer the first. For instance, Jug quite rightly points to our procedure of neglecting extra spanning clusters as a possible source for the discrepancy. However, we have demonstrated that those clusters neglected have a negligible effect on the measured value of $K'''(p_c,L)$, as follows.

We have estimated the fraction of sampled configurations that contained more than one cyclicly-spanning cluster and for BSQ we find it is 0.00094,0.00071,0.00066 for L=8,16,32 respectively. This supports the expectation that this fraction tends to zero for large L - there is only one spanning cluster in the bulk at p_c - and that consequently any effect on $K'''(p_c,L)$ should decrease with L. It is then difficult to see this as the source of the above discrepancy which increases with L.

To establish this, we have re-analysed $K'''(p_c,16)$, counting every cluster of each sampled configuration with the aid of the "ants" algorithm. From one short run of 1638400 configurations, this gives a value $K'''(p_c,16) = -12.5254$ to be compared with -12.5167 from the neglect of extra spanning clusters. From 54 such runs combined we reproduce our original estimate $K'''(p_c,16) = -17.9 \pm 1.1$. The effect of extra spanning clusters therefore is negligible in comparison to one standard deviation. The discrepancy remains.

We have not addressed ourselves to the second question. In the absence of published details, the analytic prediction of Jug (1984) is difficult to examine. At first glance however, it would appear doubtful that the crossover at the point $T=0$, $p=p_c$ (or lack of it) can be described within an expansion in dilution $q=1-p$. Even if a lack of crossover is clearly established by the GPI method, it is possible that the GPI representation of the dilute Ising model breaks down at some value $q<q_c$ of the coupling constant, in a classical analogy with the mapping between 2D bosonic and fermionic theories established by Coleman (1975).

CHAPTER 4

SCALING IN A MODEL OF IRREVERSIBLE GROWTH

4.1 Introduction to scaling in growth models

In chapters 2 and 3 we have seen how the scaling behaviour at phase transitions may be studied in terms of underlying patterns possessing some sort of scale-invariance.

Recently it has become clear that scale-invariant "fractals" and other objects with interesting scaling properties are manifestly apparent in many other phenomena of physics, chemistry and biology (Mandelbrot 1982). Among them are several phenomena associated with processes of growth and aggregation. Several models, which lead to the formation of such objects, have been introduced to describe for instance the growth of solidification fronts, flame fronts, dielectric breakdown, chemical reagents, epidemics and tumors (for reviews, see Family and Landau 1984, Pietronero and Tosatti 1985). For the physicist, the point of these models is to help him to understand how the properties of a macroscopic cluster or growth pattern depend on the microscopic rules for its growth.

A general feature is that the growth or aggregation process occurs mainly at an "active" zone on the cluster's surface, with interesting scaling properties (Plischke and Racz 1984, Family and Viscek 1985). For this reason one focuses attention on the surface structure. One

finds that surface scaling properties are, to some degree, independent of the microscopic rules for growth (see e.g. Jullien and Botet 1985, Family 1986). Then an obvious task is to identify universality classes of growth processes that share the same scaling properties (Kardar *et al* 1986) and to explain how this scaling and universality arise.

In this chapter we examine the surface properties of a simple discrete-time lattice model of random epidemic growth, first studied by Richardson (1973), who called it G[p]. The parameter p controls the virulence of the epidemic. In section 4.2 we define the model G[p] and present numerical evidence of scaling properties in two dimensions obtained from simulations performed on the ICL DAP (see e.g. Flanders *et al* 1977 for a description of this machine). We find two independent characteristic scales in the model, describing the static and dynamic scaling properties of the surface. The two scaling properties are combined into a single dynamic scaling form for the surface width. We argue that this scaling form is universal (independent of p) but that p controls the size of the scaling region, and thus induces important corrections to scaling.

In section 4.3 we compare our results with previous numerical results for other models of growth and aggregation, and note the emergence of universality classes. Very recently, Kardar *et al* (1986) have studied a Langevin equation which gives a phenomenological description of the local growth of a surface in continuous space and time. This equation appears to account for the results of a variety of growth models - including the results of our simulation of G[p] - in which universality classes may be identified using the dynamical

RG (Hohenburg and Halperin 1977). In section 4.4 we discuss the physical content of this equation in its description of G[p], and thereby identify the essential large-distance, long-time physics of this model. The universal scaling features of the surface of G[p] can then be understood in terms of the ideas of chapter 1. Section 4.5 presents our conclusions.

4.2 Growth model G[p]: numerical simulation

We have studied the following version of a model of random epidemic growth first studied by Richardson (1973): growth takes place in discrete time steps on a square lattice inside a strip of width L with cyclic boundary conditions at the edges of the strip (figure (4.1)). Lattice sites are either healthy or infected. At time t=0, all sites are healthy except for sites in the bottom layer which act as seeds for the epidemic. Then at time t the rule is that a healthy site becomes infected with probability p if it has at least one infected nearest-neighbour, and with probability 0 otherwise. Once infected, a site never recovers. Clearly, the value of p measures the virulence of the epidemic. Richardson calls this growth model G[p].

Since at each time step the entire surface is allowed to grow at once, the parallel features of the ICL DAP are uniquely suited to the numerical simulation.

Typical growth patterns for L=64 are displayed in figure (4.2). Only the surface layers are shown; the bulk of a growth pattern is compact (Richardson 1973) because all holes eventually get filled up.

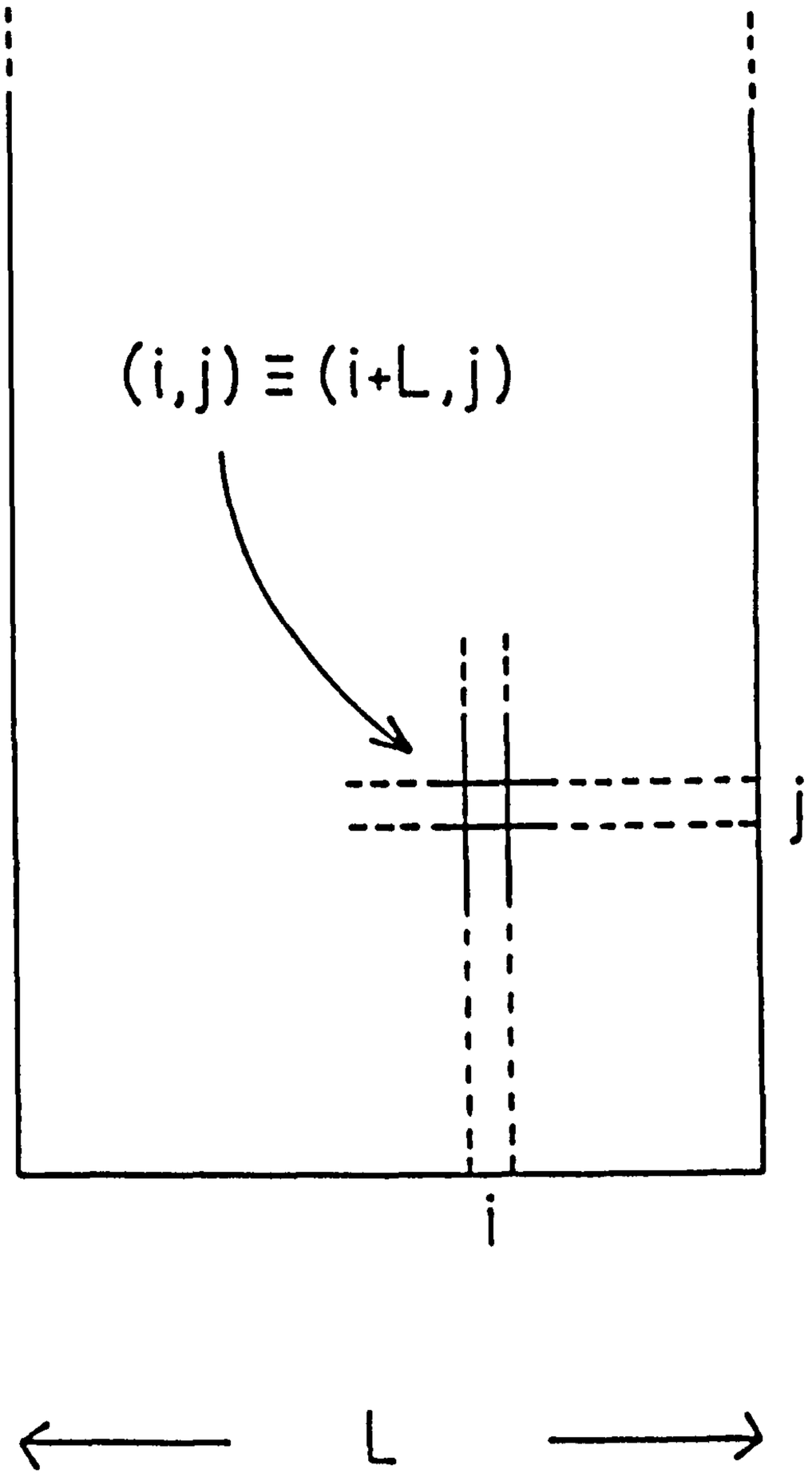

FIGURE (4.1). Strip geometry with cyclic boundary conditions at the edges.

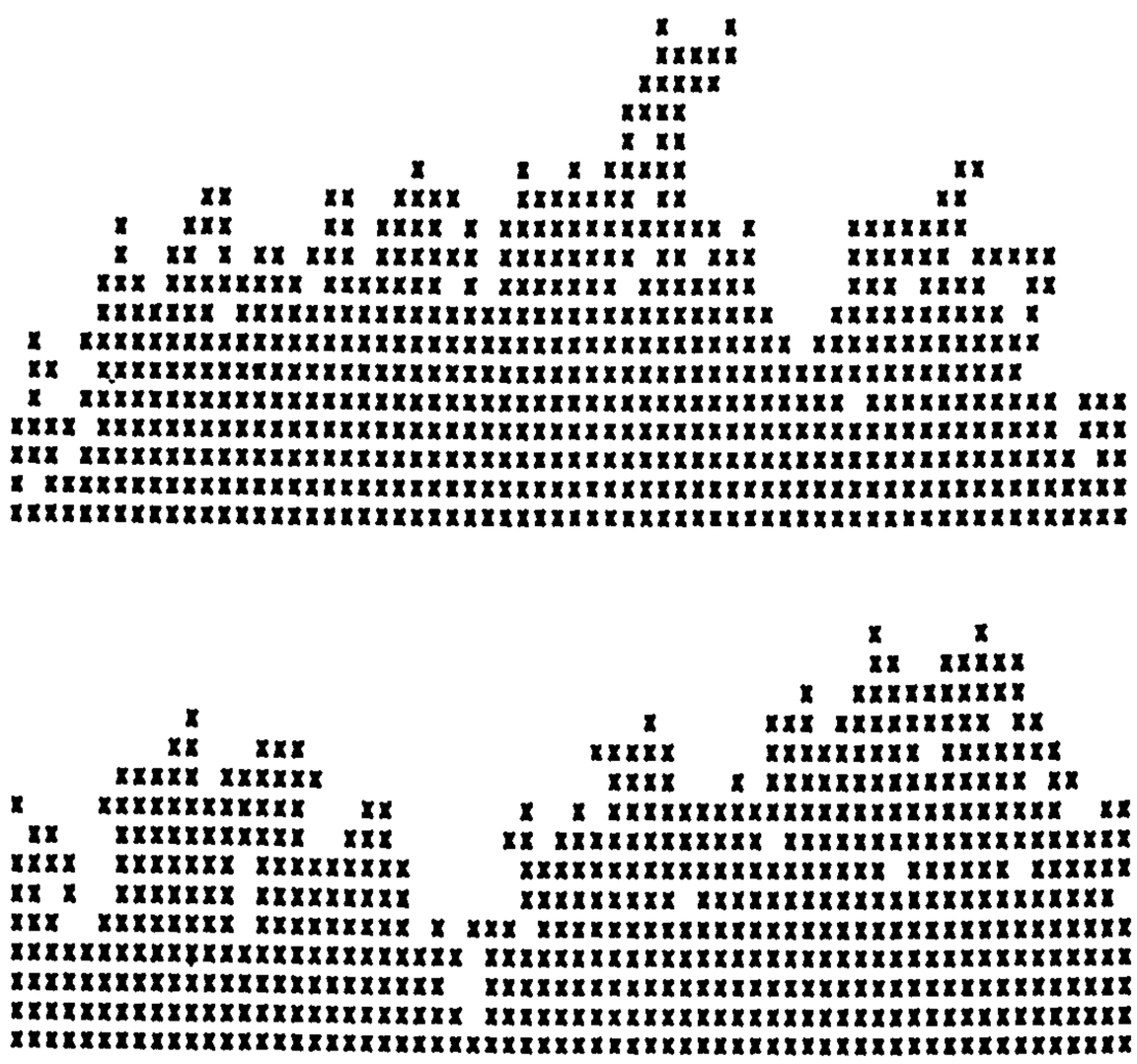

FIGURE (4.2). Typical growth patterns from epidemic model G[p].

Although the mass of the pattern is not fractal, the surface is rough. Figure (4.2) illustrates how the surface becomes less rough and has fewer holes as p increases.

Now we define exactly what we mean by the surface. It is the set of all growth sites on the pattern, where a growth site is a healthy site with at least one infected nearest-neighbour. We characterise the surface roughness by the surface thickness σ, defined from the variance

$$\sigma^2 = \frac{1}{N_g} \sum_{i=1}^{N_g} (z_i - \bar{z})^2 \qquad (4.2.1)$$

where the sum is over the N_g growth sites, z_i is the height of the i^{th} growth site above the bottom layer and

$$\bar{z} = \frac{1}{N_g} \sum_{i=1}^{N_g} z_i \qquad (4.2.2)$$

is the mean height of the surface. When there are some holes, their surface is included for convenience in the calculation of the surface thickness.

In this model, the surface thickness σ depends on three parameters: the growth probability p, the time-step t and the strip width L. The simulation results, averaged over 1000 independent growth histories, are illustrated in figure (4.3), which shows the dependence of $\sigma(p,t,L)$ on t and L when p=0.5. Similar growth profiles are obtained for other values of p.

FIGURE (4.3). Surface thickness $\sigma(0.5, t, L)$

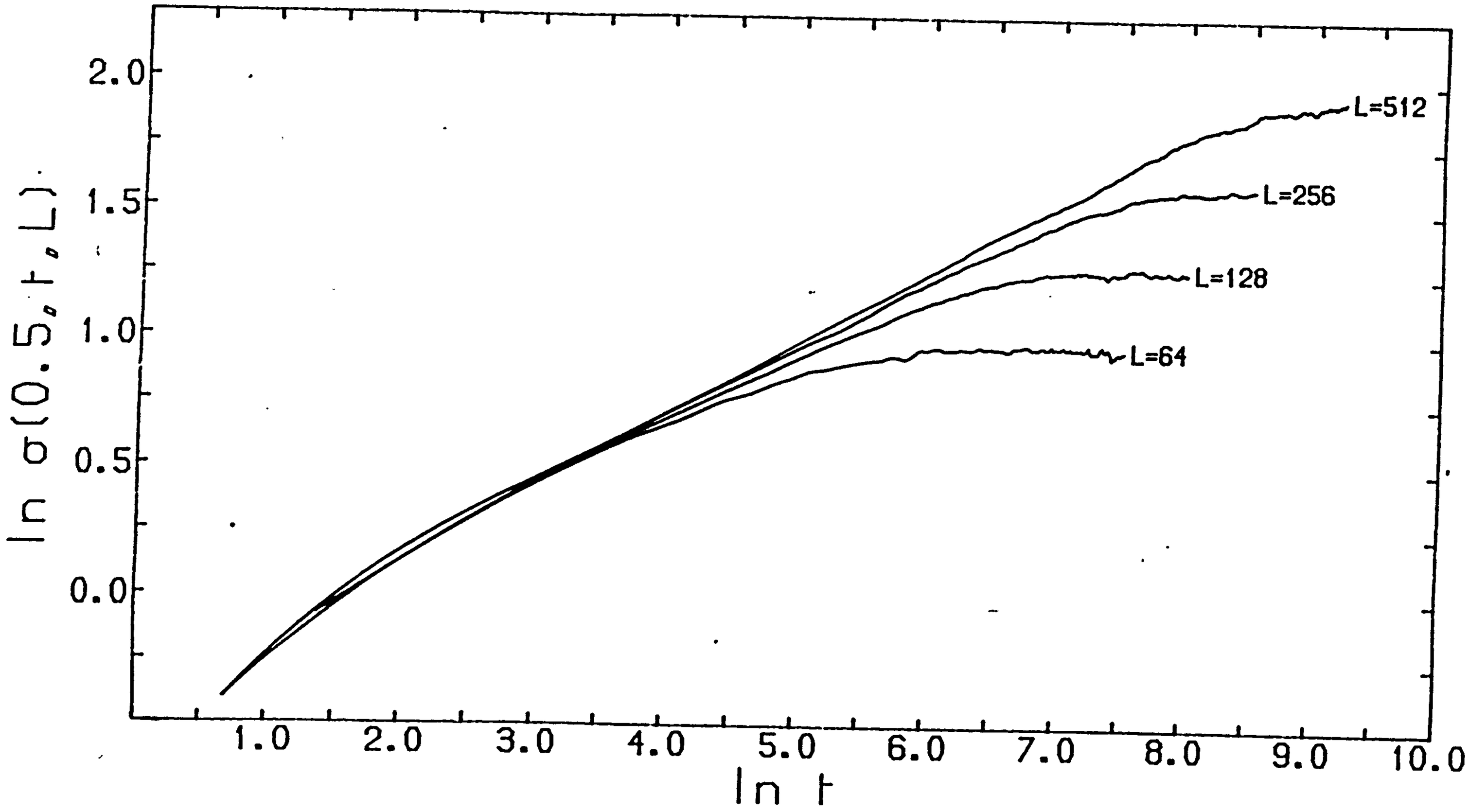

For values of t in the growth region 1 << t << L,

σ varies with t as

$$\sigma \sim t^{\beta} , \quad 1 \ll t \ll L \qquad (4.2.3)$$

which describes the dynamic scaling of the surface. From log-log plots like figure (4.3), the exponent β was estimated from a straight-line fit to the data within the growth region. Estimates of β for various values of L and p are shown in table (4.1).

We remark on the slow convergence of estimates of β as L→∞ for the smaller values of p. The data for p=0.99 yields β = 0.30 ± 0.01 with the lattice sizes we used.

In the steady-state region t >> L, the surface thickness saturates to a constant value σ(p,∞,L) depending on p and L. The dependence on L for various p values is shown in figure (4.4). The straight lines in the log-log plot indicate that

$$\sigma \sim L^{\alpha} , \quad 1 \ll L \ll t \qquad (4.2.4)$$

which describes the static scaling of the surface. The estimates of α are tabulated in table (4.2). They appear to converge to the value α=0.5 for p → 1.

In describing the asymptotic behaviour of the surface, we are guided by our understanding of asymptotic critical behaviour. If we associate a universality with the large-distance, long-time behaviour of the surface, then we do not expect the values of α and β to

TABLE (4.1). Estimates of exponent β, defined in equation (4.2.3), for various values of L and p. Errors are approximately ± 0.004

	β		
L	p=0.50	p=0.90	p=0.99
64	0.205	0.245	0.266
128	0.236	0.266	0.286
256	0.258	0.279	0.297
512	0.275	0.283	0.302

TABLE (4.2). Estimates of exponent α, defined in equation (4.2.4), for various values of p.

α	p
0.45 ± 0.01	0.3
0.46 ± 0.01	0.5
0.48 ± 0.01	0.7
0.48 ± 0.01	0.9

FIGURE (4.4). Steady-state surface thickness

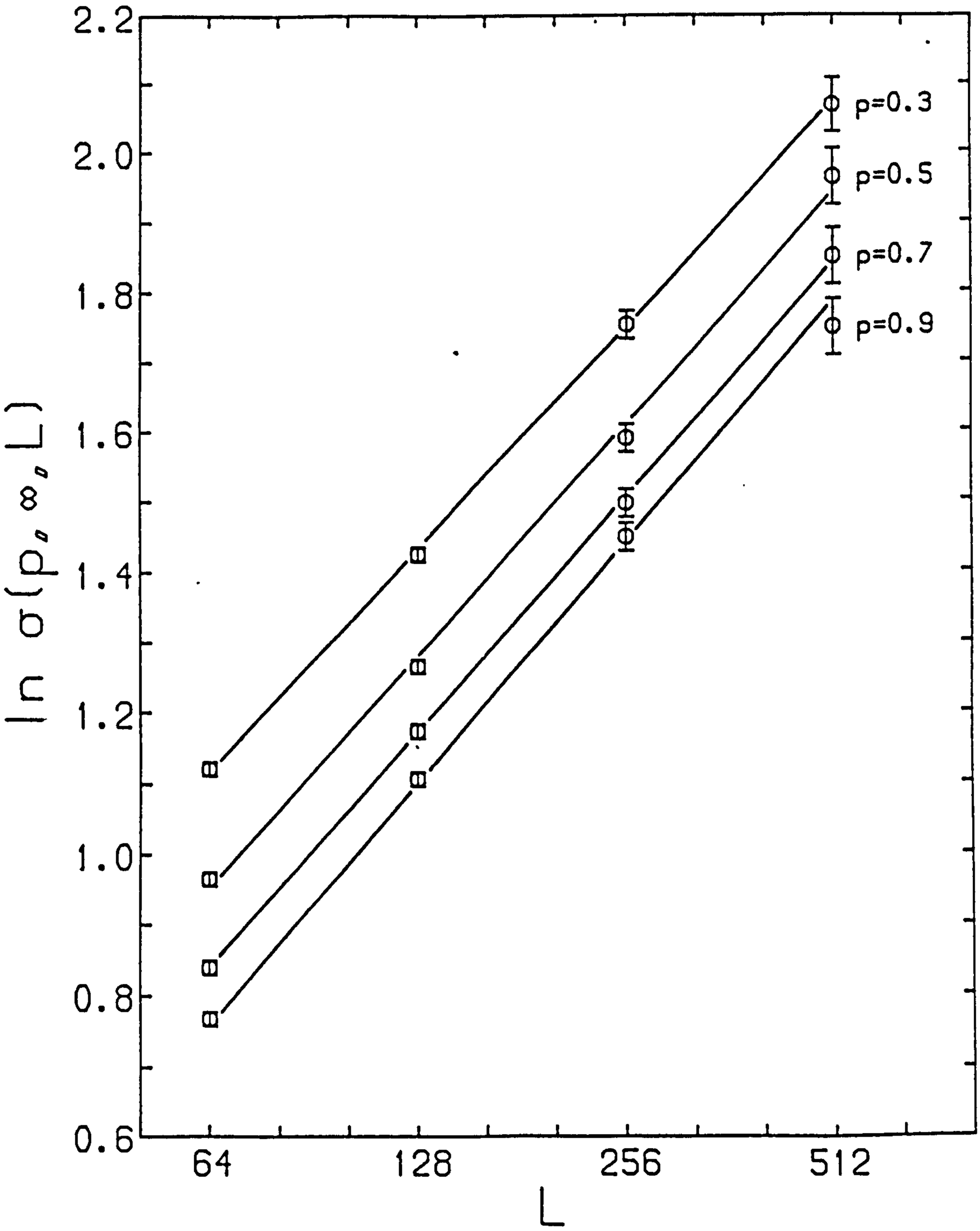

depend on $p\varepsilon(0,1)$ because the growth probability is a local feature of the surface growth. We can interpret tables (4.1) and (4.2) to mean that for small values of p, important finite-size corrections occur; we may associate these corrections with the fact, evident from figure (4.2), that the surface contains a greater number of holes which artificially increase the surface thickness.

To see this, we have plotted the surface growth in figure (4.5) for L=64 and various values of p. When $p \to 0$ we can identify four regimes. Initially the surface grows like $\sigma \sim t^{1/2}$; here the growth is a Poisson process (Family and Viscek 1985) in which the columns of the strip grow independently - this "dilute" behaviour is shared by the limit $p \to 1$ where there is an obvious duality with $p \to 0$. Then there follows a large regime where $\sigma \sim t^{0.55}$ in which the surface grows more rapidly through the formation of holes - since p is small, holes have a large average lifetime. A third, asymptotic regime is reached where $\sigma \sim t^{\beta}$ with $\beta \simeq 0.27$, which we have called the growth region. Finally the surface thickness saturates to a constant value. Note the non-zero saturation values for both $p \to 0$ and $p \to 1$.

As $p \to 1$ there is a crossover to a growth profile dominated by the asymptotic growth region. It is clear that p controls the size of the asymptotic growth region in which (4.2.3) is valid, and thus induces important corrections to scaling.

The scaling behaviours (4.2.3) and (4.2.4) can be formulated into a single dynamic scaling form for $\sigma(t,L)$:

FIGURE (4.5). Surface thickness σ(p,t,64)

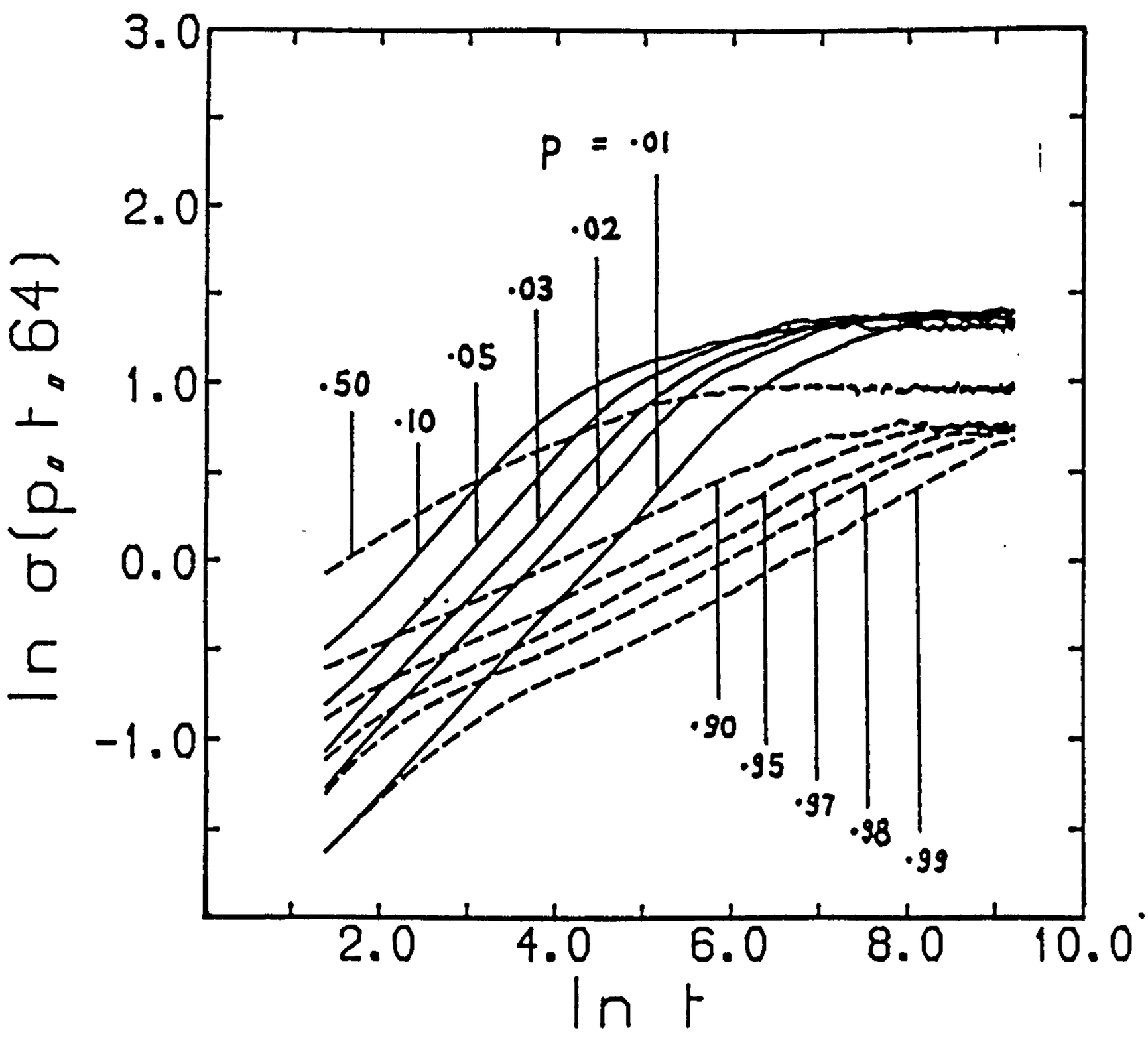

$$\sigma(t,L) \sim L^{\alpha} f\left(t/L^{\gamma}\right) \qquad (4.2.5)$$

where $\gamma=\alpha/\beta$ and the scaling function f(x) behaves like

$$f(x) \sim \begin{cases} x^{\beta} & , \quad x \to 0 \\ \text{constant} & , \quad x \to \infty \end{cases} \qquad (4.2.6)$$

Such a scaling form was first proposed by Family and Viscek (1985) for a model of ballistic aggregation, and has been applied by Jullien and Botet (1985) to the description of the surface of the Eden growth model (see section 4.3).

Since $\gamma > 1$ there are two independent characteristic scales in the model. Thus the surface is not a self-similar fractal because fractals are characterised by a single scale and a single exponent (fractal dimension). One might expect the surface to behave like a fractal coastline in the steady-state region where L is the only scale. However, this is not so. Figure (4.6) shows that the number of growth sites in the steady-state surface (the "measure" of the coastline) varies with the linear scale L like

$$N_g(\infty,L) \sim L \qquad (4.2.7)$$

in the trivial manner of a Euclidean (non-fractal) measure.

FIGURE (4.6). Growth sites vs. strip width

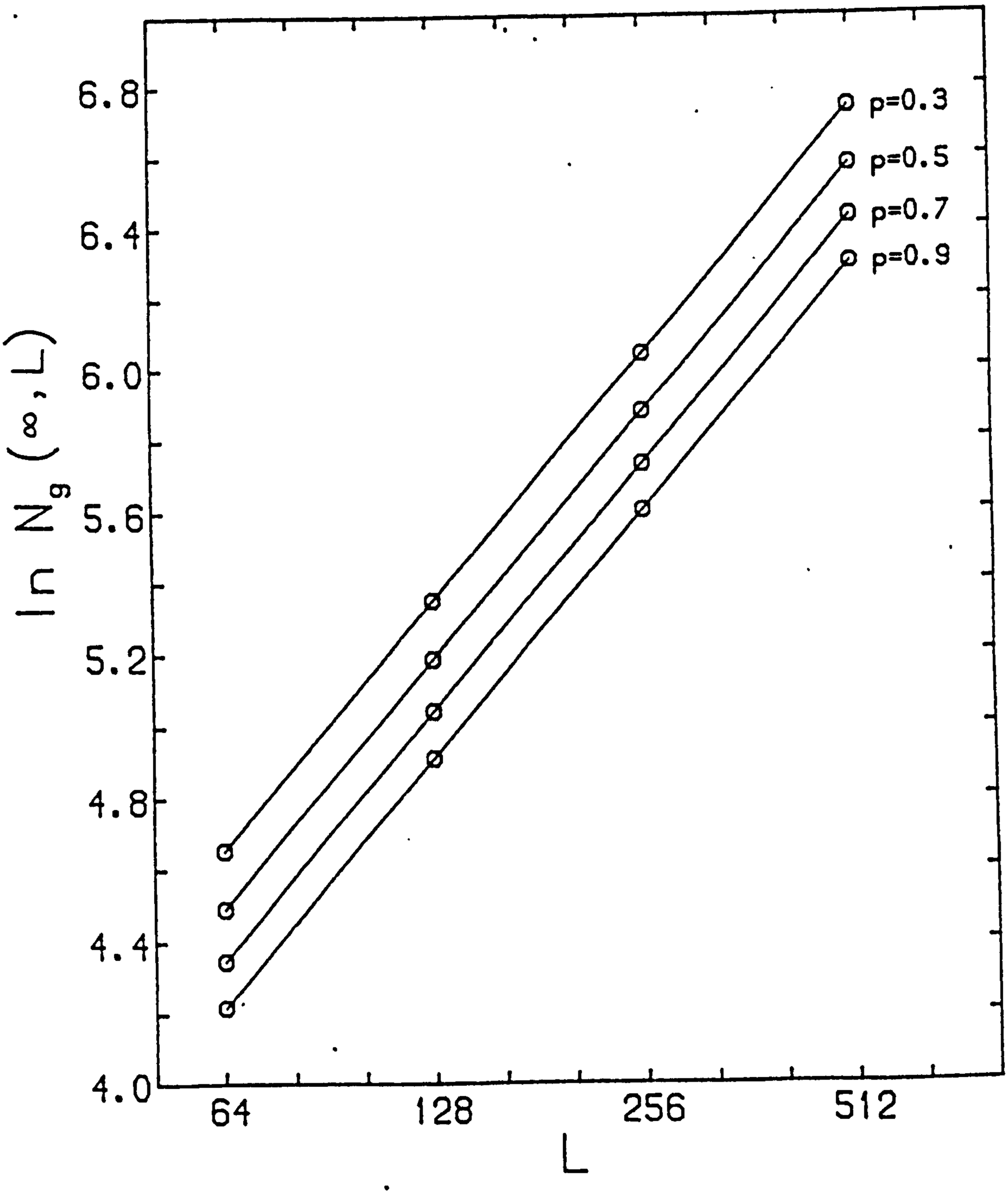

4.3 Other models: the universality class of G[p]

Now we mention some other models of growth and aggregation which can be characterised by two independent scales, and note the emergence of universality classes.

Jullien and Botet (1985) and Plischke and Racz (1986) have studied surface properties of an epidemic growth process called the Eden model (Eden 1961). In the simplest version of this model a healthy site adjacent to the surface is chosen at random and is infected with probability 1. To date, the most accurate estimates of exponents, by Plischke and Racz, are $\alpha=0.5$ and $\beta = 0.32 \pm 0.04$.

Family and Viscek (1985) have considered a model of ballistic aggregation. In this model particles are added one by one to the surface of a granular aggregate. The rule is as follows: a particle is dropped onto the randomly chosen column of a strip; the particle sticks when it arrives at the top of this column or at a site in this column adjacent to a particle in one of the neighbouring columns. It is found that $\alpha = 0.42 \pm 0.03$ and that in the growth region the surface thickness grows in time with exponent $\beta = 0.30 \pm 0.02$. (It is possible that $\alpha=0.5$ with large finite-size corrections due to the presence of holes).

From our simulations it appears that G[p] belongs to the same universality class as the Eden model and ballistic aggregation. It is a feature of all three models that the neighbouring columns of the strip are correlated. Family and Viscek (1985) note that in the absence of such correlations, the surface growth is a Poisson process

in which $\sigma \sim t^{1/2}$, corresponding to simple random deposition (RD).

Recently, Family (1986) has carried out simulations to explore the effects of surface diffusion on RD. In the simulation, like ballistic aggregation, a particle is dropped onto the randomly chosen column of a strip. However, the sticking rule is different; on reaching the surface, the particle is allowed to diffuse to neighbouring columns until it finds the column of lowest height. At this point it sticks and becomes a part of the surface. Thus, as in G[p], neighbouring columns are correlated. However, it is found that $\alpha = 0.48 \pm 0.02$ and $\beta = 0.25 \pm 0.01$, so that the surface grows at a slower rate that in G[p]. This surface diffusion model thus belongs in a different universality class from G[p].

We note that the value $\alpha=0.5$, describing the static scaling of the interface width, is common to several one-dimensional surfaces of irreversible growth, as it is for the description of surface roughening in equilibrium Ising systems (Jasnow 1980, Gallavotti 1972) and percolation (Francke 1980). However, it is a general feature that dynamic universality classes are smaller than static universality classes.

4.4 A Langevin equation for G[p]

We now discuss a phenomenological description of G[p] by a Langevin equation. This equation was proposed by Kardar *et al* (1986) as a general model for the local growth of an interface in continuous space and time. Its predictions account for the universality classes which we discussed in the previous section. At this point we

generalise to a d-dimensional lattice with a (d-1)-dimensional interface.

These authors write the following Langevin equation for the local growth of a surface, suitably coarse-grained in space and time.

$$\frac{\partial h}{\partial t} = \nu \nabla^2 h + \frac{\lambda}{2} (\nabla h)^2 + \eta(\underline{x},t) \qquad (4.4.1)$$

In the above expression, $h(\underline{x},t)$ is a continuous, single-valued function giving the height of the surface above the (d-1)-dimensional point $\underline{x}$ at time t, measured relative to its mean value. The first term on the RHS enhances the average growth of regions where h has a local minimum, and describes the surface diffusion of particles in the deposition model considered by Family (1986) (see section 4.3). ν then acts like a surface tension that wants the surface to be flat.

The second term on the RHS describes the effect of growth locally normal to the surface - it is the inclusion of this term which accounts for the universality class of G[p]. $\eta(\underline{x},t)$ is a zero-mean noise, taken to be Gaussian for convenience,

$$\langle \eta(\underline{x},t) \rangle = 0 \qquad (4.4.2)$$

$$\langle \eta(\underline{x},t)\, \eta(\underline{x}',t') \rangle = 2D\, \delta^{d-1}(\underline{x}-\underline{x}')\, \delta(t-t') \qquad (4.4.3)$$

and represents fluctuations in the surface profile about its mean height, due to the randomness in the growth, making the surface rough.

Equation (4.4.1) with $\lambda=0$ has been considered by Edwards and Wilkinson (1982) in a study of rough surfaces in granular aggregates upon which deposited particles settle under gravity. In the absence of the non-linear term, the equation is easy to solve by Fourier transforms. It may be shown directly by naive dimensional analysis that it leads to a scaling form for the surface thickness in which $\alpha=1/2$ and $\beta=1/4$. This accounts for the effect of surface diffusion on random deposition, as noted by Family (1986). In the absence of the first and second terms on the RHS, the equation describes the random deposition model in which $\sigma \sim t^{1/2}$.

When $\lambda\neq0$, the solution of (4.4.1) can only be found perturbatively, because λ couples together the different k-space modes of $h(\underline{x},t)$. However, Kardar *et al* (1986) showed that in $d=2$ the exponents are given exactly.

Their dynamical RG treatment of (4.4.1) is an extension of the ideas of chapter 1 to the study of scaling in time-dependent fluctuations (Hohenburg and Halperin 1977). When rewritten in k-space, (4.4.1) is solved perturbatively in λ. Terms in the perturbation series diverge for $d < 3$. The series is rearranged into a RG calculation by integrating out the modes with $e^{-\ell}\Lambda<k<\Lambda$. Then the parameters are rescaled as $\underline{k}'=e^{\ell}\underline{k}$, $t'=e^{-\gamma\ell}t$ and the remaining modes as $h'(\underline{k}',t')=e^{-(d+\alpha)\ell}h(\underline{k},t)$, where α and γ are the exponents appearing in the scaling form (4.2.5) for the surface thickness. The rescaled modes obey (4.4.1) with renormalised coefficients. α and γ are adjusted so that $dD/d\ell=d\nu/d\ell=d\lambda/d\ell=0$. The result in $d=2$ is $\alpha=1/2$ and $\gamma=3/2$ exactly, and hence $\beta=1/3$, close to the result for $G[p]$.

In figure (4.7) we have plotted $\sigma/L^{0.5}$ against $t/L^{1.5}$ for various L when p=0.5. The collapse onto a single scaling function for the larger values of L is in agreement with the scaling form (4.2.5) and the values $\alpha=1/2$, $\beta=1/3$.

To understand this we interpret the physical content of (4.4.1) in the context of G[p]. First, our interest in the large-distance, long-time behaviour of the model motivates us to coarse-grain our description of the surface profile with the function $h(\underline{x},t)$. This means we neglect the overhangs and holes seen in figure (4.2). Then, the surface tension term of (4.4.1) captures the large-distance relaxation effect of the rule of nearest-neighbour infection. To see this, note that a steep local minimum of h will rapidly be pinched closed by the lateral growth of opposite sides of the minimum. Any interior hole so formed can be neglected by coarse-graining. Therefore, on average, the surface height grows more rapidly at a minimum of h than at a maximum of h. The effective surface tension ν increases as $p \to 1$, as figure (4.2) illustrates. The effect is the same as the surface relaxation due to the local diffusion of grains settling under gravity.

The second term, describing growth locally normal to the surface, plays an obvious and important role in G[p]. Finally, the noise term in (4.4.1) represents the stochastic element of the growth rule. λ and D will also depend on p, although the asymptotic behaviour of the surface will not because that is controlled by the behaviour at the fixed point.

FIGURE (4.7). Surface thickness scaling function

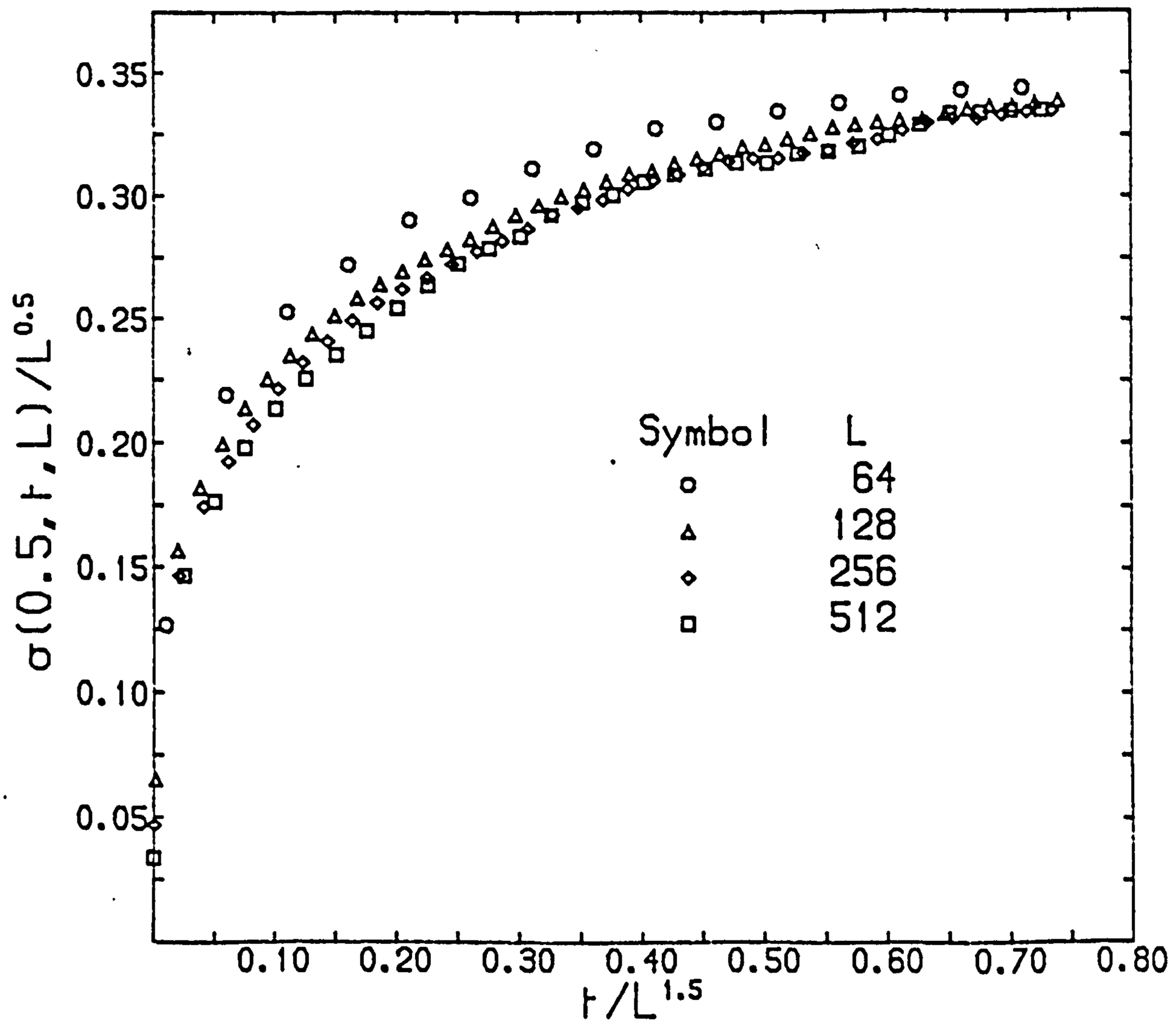

That no terms other than those appearing in (4.4.1) - higher derivatives perhaps - are required to describe the scaling properties of G[p] is evidenced by the close agreement with the simulation. Their irrelevance may be understood from RG arguments, by counting powers of momentum of additional couplings using the anomalous dimensions $\alpha=1/2$, $\gamma=3/2$ at the fixed point. In a similar way, one might generalise the noise parameterisation (4.4.3) by letting D depend on the momentum k. An expansion of D(k) for small k reveals that near the fixed point, all but the term D(k=0) are irrelevant.

We conclude that equation (4.4.1) captures the essential long-distance, long-time physics of G[p].

4.5 Conclusions

In this chapter we studied the surface properties of G[p], a simple model of random epidemic growth, first studied by Richardson (1973). From simulations in a strip geometry we found that, although the bulk and surface are not fractals, the surface has interesting scaling properties characterised by two independent scales which describe the static and dynamic scaling properties of the surface thickness. These properties were combined into a single dynamic scaling description, whose validity, we argued, was conditioned by important corrections to scaling for small values of p.

Further simulations on larger strips are required to establish this point conclusively. The version of the Eden model favoured by Jullien and Botet (1985) enhances the growth probability of sites

with a greater number of infected neighbours. This improves the asymptotic convergence of their simulation results. Such a version of G[p] is then also worth considering for future simulations. We add that the scaling corrections as $p \to 0$ are of interest in themselves; they arise from the hole structure which presumably has interesting dynamic and static scaling properties (Botet 1986).

Then we noted that the values of the exponents α and β were in close agreement with the predictions of a Langevin equation, proposed by Kardar *et al* (1986) as a phenomenological description of a growing interface, and which these authors note can be solved exactly within a dynamical RG treatment in d=2. We concluded that this equation captures the essential large-distance, long-time physics of G[p], namely, the growth of sites locally normal to the surface and the competition between surface relaxation and surface roughening, arising from the stochastic rule for infection of healthy sites by nearest-neighbour infected sites.

We were then able to understand the universal, scaling properties of the surface structure in terms of the ideas of chapter 1.

REFERENCES

Adler J 1986 Phys. Rev. Lett. 57, 918

Aharony A 1976 in "Phase Transitions and Critical Phenomena" vol.6 eds. Domb C and Green MS (New York: Academic)

Amit DJ and Kotliar GB 1980 Nuc. Phys. B170, 187

Amit DJ 1984 "Field Theory, the Renormalisation Group and Critical Phenomena" revised 2nd. edition (New York: McGraw-Hill)

Barber MN 1983 in "Phase Transitions and Critical Phenomena" vol.8 eds. Domb C and Lebowitz JL (New York: Academic)

Binder K 1979 ed. "Monte-Carlo Methods in Statistical Physics I" (Heidelberg: Springer-Verlag)

Binder K 1981 Z. Phys. B43, 119

Botet R 1986 Private communication

Brezin E 1982 J. Physique (Paris) 43, 15

Brezin E, Le Guillou JC and Zinn-Justin J 1976 in "Phase Transitions and Critical Phenomena" vol.6 eds. Domb C and Green MS (New York: Academic)

Brezin E and Wallace DJ 1973 Phys. Rev. B7, 1967

Brezin E and Zinn-Justin J 1976 Phys. Rev. B14, 3110

Bruce AD 1981 J. Phys. C14, 3667

Bruce AD and Wallace DJ 1983 J. Phys. A16, 1721

Coleman S 1975 Phys. Rev. D11, 2088

den Nijs MPM 1979 J. Phys. A12, 1857

Deutscher G, Zallen R and Adler J 1983 eds. "Percolation Structures and Processes" Ann. Israel Phys. Soc. vol.5 (Bristol: Adam Hilger)

Dewar R and Harris CK 1985 in "Fractals in Physics" Proc. 6th Trieste

Int. Symp. eds. Pietronero L and Tosatti E (Amsterdam: North Holland) p.145

Dewar R and Harris CK 1986 Edin. Univ. preprint 86/368: in print

Domb C and Pearce CJ 1976 J. Phys. A9, L137

Dotsenko VS and Dotsenko VS 1982 J. Phys. C15, 495

Eden M 1961 in "Proc. 4th Berkeley Symp. on Mathematics, Statistics and Probability" vol.4 ed. Neyman F (Berkeley: Univ. of California)

Edwards SF and Wilkinson DR 1982 Proc. R. Soc. Lond. A381, 17

Elitzur S 1979 IAS preprint

Elliot RJ, Heap BR, Morgan DJ and Rushbrooke GS 1960 Phys. Rev. Lett. 5, 366

Essam JW 1980 Rep. Prog. Phys. 43, 833

Family F 1986 J. Phys. A19, L441

Family F and Landau DP 1984 eds. "Kinetics of Aggregation and Gelation" (Amsterdam: North Holland)

Family F and Viscek T 1985 J. Phys. A18, L75

Ferer M, Moore MA and Wortis M 1973 Phys. Rev. B8, 5205

Fisher ME 1967 Rep. Prog. Phys. 30, 615

Flanders PM, Hunt DJ, Reddaway SF and Parkinson D 1977 in "High Speed Computer and Algorithm Organisation" eds. Kuck *et al* (New York: Academic) p.113

Francke H 1980 Z. Phys. B40, 1961

Gallavotti G 1972 Commun. Math. Phys. 27, 103

Goldstone J 1961 Nuovo Cimento 19, 154

Grover M 1972 Phys. Rev B6, 3546

Hohenburg PC and Halperin BI 1977 Rev. Mod. Phys. 49, 435

Hubbard J 1972 Phys. Lett. 39A, 365

Janke W and Kleinert H 1986 Nuc. Phys. B270, 154

Jasnow D 1980 Rep. Prog. Phys. 47, 1059

Jug G 1984 Phys. Rev. Lett. 53, 9

Jug G 1985 Phys. Rev. Lett. 55, 1343

Jug G 1986 J. Phys. A19, 1459

Jullien R and Botet R 1985 J. Phys. A18, 2279

Kadanoff LP 1966 Physics 2, 263

Kardar M, Parisi G and Zhang YC 1986 Phys. Rev. Lett. 56, 889

Kasteleyn PW and Fortuin CM 1969 J. Phys. Soc. Japan 26, 11

Kesten H 1983 "Percolation Theory for Mathematicians" (Boston: Birkhauser)

Kesten H 1986 Phys. Rev. Lett. 56, 1210

Lubensky TC 1977 Phys. Rev. B15, 311

Lubensky TC 1979 in "Ill-Condensed Matter" Les Houches Lecture Notes vol. 31 eds. Balian R *et al* (Amsterdam: North Holland) p.405

Ma SK 1976 "Modern Theory of Critical Phenomena" (Benjamin/Cummings)

Mandelbrot BB 1982 "The Fractal Geometry of Nature" (New York: Freeman)

McKane A and Stone M 1980 Nuc. Phys. B163, 169

Mermin ND and Wagner H 1966 Phys. Rev. Lett. 17, 1133

Metropolis N, Rosenbluth A, Rosenbluth M, Teller A and Teller E 1953 J. Chem. Phys. 21, 1087

Migdal AA 1975 Zh. Eksp. Teor. Fiz. 69, 1457

Mouritsen OG 1984 "Computer Studies of Phase Transitions and Critical Phenomena" (Heidelberg: Springer-Verlag)

Nienhuis B, Riedel EK and Schick M 1980 J. Phys. A13, L189

Pietronero L and Tosatti E 1985 eds. "Fractals in Physics" Proc. 6th Trieste Int. Symp. (Amsterdam: North Holland)

Plischke M and Racz Z 1984 Phys. Rev. Lett. 53, 415

Plischke M and Racz Z 1986 Phys. Rev. A32, 3825

Polyakov AM 1975 Phys. Lett. B59, 79

Ravndal F 1976 "Scaling and Renormalisation Groups" (Copenhagen: NORDITA)

Reddaway SF, Scott DM and Smith KA 1975 Computer Physics Communications 37, 351

Richardson D 1973 Proc. Camb. Phil. Soc. 74, 515

Samuel S 1980 J. Math. Phys. 21, 2806

Savit R 1978 Phys. Rev. B17, 1340

Savit R 1980 Rev. Mod. Phys. 52, 453

Stauffer D, Ferer M and Wortis M 1972 Phys. Rev. Lett. 29, 345

Stephen MJ and Grest GS 1977 Phys. Rev. Lett. 38, 567

Sykes MF and Essam JW 1964 J. Math. Phys. 5, 1117

t'Hooft G and Veltman M 1972 Nuc. Phys. B44, 189

Villain J 1975 J. Physique (Paris) 36, 581

Wallace DJ and Zia RKP 1978 Rep. Prog. Phys. 41, 1

Widom B 1965 J. Chem. Phys. 43, 3898

Wilson KG 1971a Phys. Rev. B4, 3174

Wilson KG 1971b Phys. Rev. B4, 3184

Wilson KG and Kogut J 1974 Phys. Rep. 12C, 75